UNIVERSITÀ VITA-SALUTE SAN RAFFAELE

CORSO DI DOTTORATO DI RICERCA INTERNAZIONALE IN MEDICINA MOLECOLARE

Curriculum in IMMUNOLOGIA E ONCOLOGIA DI BASE E APPLICATE

ELUCIDATING THE ROLE OF PROMYELOCYTIC LEUKEMIA GENE IN CLEAR CELL RENAL CELL CARCINOMA

DoS: Dr. Rosa Bernardi

Second Supervisor: Prof. Andrew Tee

Tesi di DOTTORATO di RICERCA di Chiara Menegazzi

matr. 017574

Ciclo di dottorato XXXVI

SSD BIO/13-Biologica Applicata

Anno Accademico 2022/2023

CONSULTAZIONE TESI DI DOTTORATO DI RICERCA

Il/la sottoscritto/*I* **Chiara Menegazzi**

Matricola / *registration number* **017574**

nat_ a/ *born at* **Pordenone (PN)**

il/*on* **31/01/1996**

autore della tesi di Dottorato di ricerca dal titolo / *author of the PhD Thesis titled*

Elucidating the role of promyelocytic leukemia gene in clear cell renal cell carcinoma

□ AUTORIZZA la Consultazione della tesi / *AUTHORIZES the public release of the thesis*

√ NON AUTORIZZA la Consultazione della tesi per **12** mesi /*DOES NOT AUTHORIZE the public release of the thesis for **12** months*

a partire dalla data di conseguimento del titolo e precisamente */ from the PhD thesis date, specifically*

Dal / *from* **15/12/2023** Al / *to* **14/12/2024**

Poiché /*because*:

□ l'intera ricerca o parti di essa sono potenzialmente soggette a brevettabilità/ *The whole project or part of it might be subject to patentability;*

√ ci sono parti di tesi che sono già state sottoposte a un editore o sono in attesa di pubblicazione/ *Parts of the thesis have been or are being submitted to a publisher or are in press;*

□ la tesi è finanziata da enti esterni che vantano dei diritti su di esse e sulla loro pubblicazione/ *the thesis project is financed by external bodies that have rights over it and on its publication.*

E' fatto divieto di riprodurre, in tutto o in parte, quanto in essa contenuto / *Copyright the contents of the thesis in whole or in part is forbidden*

Data /Date **01/12/2023** Firma /Signature 

DECLARATION

This thesis has been:

- composed by myself and has not been used in any previous application for a degree. Throughout the text I use both 'I' and 'We' interchangeably.

-has been written according to the editing guidelines approved by the University.

Permission to use images and other material covered by copyright has been sought and obtained. For the following image/s (specify), it was not possible to obtain permission and is/are therefore included in thesis under the "fair use" exception (Italian legislative Decree no. 68/2003).

All the results presented here were obtained by myself, except for:

1) ***RNA-sequencing data and bioinformatic analysis***

   RNA sequencing analysis and Bioinformatic analysis (Results, chapter 3.2.1, figure 19) was performed in collaboration with Dr. Matilde Simoni, Preclinical models of cancer Unit, San Raffaele Scientific Institute, Milan, Italy and Dr. Francesca Genova, Center for Omics Sciences, San Raffaele Scientific Institute, Milan, Italy.

2) **Lentiviral and retroviral vectors production**

   Lentiviral vectors (Results, chapter 3.1.2, figure 17; Results, chapter 3.3.3., figure 31) and retroviral vector (Result, chapter 3.3.1, figure 24) production were performed in collaboration with Dr. Matilde Simoni, Preclinical models of cancer Unit, San Raffaele Scientific Institute, Milan, Italy. Lentiviral vector production (Results, chapter 3.3.3, figure 30) was performed in collaboration with Dr. Federico Rossari, Targeted Cancer Gene Therapy Unit, San Raffaele-Telethon Institute for Gene Therapy, Vita-Salute San Raffaele University, Milan, Italy. Lentiviral vector production (Results, chapter 3.3.4, figure 32) was performed in collaboration with Dr. Oronzina Botrugno Functional genomics of cancer Unit, San Raffaele Scientific Institute, Milan, Italy.

3) ***Quantitative real time-PCR data***

   Quantitative real time PCR (Results, chapter 3.3.2, figure 25) was performed in collaboration with Dr. Matilde Simoni, Preclinical models of cancer Unit, San Raffaele Scientific Institute, Milan, Italy.

All sources of information are acknowledged by means of reference.

DEDICATION

I extend my sincere gratitude to the members of my laboratory—Matilde, Cristina, Martina, and Daniela—whose unwavering support has been instrumental in achieving this life success. A special acknowledgment goes to: my primary supervisor, Rosa, for her close companionship throughout this academic journey, during which I felt listened and guided. Her lessons, especially in critical thinking will profoundly influence my academic and personal growth. I am also indebted to my second supervisor, Andrew Tee, whose wise advices has been valuable in shaping this work. Finally, I am especially grateful to Matilde, whose mentorship exhibited patience and support and from whom I have learned invaluable skills and techniques in the laboratory.

ABSTRACT

Clear cell Renal Cell Carcinoma is the most common type of RCCs accounting for 75 % of all cases. It has been estimated that 50 % of patients develop metastasis within 3 to 30 years after tumor removal. The majority of the patients with metastasis develop treatment resistance, therefore the urge of new treatment is imminent. Recent emerging drugs include inhibitors of HIF2α, a hypoxia-induced factor whose expression is deregulated in ccRCC. Preliminary results from our laboratory suggested that PML is overexpressed in RCC and that it correlated with poor prognosis. Here the role of PML as an oncogene was further tested by bioinformatics analysis and *in vitro* studies. We found that *PML* silencing induced a stable and p53-dependent growth arrest. Moreover, by using SA-β-gal assay we showed that knocking down *PML* caused ccRCC cells to enter senescence after long term *PML* silencing. By performing RNA sequencing on *PML*-silenced RCC4 cells we confirmed the phenotypes observed *in vitro* and *in vivo* upon *PML* silencing and we identified genes that are positively regulated by HIF2α. This prompted us to hypothesize that PML regulates ccRCC proliferation through HIF2α. However, overexpression of HIF2α in *PML*-silenced cells failed to reverse the phenotype. Finally, we interrogated the transcriptional network regulated upon *PML* silencing and identified a number of transcription factors whose responsive elements are enriched in PML-regulated genes. Within these genes, we observed an enrichment of SP1 binding sites. Because SP1 is a known interactor of both PML and p53 we tested a possible interaction with PML in ccRCC cells. By double immunofluorescence, we demonstrated spatial colocalization of SP1 and PML and proposed SP1 as a valid candidate to be tested for its involvement in the regulation of p53-mediated senescence.

TABLE OF CONTENTS

Chapter 1. INTRODUCTION 10

1.1. The promyelocytic leukemia gene -overview 10

1.1.1. The oncoprotein PML-RARα and degradation by ATRA/ATO 10

1.1.2. PML isoforms and protein structure 12

1.1.3. Formation of PML-NBs 13

1.1.4. PML regulation by transcriptional and translational machineries 14

1.1.5. Functions of PML 15

1.2. Renal Cell Carcinoma 19

1.2.1. ccRCC and its genetics 20

1.2.2. The role of PML in ccRCC 21

1.3. HIF1α and HIF2α 22

1.3.1. The Role of HIF1α/HIF2α in response to hypoxia 22

1.3.2. The Role of HIF1α/HIF2α in ccRCC 24

1.3.3. The role of HIF1α and HIF2α on p53 25

1.4. Therapy in Renal cell Carcinoma 26

1.5. Preliminary data 27

1.5.1. PML expression in ccRCC 27

1.5.2. The effect of PML silencing on ccRCC expansion in vitro and in vivo 28

1.5.3. The effect of PML silencing on p53 and HIF transcription factors in ccRCC 31

Chapter 2. AIM OF THE WORK 33

2.1. AIM 1. Define the function of PML in ccRCC progression; 33

2.2. AIM 2. Analyze the gene expression network upon *PML* silencing in ccRCC cells; . 33

2.3. AIM 3. Explore the molecular mechanisms of PML-mediated control of proliferation. 33

Chapter 3. RESULTS 34

3.1. AIM 1. Define the function of PML in ccRCC progression 34

3.1.1. Bioinformatics analysis reveals PML overexpression in ccRCC 34

3.1.2. Evaluating the effect of long PML silencing in RCC4 cells 38

3.1.3. The effect of PML silencing on senescence 40

3.2. AIM 2. Global analysis of gene expression regulation upon PML silencing in ccRCC cells 41

3.2.1 Defining the effect of PML silencing on the RCC4 transcriptome 41

3.2.2. Comparisons of gene expression changes induced by PML silencing in RCC4 with other studies.....46

3.3. AIM 3. Explore the molecular mechanisms of PML-mediated control of proliferation 50

3.3.1. The role of p53 in cell proliferation in RCC4.....50

3.3.2. The role of PML in the regulation of HIF2α-induced genes 52

3.3.3. HIF2α rescue experiments in RCC4 cells upon PML silencing 55

3.3.4. The effect of arsenic trioxide on ccRCC in vitro 60

3.3.5. The identification of putative transcription factors regulating pathways downstream of PML.....61

Chapter 4. DISCUSSION..... 67

4.1. Future perspectives..... 70

Chapter 5. MATERIALS AND METHODS..... 72

5.1 Applied bioinformatics analysis..... 72

5.2. Senescence-associated β-Galactosidase staining 72

5.3. RNA extraction and RNA sequencing 72

5.4. Functional enrichment analysis 73

5.5. Cell culture 74

5.6. Western Blotting 74

5.7. Cell Proliferation and focus forming assay 75

5.8. Focus forming assay 76

5.9. Lentivirus production and cell transduction..... 76

5.10. Retrovirus production and cell transduction 77

5.11. Quantitative real time (qRT) PCR 78

5.12. Generation of cancer cell lines expressing luciferase and treatment with ATO... 78

5.13. Immunofluorescence..... 79

5.14. Statistical analysis 79

5.15. Reagents and treatments 80

5.16. List of antibodies 80

Chapter 5. REFERENCES 81

ACRONYMS AND ABBREVIATIONS

Akt – Ak strain transforming

AMPK–5'AMP-activatedproteinkinase

ANGPT2–Angiopoietin2

ANGPTL4–Angiopoietin-like4

APL – Acute Promyelocytic Leukemia

ARF – ADP-ribosylation Factor

ATO – Arsenic Trioxide

ASF1 – Anti-Silencing Function 1 Histone Chaperone

ATRA – All Trans Retinoic Acid

B – B-box

BAP1 – BRCA1 Associated Protein 1

BCL-B – Cell Lymphoma

BNIP3 – BCL2/Adenovirus E1B 19 kDa protein-interacting protein 3

CBP – Creb Binding Protein

c-Myc – cellular Myc

CC – Coiled Coil domain

CCND1 – Cyclin D1

CEBP – CCAAT/Enhancer Binding Protein

CDKN2A – cycline-dependent kinase inhibitor 2A

CDK – Cycline-dependent Kinase

ChRCC – Chromophobe Renal Cell Carcinoma

CML – Chronic Myeloid Leukemia

CSCs – Cancer Stem Cells

CXCL-C-X-C Motif Chemokine Ligand 1

E2F – E2 Transcription Factor

eIF4E – eukaryotic Initiator of Translation Factor 4

EPAS – Endothelial PAS domain-containing protein 1

EPO – Erythropoietin

ER – Endoplasmic Reticulum

FACS – Fluorescence Assisted Cell Sorting

FAO – Fatty Acid Biosynthesis

FDA – Food and Drug Association

GLUT1 – Glucose Transporter 1

HDAC7 – Histone Deacetylase 7

HIF – Hypoxia-Inducible Factors

HIPK2 – Homeodomain-Interacting Protein Kinase 2

HIRA – Histone Cell Cycle Regulator

HK1 – Hexokynase 1

HRE – Hypoxia-responsive Element

HSV – Herpex Simplex Virus

HUVEC – Human Umbilical Vein Endothelial Cells

IF - immunofluorescence

IHC – Immunohistochemistry

JARID1B – histone demethylase

LOX – Lysyl Oxydase

MAM – Mitochondrial associated membranes

MDM2- Mouse Double Minute 2,

MEFs – Murine Embryonic Fibroblasts

MHC – Major Histocompatibily Complex

MMP – Metalloproteinase

mTORC – Mammalian Target of Rapamycin Complex

NB-Nuclear Body

N-coR – Nuclear Repressor Complex

NES – Nuclear Exclusion Signal

NFK – Nuclear Factor Kappa

NGFR – Nerve Growth Factor Receptor

NLS – Nuclear Localization Signal

NSCLC – Non-Small Cell Lung Cancer

O2 – Molecular Oxygen

Oct4 – Octamer Binding Transcription Factor 4

ODD – Oxygen-dependent Degradation Domain

ORO – Oil red O

PAS – Per-ARNT-Sim

PBRM1 – Polybromo 1

Protein 1 PDH – Pyruvate Dehydrogenase

PDK1 – Pyruvate Dehydrogenase Kinase

PDL-1 – Programmed Death-ligand 1

PDX – Patient-derived Xenografts

PHD – Prolyl Hydroxylase

PI – Propidium Iodide

PI3K – Phosphatidylinositol 3-kinase

PML – Promyelocytic Leukemia Protein

pO2 – Partial Oxygen Pressure

PPAR – Peroxisome Proliferator Activated Receptor

PTEN – Phosphatase and tensin homolog

qRT-PCR – quantitative Real Time Polymerase Chain Reaction

pRCC – Papillary Renal Cell Carcinoma

R – Ring Finger

RAR − Retinoic Acid Receptor

RARE-Retinoic Acid Response Elements

Ras – Rat Sarcoma

RCC – Renal Cell Carcinoma

RING – Really Interesting New Gene

SA-β-Gal – Senescence associated -Beta-Galactosidase

SASP – Senescence Associated Secretory Phenotype

SATB1-Special AT-Rich Sequence Binding Protein 1

SCP1 – Small C-terminal domain phosphatase

SET – Su(var)3-9-Enhancer-of-zeste and Trithorax

shRNA – short hairpin RNA

SIM – SUMO interacting motif

Ski – Sloan-Kettering Institute Proto-Oncogene

SOX2 – Sex Determining Region 2

SP1 - Stimulatory Protein 1.

SREB – Sterol Regulatory Element Binding Transcription Factor

STAT – Signal Transducer and Activated Transcription

SUMO – Small ubiquitin modifier

TBX2 – T-Box transcription factor 2

TCGA-KIRC – The Cancer Genome Atlas and the Clinical Proteomic Tumor Analysis Consortium of the National Cancer Institute

TCGA-KIRP – The Cancer Genome Atlas Cervical Kidney Renal Papillary cell carcinoma

TGF – Transforming Growth Factor

TEM – Transmission Electron Microscopy

TLR – Toll like Receptor

TKI – Tyrosine Kinase Inhibitor

TNBC – Triple Negative Breast Cancer

TNF – Tumor Necrosis Factor

TRIM19 – TRIpartite Motif

UBC9 – Ubiquitin conjugating enzyme 9

USF1 - Upstream Stimulating Factor 1

VEGFA – Vascular Endothelial Growth Factor A

VEGFR-Vascular Endothelial Growth Factor Receptor

VHL – Von Hippel Lindau

WB – Western Blotting

YY1-Yin-Yang 1

LIST OF FIGURES AND TABLES

Figure 1.Representation of the different PML isoforms and their structure.....12

Figure 2. Pie chart of the different subtypes of RCCs and their incidence.....20

Figure 3. VHL loss of function is the only clonal genetic aberration in ccRCC.....21

Figure 4.VHL targets the hypoxia-inducible transcription factors HIF1α.....23

Figure 5.The effect of HIF2α on VHL-null ccRCC proliferation in vitro. 25

Figure 6. PML is overexpressed in ccRCC. 28

Figure 7. The efficiency of the Tet-On inducible system in silencing PML in ccRCC cell lines. 28

Figure 8. PML knockdown inhibits cell proliferation and survival capacity. 29

Figure 9. PML knockdown leads to cell cycle arrest in G0/G1 phase.....29

Figure 10. PML silencing causes tumor shrinkage in vivo.....30

Figure 11. PML silencing causes p53 and p21 upregulation. 31

Figure 12.PML silencing causes HIF1α upregulation and HIF2α downregulation .32

Figure 13.Bioinformatics analysis of PML mRNA and protein expression in ccRCC compared to adjacent normal tissue. 35

Figure 14.Comparative analysis of PML expression across tumor types.....36

Figure 15.Survival probability of PML expression along time.....37

Figure 16.Correlation between PML expression and age, race and gender. 38

Figure 17. PML silencing drives stable growth arrest. 40

Figure 18. PML silencing cause senescence in vitro. 41

Figure 19. PML silencing induces altered mRNA expression of 2192 genes. 42

Figure 20. PML silencing causes downregulation of pathways related to cell cycle and proliferation. 43

Figure 21. PML silencing causes upregulation of pathways related to senescence and inflammation 46

Figure 22. PML silencing causes upregulation of 22 senescence markers which are common to 15 transcriptomic studies of senescence.....48

Figure 23.. PML silencing causes upregulation of 81 soluble SASP which are related to inflammation and extracellular matrix organization.....49

Figure 24. Loss of p53 function rescues proliferation. 51

Figure 25. PML negatively regulates HIF1α -target genes and positively regulates HIF2α -target genes. *52*

Figure 26. PML and HIF2α co-regulate genes that are involved in cell cycle and DNA replication in vivo *53*

Figure 27. PML and HIF2α co-regulate genes that are involved in cell cycle and DNA replication in vitro. *54*

Figure 28.PML regulates few genes that are bound by HIF2α. *55*

Figure 29. Retroviral-mediated infection of wild-type RCC4 cells with two plasmids expressing a mutant HA-HIF2α and shRNAs against PML failed to provide an HIF2α overexpression system. *56*

Figure 30. HIF2α overexpression does not rescue proliferation. *58*

Figure 31. HIF2α silencing does not affect cell proliferation in RCC4 and A498. ..... *59*

Figure 32.Arsenic trioxide (ATO) treatment inhibits cell growth in ccRCC *61*

Figure 33.33 transcription factors have been identified in multiple different cellular contexts as transcriptional regulators of PML-activated genes in RCC4. ..... *63*

Figure 34. 33 transcription factors have been identified in multiple different cellular contexts as transcriptional regulators of PML-repressed genes in RCC4. ..... *65*

Figure 35. PML and SP1 colocalize in ccRCC RCC4 cells. *66*

Chapter 1. INTRODUCTION

1.1. The promyelocytic leukemia gene -overview

The promyelocytic leukemia (*PML*) gene was first identified in a patient with acute promyelocytic leukemia (APL) in 1990 (De Thé *et al*, 1990). *PML* generates multiple isoforms, all of which contribute to the assembly of PML nuclear bodies (PML-NBs), a specialized subnuclear donut-like structure that lacks a membrane. The PML protein, acting as a central component of PML-NBs, displays remarkable dynamic behavior by moving fluidly between the nucleoplasm and PML-NBs, as well as among different PML-NBs within the nuclear matrix. Many groups have demonstrated that PML-NBs play a role in various cellular processes, such as transcriptional regulation, post-translation modifications, antiviral response, apoptosis, stem cell maintenance and metabolism. Thus, deregulated PML expression and dysregulation of PML-NBs formation can profoundly affect important and vital cell functions, leading mainly to tumor onset. In this chapter I will first describe the *PML* gene, its product isoforms and the biogenesis and functions of PML NBs. Finally, I will describe the dual role of as tumor suppressor and oncogene.

1.1.1. The oncoprotein PML-RARα and degradation by ATRA/ATO

More than 95 % of APL patients harbor an oncogenic fused gene PML-RARα assigning an essential role for this protein in leukemogenesis (Di Croce, 2005). The fusion between the *RARα* gene, which maps to chromosome 17q21 and the *PML* gene, which maps to chromosome 15q22, occurs after the t(15;17) translocation, leading to the fused product PML-RARα (de Thé *et al*, 1991; Kakizuka *et al*, 1991). This protein creates homodimers that inhibits the activation of key genes essential for the differentiation of granulocytes. They do so by associating with a set of various retinoic acid response elements (RAREs) found in the regulatory regions of these genes. Simultaneously, they recruit a corepressor (CoR) complex containing different proteins to both the PML and RARα components.

The involvement of PML-RARα in the disease progression of APL raised the possibility of a molecular mechanism underlying the specific response to all-*trans* retinoic acid (ATRA) therapy, which expanded the therapeutic landscape in APL, initially treated only

with chemotherapy (Fenaux *et al*, 1995). Indeed studies have shown that APL patients achieve an impressive complete emission rate of 90 % when treated with ATRA (Creutzig *et al*, 2010; Ades *et al*, 2009). ATRA induces a conformational change in PML-RARα, resulting in the disassociation of the corepressor (CoR) complex from the receptor. Simultaneously, proteins with histone acetylase (HAT) properties as part of the coactivator complex act to open and modify the chromatin structure, making it more accessible and permissive for gene transcription and consequently differentiation. Recent transcriptome and proteome analyses provide substantial evidence for this coregulator exchange model, with numerous genes responsible for the initiation and promotion of differentiation of granulocytes being modulated. This includes the upregulation of granulopoiesis-associated transcription factors C/EBPs and cytokines receptors such as the G-CSFR, which initiate the downstream signaling cascade that involves various proteins such as protein kinases and phosphatases. It's crucial to emphasize that ATRA not only induces a caspase-mediated cleavage of the PML-RARα chimeric protein but also triggers its degradation through the ubiquitin/proteasome system (UPS). This mechanism extends to both PML-RARα and RARα.

Since the late 1990s, arsenic trioxide (ATO) has been incorporated into APL treatment regimens, significantly enhancing outcomes for patients with refractory or relapsed APL as well as those newly diagnosed (Niu *et al*, 1999). Combining ATRA with ATO has demonstrated a more pronounced reduction in PML-RARα transcript levels and prolonged survival in newly diagnosed APL patients, surpassing the efficacy of therapy with ATRA or ATO alone (Zhu & Huang, 2014; Lo-Coco et al, 2013).

Similar to ATRA, ATO induces PML-RARα degradation and reconstitution of PML-NBs (de Thé *et al*, 2012). However, unlike ATRA, ATO binds directly to the cysteine residues in the zinc fingers of the PML RBCC domains (Zhang *et al*, 2010). This binding induces a conformational change in the protein that facilitate the oligomerization of PML and increases the PML-RARα aggregates, concurrently fostering the SUMOylation of proteins through interactions with the small ubiquitin-like protein modifier (SUMO)-conjugating enzyme UBC9 (Zhang *et al*, 2010; Lallemand-Breitenbach *et al*, 2008).

The interaction with UBC9 leads to increased SUMOylation exposing polySUMO chains to the direct binding of the E3 ubiquitin ligase RNF4 which mediates the ubiquitination of both PML and the PML-RARα oncoprotein via proteasomal-mediated degradation

(Geoffroy *et al*, 2010; Tatham *et al*, 2008). ATO can also trigger PML and PML-RARα degradation by triggering oxidative stress facilitating aggregation of PML into PML-NBs.

1.1.2. PML isoforms and protein structure

The *PML* locus is 35 kb long and is composed of nine exons. Through alternative splicing these exons transcribe different *mRNA* transcripts producing 11 human protein PML isoforms with varying properties. These isoforms result from alternative splicing, share the same N-terminal region but differ at the C-terminal region. We will describe only 7 out of 11 PML isoforms, that have been fully characterized and designated as PML I-VII according to Jensen and colleagues (Figure 1) (Jensen *et al*, 2001). With the exception of isoform VII which is cytoplasmic, PML I-VI are nuclear and share constitutive exons 1-3 as well as putative alternative exons (4-6). Instead, exons 7 and 8 can be subdivided into exons 7a, 7b, 8a, and 8b (Uggè *et al*, 2022).

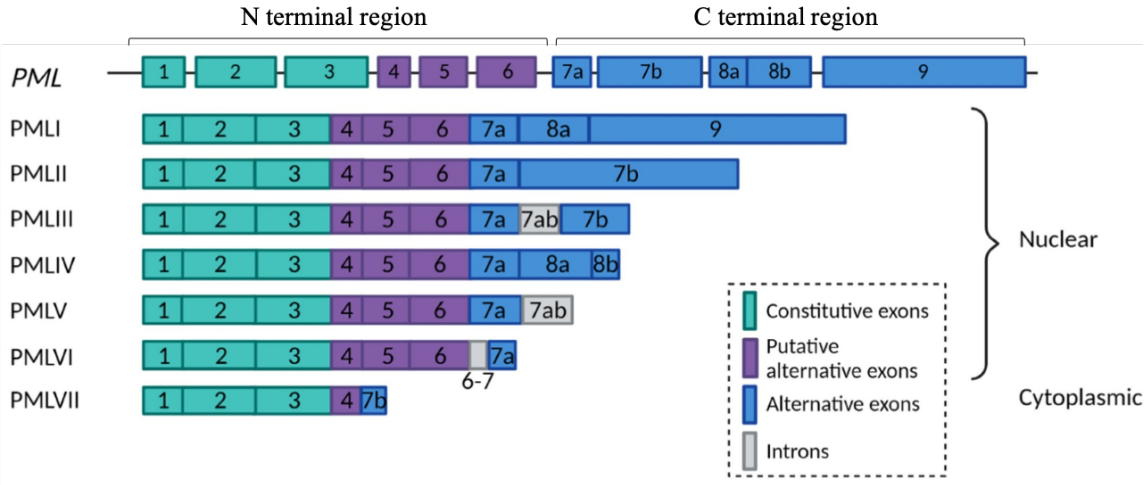


Figure 1.Representation of the different PML isoforms and their structure.
7 out of 11 PML isoforms have been characterized, namely PMLI-VII. PML I is the longest and PMLVII is the shortest. All 7 isoforms contain constitutive exons 1-3 (green). All except for PMLVII contain putative alternative exons 4, 5 and 6 (purple). PML isoforms differ in their C terminal region containing alternative exons 7-9 (blue). PMLIII, PMLV and PMLVI isoforms harbor introns between exons. Modified from Uggè et al. (Uggè *et al*, 2022).

The PML protein is a member of the tripartite motif protein family (TRIM), corresponding to TRIM19. The highly conserved exons 1-3 at the N-terminal domain encode a RBCC motif, containing one Really Interesting New Gene (RING) finger, two B boxes (B1 and B2) and a α-helical coiled-coil (CC) domain, all located at amino acids

57–253 in exons 1–3. The RBCC motif in PML is crucial for the initial assembly of PML-NBs, as well as for homo and hetero oligomerization and interactions with other proteins (Jensen *et al*, 2001). Mutation in the cysteine residues C62A/C65A results in failed PML-NB formation, dispersion of resident proteins within the nucleus, failed PML SUMOylation and escape from ATO-induced PML degradation (Voisset *et al*, 2018). Moreover, in APL, the RING domain is required for the transforming potential of PML-RARα (Jensen *et al*, 2001). Instead, the C terminal region of PML is subject to alternative splicing thus it is responsible for the different functions of PML isoforms and contains various motifs: a nuclear localization signal (NLS), an essential SUMO-binding domain or SUMO-interacting motif (SIM); a nuclear exclusion signal (NES) in PML-I (Nisole *et al*, 2013). The specific function and interaction partners of each isoform are determined by these C-terminal differences. For example, while all isoforms share a nuclear localization signal (NLS), PML VII, the shortest isoform, stands out by being primarily located in the cytosol. In contrast, PML I, the longest isoform, is unique in possessing a Nuclear Export Signal (NES), allowing it to be dually localized in both the nucleus and the cytoplasm (Condemine *et al*, 2006). PMLI harbors a motif similar to exonuclease-III, partially shared with PML IV, and contributes to nucleolar localization during genotoxic stress (Condemine *et al*, 2007). Furthermore, PMLV includes an α-helix crucial for the formation of PML-NBs, as expounded upon later (Geng *et al*, 2012). The SIM domain is present exclusively in PMLI–V and is responsible for the interaction of PML with other SUMOylated proteins, a process pivotal for the assembly and organization of PML-NBs, though not indispensable for the initiation process of PML-NB assembly (Sahin *et al*, 2014). Additionally, PMLI and PMLIV possess an additional SUMOylation site in exon 8a (Nisole *et al*, 2013). PML itself is extensively modified by SUMOylation (Seeler & Dejean, 2017). PML SUMOylation mainly occurs at three lysine sites K65, K160 and K490 (Kamitani *et al*, 1998) within the RBCC region and in proximity to the NLS.

1.1.3. Formation of PML-NBs

When PML proteins aggregate they contribute to the establishment of punctate and stress-responsive structures known as PML-NBs. These are proteinaceous not static structures primarily consisting of PML proteins, which reside at the outer shell of this super-complex where they can interact with a select group of resident proteins and a

multitude of transient clients (Sahin Umut *et al*, 2014). These bodies typically measure between 0.2 and 1.0 μm in size, with the number of PML-NBs per nucleus ranging from 5 to 30 (Boisvert *et al*, 2000; Dellaire & Bazett-Jones, 2004). The size and number can vary substantially between cell types, cell cycle phases and upon stress or DNA damage (Dellaire & Bazett-Jones, 2004). Indeed, in interphase, PML-NBs appear as stable through extensive contacts with surrounding chromatin (Eskiw *et al*, 2004). As cells enter the S phase, chromatin condensation causes PML-NBs to undergo fission, producing PML microbodies associated with chromatin (Dellaire *et al*, 2006). Interestingly, the dynamic nature of PML-NBs is reflected by their ability to exist as liquid-like droplets formed by liquid-liquid phase separation (Banani *et al*, 2016; Corpet *et al*, 2020; Hoischen *et al*, 2018).

The establishment of PML-NBs involves a series of intricate steps, involving oxidation-driven cross-linking, self-oligomerization, poly-SUMOylation, and interactions with SUMO/SIM motifs (Hoischen *et al*, 2018). Specifically, these steps include: i) Initiation involves the formation of oxidation-driven covalent disulfide bridges and noncovalent interactions between RBCC domains, particularly attributed to the RING and B1 elements (Wang *et al*, 2018; Li *et al*, 2019b). These multimers spontaneously self-organize into the outer shell of the PML nuclear body. ii) Subsequent SUMOylation of PML is followed by further self-multimerization through SUMO/SIM interactions. iii) The engagement of the SUMO-conjugating enzyme UBC9, which is recruited to the PML nuclear body to mediate poly-SUMOylation, contributing to the maturation of PML bodies and the establishment of a peripheral scaffold within the nuclear body. iv) Finally, the recruitment of SUMOylated or SIM-containing client proteins completes the maturation process of PML-NBs.

1.1.4. PML regulation by transcriptional and translational machineries

PML is a sensor of stress and its expression can be regulated by various stress stimuli and molecular mechanisms. Upon environmental stimuli such as hypoxia, osmotic stress, heat shock, oxidative stress, oncogenic stress, viral infection, cytokine and hormone release and DNA damage, different transcriptional and translational machineries promote *PML* mRNA and protein expression, PML post-translational modifications affecting protein stability and localization and interaction with other proteins.

At the transcriptional level, extracellular stimuli involving interferons via STAT1, tumor necrosis factor alpha (TNFα) via STAT2, IRF3, IRF8, and oncogenic stress via RAS/p53, all lead to upregulation of *PML* mRNA (Stadler *et al*, 1995; Dror *et al*, 2007; Chelbi-Alix *et al*, 1995; Cheng *et al*, 2012; de Stanchina *et al*, 2004; Ferbeyre *et al*, 2000). Instead, cytokine and hormone release lead to the downregulation of *PML* mRNA via STAT3 and STAT6 (Yamada *et al*, 2014).

At the post-transcriptional levels, oncogenic stress mediated by expression of K-RAS augments translation of *PML* mRNA via mTOR/eIF$_4$E signaling (Scaglioni *et al*, 2012). TNFα can also induce increased PML protein levels, a process mediated the activation of the internal ribosome entry site (IRES) by p38-MNK1 (Hsu *et al*, 2016).

1.1.5. Functions of PML

PML is capable of regulating transcription, *mRNA* translation, protein post-translational modifications and protein-protein interactions (Hsu & Kao, 2018). The different functions of PML rely not only on PML found in PML-NBs, but also in the nucleoplasm and in the cytoplasm, such as within mitochondrial associated membranes (MAMs) and endoplasmic reticulum (ER) (Lin *et al*, 2004; Missiroli *et al*, 2016). PML exerts a plethora of functions under pathological and physiological contexts. PML has been shown to enhance apoptosis in both the nuclear and cytoplasmic compartments. Moreover, cytoplasmic PML is primarily linked to antiviral responses (Hsu & Kao, 2018). Other functions include senescence, stemness maintenance, inflammation and metabolism. PML exerts these functions through its interaction with protein interactors, that up to now account for more than 200 (Previati *et al*, 2018). Below I will give a general overview of the main functions exerted by PML.

1.1.5.1. Transcriptional regulation

It is important to emphasize the complexity of studying PML's transcriptional functions, given its dualism between PML-NBs and nucleoplasmic PML. PML's impact on transcription is exerted through both indirect mechanisms, modulating the activity of transcriptional regulatory proteins, and more direct interactions with specific chromatin regions. Indirect mechanisms are evident by the capability of PML-NBs to sequester transcription factors, such as p53 and DAXX, into the PML-NBs, blocking their access

to chromatin. Another indirect example of transcriptional control by PML is the transcriptional repression of E2F factors permitted by the re-localization of the E2F/Rb complexes along with heterochromatin proteins into the PML-NBs upon senescence induction (Vernier *et al*, 2011). However, PML is also implicated in both promoting and inhibiting transcription through interactions with specific chromatin modifiers. Many transcriptional coactivators, such as histone acetyltransferase (CBP), along with transcriptional corepressors (Ski and N-coR), are indeed found in colocalization with PML-NBs. Indeed, many transcriptional coactivators, such as histone acetyltransferase (CBP) and transcriptional corepressors (Ski and N-coR) colocalize with PML-NBs (Bernardi & Pandolfi, 2007; Khan *et al*, 2001). Likewise, HDAC7 repressive activity is inhibited by TNFα-induced increased PML NBs in HUVEC (Gao *et al*, 2008b, 2008a). Although PML cannot bind directly to DNA and PML-NBs are devoid of DNA, an association of PML with chromatin regions, encompassing both euchromatin and heterochromatin has been demonstrated (Boisvert *et al*, 2000; Wang *et al*, 2004). An example of specific chromatin regions includes the major histocompatibility complex (MHC) locus. In particular PML associates with this locus by interacting with SATB1 and promoting chromatin looping between regions (P. *et al*, 2007). Interestingly, PML can also act as a regulator of epigenetic inheritance through its binding to heterochromatin region and direct repression of histone H3.3 deposition (Delbarre & Janicki, 2021).

1.1.5.2. Post translational modifications

PML can either activate or repress the activity of various proteins through sequestration into PML-NBs or by facilitating protein-protein interactions, both processes followed by post-translational modifications mediated by PML. One of the most studied PML interactor is p53, which moves to PML-NBs during cellular stresses, where it undergoes SUMOylation, phosphorylation and acetylation (Matt & Hofmann, 2018). Phosphorylation and acetylation of p53 are mediated by histone modulators HIPK2 and CBP, respectively, when all three proteins are recruited to PML-NBs (Hofmann *et al*, 2002; D'Orazi *et al*, 2002).

1.1.5.3. Antiviral response

PML participates to the regulation of innate immunity and acute inflammatory response, impacting anti-bacterial macrophage activity and modulating the Toll-like receptors (TLR)/NF-kB pathway in response to infections, especially viral infections (Lunardi *et al*, 2011). For this reason, PML-NBs can be disrupted by viral proteins that can also affect PML re-localization outside the nucleus. One such example is the infected cell protein (ICP) 0 of HSV-1 (ICP0), which causes both proteosome-dependent degradation of PML (Maul & Everett, 1994) as well as re-localization of PML into viral cellular compartments and export in the cytoplasm (McNally *et al*, 2008). Indeed, increased alternative splicing and oxidative stress lead to accumulation of cytoplasmic PML as a mean for weakening host defenses (McNally *et al*, 2008; Guo *et al*, 2014).

1.1.5.4. Apoptosis

PML-NBs may influence apoptosis via diverse pathways. These mainly include acting as platforms for transcriptional modification and activation of the tumor suppressor p53. For example, PML sequesters p53 ubiquitin ligase MDM2 inside nucleoli leading to p53 stabilization and apoptosis (Bernardi *et al*, 2004). Moreover, PML-null mice are less sensitive against death-receptor mediated apoptosis by stimulation of CD95L and TNFα (Wang *et al*, 1998). Cytoplasmic PML can also initiate apoptosis. Missiroli and colleagues demonstrated that PML at MAMs facilitates Ca^{2+} import into mitochondria, a key step for initiating apoptosis and that PML-null mouse embryonic fibroblasts (MEFs) gain resistance in ER-stress induced apoptosis (Missiroli *et al*, 2016).

1.1.5.5. Cancer stem cell maintenance and drug-resistance

PML can regulate stemness in different type of stem cells, both in pathological and normal settings. In chronic myeloid leukemia, *PML* inhibition suppresses quiescent leukemia-initiating stem cells (Ito *et al*, 2008). PML can also maintain normal hematopoietic stem cells stemness through peroxisome proliferator-activated receptor δ (PPAR-δ)–fatty-acid oxidation (FAO) pathway (Ito *et al*, 2012). Moreover, PML's involvement is also evident in mouse embryonic stem cells, where it influences the expression and activation of key transcription factors, including OCT4, MYC, NANOG, STAT3, and REST (Zhou & Bao, 2014). PML appears to contribute to an open chromatin

conformation in the Oct4 promoter region, thereby influencing consistent expression in stem cells. Studies on developmental processes, such as mammary secretory epithelium development and nervous system development, further emphasize PML's crucial role in maintaining cell stemness during normal development (Li *et al*, 2009; Regad *et al*, 2009).

1.1.5.6. Metabolism

PML plays an acknowledged role in modulating cellular physiology, particularly in controlling pro-surviving metabolic processes (Cheng *et al*, 2013; Carracedo *et al*, 2012). The function of PML on metabolism can vary based on factors such as mouse strain, diet, and age (Kim *et al*, 2011). In mouse models with obesity fed with a Western diet, the absence of PML has been associated with an increased rate of glucose and fatty acid metabolism, leading to a reduction in obesity-related symptoms (Cheng *et al*, 2013). PML KO in these mice led to AMPK activation and the upregulation of genes involved in lipid metabolism (cholesterol biosynthesis and FAO) in adipose tissue, skeletal muscle and liver (Cheng *et al*, 2013). Moreover, when energy is low, PML-NBs are proposed to re-arrange affecting the expression of genes downstream of important energy modulators such as RELA and NF-kB transcription factors, leading to metabolic changes (Cheng *et al*, 2013). In another study, it was shown that *PML KO* augments the metastatic potential of prostate cancer, by indirectly modulating the SREBP-lipogenesis, the latter signature being highly associated with metastasis in this tumor (Chen *et al*, 2018).

1.1.5.7. PML, senescence and p53 regulation

PML's involvement in regulating p53 was initially demonstrated in primary fibroblasts during oncogene-induced senescence. Research findings converged to indicate that PML promotes p53 post-translational modifications (PTMs) crucial for RAS-induced senescence (Ferbeyre *et al*, 2000). Separate studies emphasized PML's necessity for p53-activated apoptosis (Gottifredi & Prives, 2001). Beside p53, PML’s induction of senescence involves the retinoblastoma (Rb) protein which via regulation of E2Fs induces cell cycle exit (Vernier *et al*, 2011). Beside p53 and pRb, other less predominantly inducers of senescence exist. Notably, chromatin regulatory factors like HIRA and ASF1, interact with the heterochromatin protein HP1 inside the PML-NBs, driving the formation of heterochromatin foci around proliferation-promoting genes (Zhang *et al*, 2005).

Additionally, PML can bind to the promoter of TBX2, inactivating its transcriptional activity and promoting senescence (Martin *et al*, 2012a).
Under conditions of stress induction, such as oncogene expression or irradiation, PML-NBs recruit regulators of p53, including HIPK2, CBP, or ARF, thereby enhancing p53 acetylation or phosphorylation (Ivanschitz *et al*, 2013). Importantly, only PMLIV among the other isoforms, contributes to p53-mediated senescence, thanks to its distinctive C-terminus sequence. This sequence facilitates PML binding of ADP-ribosylation factor (ARF) that protects p53 from MDM2-driven degradation through SUMOylation (Ivanschitz *et al*, 2015).

1.1.5.8.PML dual role as tumor suppressor and oncogene

Even though *PML* locus is rarely mutated in tumors, PML expression by immunohistochemistry was found to be reduced in a number of human cancers compared to normal tissues, such as central nervous system (CNS) tumors, colon adenocarcinomas, lung tumors, prostate adenocarcinomas, breast adenocarcinomas, germ cell tumors, non-Hodgkin's lymphomas (Gurrieri *et al*, 2004). Moreover, PML loss in prostate, breast, and CNS tumors, leads to tumor invasiveness and bad prognosis (Gurrieri *et al*, 2004). While many tumors show decreased PML expression levels, there are some exceptions where PML expression is found increased. For example, in triple negative breast cancer (TNBC), PML expression levels are increased and correlate with poor prognosis (Huber *et al*, 2009). Indeed, PML in TNBC has pro-metastatic function (Ponente *et al*, 2017). *In vitro* experiments also demonstrated that PML overexpression in TBNC protects human cancer cell from anoikis via increased fatty acid oxidation (Carracedo *et al*, 2012). In chronic myeloid leukemia (CML) treatment with arsenic trioxide, which disassemble PML-NBs, causes cells to exit from quiescence and blocks cancer stem cells (CSC) differentiation (Ito *et al*, 2008). In ovarian cancer, PML is highly expressed, playing a role in cell proliferation and colony formation (Liu *et al*, 2017).

1.2. Renal Cell Carcinoma

With more than 400,000 newly diagnosed cases, renal cell carcinomas (RCCs) are the seventh most common type of cancer in the world (Fitzmaurice *et al*, 2017). RCCs account for 140,000 deaths each year, caused by disease progression into metastatic

RCCs developing in 20-30 % of patients (Ljungberg *et al*, 2011). Therefore, for its poor prognosis, RCC represent a serious threat for the population.

RCC is subdivide in four main histological subtypes, namely clear cell renal cell carcinoma (ccRCC), papillary renal cell carcinoma (pRCC) and chromophobe renal cell carcinoma (chRCC), which constitute more than 90 % of all RCCs (Figure 2) (Shuch *et al*, 2015). The remaining subtypes are less frequent with an incidence of approximately 2 % (Shuch *et al*, 2015).

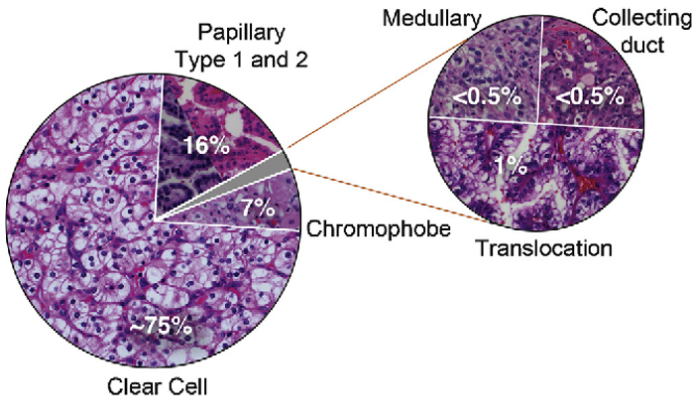


Figure 2. Pie chart of the different subtypes of RCCs and their incidence.
The majority (>90 %) of the subtypes comprise of ccRCC, pRCC and chRCC. Only 2 % of the total RCCs are medullary, collecting duct and translocation subtypes. Images taken from (Shuch et al, 2015).

1.2.1. ccRCC and its genetics

Clear cell renal cell carcinoma (ccRCC) represents the most common histological subtype of all RCCs, accounting for 75 % of all cases (Rini *et al*, 2009). ccRCC originates from the epithelium of the proximal convoluted tubule (renal cortex). Histologically, ccRCC is characterized by the presence of clear (lipid and glycogen-rich) and eosinophilic cytoplasm (Frew & Moch, 2015). ccRCC can be sporadic (95 %) or hereditary (5 %), the latter due to the loss of function of Von Hippel-Lindau (VHL) protein (Frew & Moch, 2015). 90 % of sporadic ccRCC develop a mutation in the *VHL* gene, caused by a truncal genetic event that sees the deletion of one allele on the 3p chromosome (Figure 3). The subsequent loss of VHL protein function is crucial for initiating early steps in tumor formation. In addition, tumor development and progression are further promoted by mutations in other genes with a prevalence in epigenetic regulatory genes (Greenman *et al*, 2007; Varela *et al*, 2011; Peña-Llopis *et al*, 2012;

Brugarolas, 2014) including *PBRM1* (32.9 %), *SETD2* (11.2 %), *BAP1* (10.1 %), *KDM5C (*6.7 %). Other alterations include mutations and chromosomal copy number alterations (Sato *et al*, 2013) in cell-cycle regulatory genes such as *CDKN2A* (deletion, 16 %), and MYC (copy number gain, 23 %) and PI3K pathway genes *PIK3CA* (mutation, 5 %), *PTEN* (mutation, 2 %), *MTOR* (mutation, 6 %) and *TSC1* (mutation, 2 %). In contrast with other tumor types, *TP53* is infrequently mutated in ccRCC (mutation, 2.2 %), Unlike *VHL* inactivation, which constitutes a clonal genetic aberration event, these mutations occur later and recurrently in ccRCC, cooperating with pVHL in the evolution of this disease (Figure 3) (Sato *et al*, 2013).

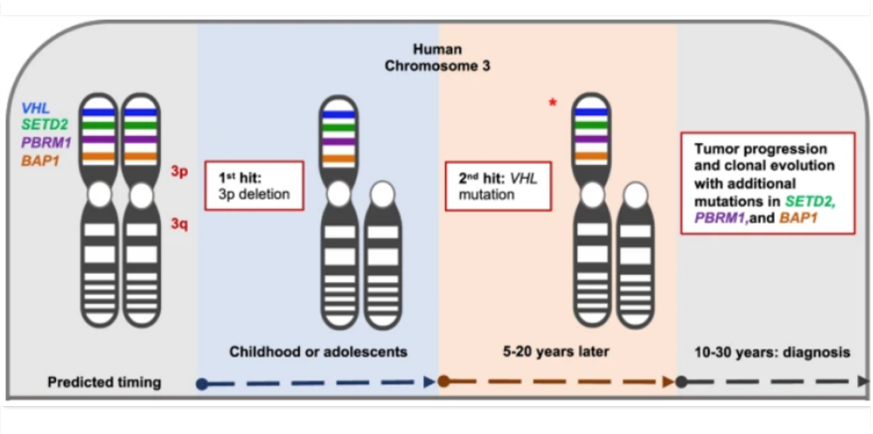


Figure 3. VHL loss of function is the only clonal genetic aberration in ccRCC.
VHL mutation can occur even 5-20 years later than 3p deletion occurring in childhood or adolescence. Diagnosis occurs much later, when the tumor has progressed following additional mutation in epigenetic factors including SETD2, PBRM1 and BAP1. Image taken from (Wolf *et al*, 2020).

1.2.2. The role of PML in ccRCC

PML has not been well characterized in ccRCC. Studies describing PML in ccRCC date back to 2014 where PML was suggested to be playing tumor suppressive functions. In this study overexpression of the SCP1 phosphatase, which promotes PML stability, inhibited tumor growth (Lin *et al*, 2014). In striking contrast with this study, four recent studies suggested a tumor-promoting function of PML in this disease. The first study highlighted a correlation between PML expression and clinical features, such as metastasis, cancer stage and survival status (Li *et al*, 2019a). Subsequently, Luo and colleagues use the public TGCA dataset to set up a model for identifying prognostic markers in ccRCC (Luo *et al*, 2023). Among the differentially significantly expressed

cuproptosis-related ferroptosis genes, they identified PML, which was positively correlated with worse overall survival, Moreover, in the same year Wu *and colleagues* identified PML as a prognostic TGF-ß signaling-related gene that was significantly differentially expressed in tumor tissues compared to normal tissue (Wu *et al*, 2023). Finally, another group confirmed PML as a possible prognostic marker gene in ccRCC, demonstrating its enhanced expression in tumors compared to normal tissues (Wang *et al*, 2023).

1.3. HIF1α and HIF2α

1.3.1. The Role of HIF1α/HIF2α in response to hypoxia

The pVHL protein exerts different functions in untransformed cells (Gerlinger *et al*, 2012). Some of its functions include maintaining the primary cilium, stabilizing microtubules, controlling ECM formation, and others (Haase, 2009). Its main function however is to serve as an element together with the other components of the E3 ubiquitin ligase complex (Elongin B, Elongin C, Cullin 2 and Rbx1) in the recognition of specific substrates (Cardote *et al*, 2017). The pVHL-E3 ligase fulfills a critical function in the oxygen-sensing pathway of metazoans, ubiquitinating and degrading hypoxia-inducible factors HIF-α (Ivan *et al*, 2001). During normoxia, 2-oxoglutarate-dependent dioxygenases (prolyl-4-hydroxylase domain (PHD) proteins) hydroxylate HIF-α factors on proline residues (Pro402, Pro564 for HIF1, Pro405 and Pro531 for HIF2), and their activity relies on ascorbate, 2-oxoglutarate, and oxygen beside oxygen (Figure 4) (Schofield & Ratcliffe, 2004). This process enables binding of the pVHL-E3 ligase complex to the α subunit of the oxygen-dependent degradation (ODD) of HIF-α, promoting ubiquitin-mediated degradation of HIF-α via proteosome-mediated degradation (Figure 4) (Huang *et al*, 1998; Ohh *et al*, 2000). Under hypoxia, the lack of oxygen does not allow recognition of HIF-α by PHDs, leading to HIF-α stabilization and dimerization with HIF1β that together bind hypoxia responsive elements (HRE) on DNA (Figure 4). Thus, pVHL loss of function recapitulates a hypoxic environment where HIF1α and HIF2α are constitutively expressed, and for this reason it is referred to as pseudohypoxia (Figure 4).

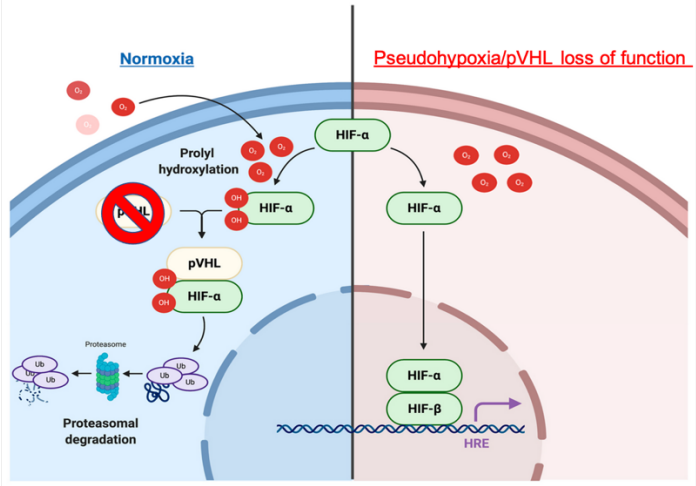


Figure 4.VHL targets the hypoxia-inducible transcription factors HIF1α.
Under normoxia, the HIF-α transcription factors are degraded by pVHL-mediated ubiquitination. Loss of functional pVHL protein mimics a hypoxic environment in which the HIF-α transcription factors escape degradation. Image taken from (Vito et al.,2020).

In the realm of the adaptation response to hypoxia, HIF1α and HIF2α bind to HRE and regulate many cellular functions, both cell autonomous e non cell autonomous. These include angiogenesis/O_2 supply (via VEGFA, ANGPT2, CXCL12, EPO), stemness/self-renewal (via OCT4, JARID1B), cell proliferation (via CCND1, TGFA, EPO), autophagy (via BNIP3, NOX, etc.), cell migration and invasion (via LOX, ANGPTL4, MMP9) and metabolism (via GLUT1, HK1, PDK1). In hypoxic conditions, HIF1α complexes stimulate the expression of genes involved in glycolysis (Hu *et al*, 2003), pro-angiogenic functions, and pH regulation (Kalinowski *et al*, 2016). The *EPAS1* gene encodes HIF2α, which is produced in specific cell types constituting the endothelium, the heart and the liver (Zhao *et al*, 2015), where it promotes the expression of matrix metalloproteinases and erythropoietin (Keith *et al*, 2012). While angiogenesis is initiated by HIF1α, HIF2α plays a crucial role in ensuring the appropriate development and maturity of vascular network (Koh & Powis, 2012). HIF1α accumulates earlier and decreases more rapidly (upon severe hypoxia: $pO_2 < 1\%$) than HIF2α during prolonged hypoxia (upon mild hypoxia $pO_2 < 5\%$) (Magliulo & Bernardi, 2018), leading to a transition known as the HIF switch (Cabaj *et al*, 2022), caused by lower HIF1α mRNA stability compared to *EPAS1 mRNA* (Serocki *et al*, 2018). HIF1α activity in hypoxia promotes anaerobic glycolysis, potentially reactivating PHDs and influencing the HIF switch by affecting HIF-2α expression (Hagen *et al*, 2003).

1.3.2. The Role of HIF1α/HIF2α in ccRCC

Both HIF1α and HIF2α can significantly impact tumor progression by exerting shared functions such as metabolism, angiogenesis, and invasion. Tumor cells often exhibit elevated expressions of both HIF1α and HIF2α, which have been correlated to tumor progression (Keith *et al*, 2012). Initially perceived as having overlapping functions, recent insights highlight diverse and sometimes opposing roles played by HIF1α and HIF2α within the same tumor type.

In distinct tumor contexts, HIF1α and HIF2α have been observed to regulate cell cycle progression by inhibiting or enhancing c-MYC, respectively (Koshiji *et al*, 2004; Gordan *et al*, 2007). The specific impacts of HIF1α and HIF2α on c-MYC provide a mechanistic rationale for the involvement of HIF2α in clear cell renal cell carcinomas (ccRCCs) associated with VHL disease (Raval *et al*, 2005; Mandriota *et al*, 2002). Notably, in VHL disease, the hereditary cancer syndrome linked with germline *VHL* mutation, there is a gradual reduction in HIF1α expression, while HIF2α expression rises during the development of ccRCCs (Raval *et al*, 2005; Mandriota *et al*, 2002).

While HIF1α promotes, rather than inhibit, many tumor types of non-renal origin, in ccRCC it is described more often as a tumor suppressor (Semenza, 2003). In ccRCC, re-expressing HIF1α in cells lacking wild type HIF1α slows tumor progression. Moreover, in ccRCC expression of HIF1α and HIF2α-bound genes correlate with better and poor prognosis, respectively (Salama *et al*, 2015). Similarly, in colorectal cancer (CRC), HIF2α exhibits pro-tumoral activity by inducing a pro-inflammatory milieu that promotes the production of cytokines and chemokines (Xue *et al*, 2012; Triner & Shah, 2016).

Independent studies in pVHL-deficient human ccRCC xenografts highlight the HIF2α subunit as the key driver of proliferation, contrasting with the limited impact of HIF1α (Raval *et al*, 2005; Kondo *et al*, 2003, 2002; Cho *et al*, 2016). However, the effect of HIF2α on cell proliferation in vitro within ccRCC remains contentious and contradictory (Figure 5) (Wallace *et al*, 2016; Raval *et al*, 2005; Cho *et al*, 2016; Stransky *et al*, 2022; Shen *et al*, 2011; Gordan *et al*, 2008; Kondo *et al*, 2003; Arnaiz *et al*, 2021). In general, RNA-induced silencing of HIF2α or pharmacological targeting by two new HIF2α inhibitors (PT2385 or PT2399) does not affect the proliferation of RCC4, 786-O, and A498 cell lines, unless cells are grown in soft agar, which is a more restrictive condition where single cells form colonies. Therefore, albeit oncogenic *in vivo*, HIF2α does not

appear to be essential for proliferation *in vitro*, in standard growth conditions. However, a few papers demonstrated contradictory results for RCC4 (Figure 5). The molecular mechanisms and acquired mutations that could account for the variation in HIF2α dependency in RCC4 cells are still unknown.

Cell	Effect of PT2385 (standard growth condition)	Effect of PT2399 (soft agar)	Effect of RNAs targeting EPAS1 (standard growth condition)	Author/s
RCC4 *wt* (*VHL*$^{-/-}$)	NO	ND	NO YES	Arnaiz; Shen, Gordan
786-O *wt* (*VHL*$^{-/-}$)	NO	YES	NO	Arnaiz; Stransky; Cho; Wallace; Kondo
A498 *wt* (*VHL*$^{-/-}$)	ND	YES	NO	Cho; Wallace; Kondo

Figure 5.The effect of HIF2α on VHL-null ccRCC proliferation in vitro.
Studies that have investigated the effect of PT2385, PT2399, RNA-induced silencing on RCC4, 796-O and A498 cells. NO=no effect; YES=significant inhibition; ND=not determined.

1.3.3. The role of HIF1α and HIF2α on p53

HIF1α and HIF2α exhibit contrasting effects on the activation of p53, particularly in response to insufficient oxygen levels. In hypoxic region of solid tumors p53 accumulate fast and associates with cells undergoing apoptosis, especially under low pH conditions and nutrient scarcity (Pan *et al*, 2004). In the beginning, it was suggested that HIF1α enhances the stability of functionally active wild type p53 through a direct physical interaction (An *et al*, 1998). However, subsequent reports indicated that HIF1α binds MDM2, suppressing its ubiquitination activity on p53 and promoting its nuclear export (Chen *et al*, 2003). Conversely, HIF2α indirectly regulate p53 through multiple mechanisms, involving p53 phosphorylation and stabilization (Bertout *et al*, 2009; Scortegagna *et al*, 2003). Loss of HIF2α leads to increased ATM activity, DNA double-strand breaks, and elevated ROS after ionizing radiation (Scortegagna *et al*, 2003). HIF2α inhibition in renal cell carcinoma (RCC) activates p53 by enhancing ROS accumulation,

causing cell cycle arrest potentially contributing to resistance to radiation therapy in HIF2α-expressing RCCs (Bertout *et al*, 2009). Parallel studies indicate that in RCC4$^{VHL-/-}$ and 786-O$^{VHl-/-}$ ccRCC cells, HIF2α overexpression suppresses p53 via a pathway involving growth factor receptors, AKT, and MDM2, fostering the survival of tumor cells upon exposure to radiation and chemotherapy (Roberts *et al*, 2009).

1.4. Therapy in Renal cell Carcinoma

The current treatment available for localized ccRCC is surgical removal. As the tumor expands, chemotherapeutic agents are used, challenged by drug resistance. Between 2000-2010 tyrosine kinase inhibitors (TKIs), such as VEGFR inhibitor sunitinib, and mTOR inhibitor everolimus, were used to treat ccRCC (Gossage *et al*, 2015), as the PI(3)K/AKT pathway emerged as a compelling therapeutic target in ccRCC (Motzer *et al*, 2008; Hudes *et al*, 2007). Studies have demonstrated a correlation between poor prognosis in ccRCC patients and a metabolic shift towards increased dependency on the pentose phosphate shunt, decreased AMPK, reduced Krebs cycle activity, heightened glutamine transport, and enhanced fatty acid production (Comprehensive molecular characterization of clear cell renal cell carcinoma, 2013). These findings align with an analysis of *VHL-/-* ccRCC cell lines demonstrating a dependency of these cell lines on the utilization of glutamine in its reduced form to synthesize lipids (Metallo *et al*, 2012). Future investigations to unravel the roles of commonly mutated genes in ccRCC mapped to chromosome 3 (PBRM1, SETD2, and BAP1) and their potential involvement in the associated metabolic remodeling during disease progression hold promise for shaping effective therapeutic strategies for this condition.

As for now, the first-line of therapy in ccRCC is represented by immune checkpoint inhibitors, including pembrolizumab, nivolumab, and ipilimumab, sometimes used in combinations with TKIs, such as axitinib, cabozantinib, and lenvatinib (Atkins & Tannir, 2018; Choueiri & Motzer, 2017; Powles *et al*, 2020). Advances in the therapeutic landscape of this tumor are challenging because of variability of responses seen among patients due to the highly heterogeneity of the tumor segments in ccRCC (Li *et al*, 2023). Recently, combination of histopathologic, proteogenomic, and metabolomic data from hundreds of different tumor segments highlighted the intra-tumoral heterogeneity of this tumor, shedding light on the significance of genetic instability and enhanced

hypermethylation as markers for poor patient outcome (Li *et al*, 2023). For this reason implementation of demethylating agents have been suggested (Li *et al*, 2023; Chen *et al*, 2020).

The involvement of HIF2α in ccRCC led to the design of drugs inhibiting HIF2α, these comprising of small molecules ligands, called PT2385, PT2399 and PT2977. All these molecules can bind to the hydrophobic motif in the PAS-B domain of HIF2α, inducing a conformational change that blocks the formation of HIF2α/HIF1β complex and suppress downstream activation of genes (Key *et al*, 2009; Rogers *et al*, 2013; Scheuermann *et al*, 2009). Both PT2385 and PT2399 suppress tumor progression faster than sunitinib (Wallace *et al*, 2016). Although well-tolerated, the drug pharmacokinetics of these drugs was not very efficient, leading to the second-generation of HIF2α inhibitor, PT2977 (Courtney *et al*, 2018). Recently a structural analogue of PT2399, named Belzutifan gained FDA approval for treating patients with VHL-associated RCC after showing promises *in vitro* and *in vivo* (source: FDA website, http://www.fda.gov/cder/approval/index.htm). Despite remarkable advances, drug resistance due to mutations in the HIF2α pocket or HIF1β remains a challenge (Chen *et al*, 2016).

By integrating genomic and functional analysis recent experiments demonstrated that similarly to p53, HIF2α can control the expression of genes by enabling their association with nuclear speckles, which are nuclear bodies containing RNA-binding proteins and specific non-coding RNAs (Alexander *et al*, 2023). This physical association influences patient survival and is correlated with poor prognosis (Alexander *et al*, 2023). Manipulation of speckles-targeting motifs will be a valuable way to regulate gene expression in the realm of cancer therapy.

1.5. Preliminary data

1.5.1. PML expression in ccRCC

Preliminary analyses conducted in collaboration with Dr. Sabina Signoretti at the Brigham and Women's Hospital in Boston show that PML is overexpressed in ccRCC specimens compared to normal kidney parenchyma (Figure 6A). Consistently, PML protein levels are higher in ccRCC cell lines compared to the normal kidney HEK293 cell line as well as other cell lines, including cells representative of tumor types where PML

expression is maintained high (chronic myeloid leukemia cells) (Ito *et al*, 2008) (Figure 6B). Finally, high PML expression correlated with increased Furnham grade, a predictor of poor prognosis (Figure 6C). Taken together, these observations suggested that PML does not exert tumor suppressive functions in ccRCC.

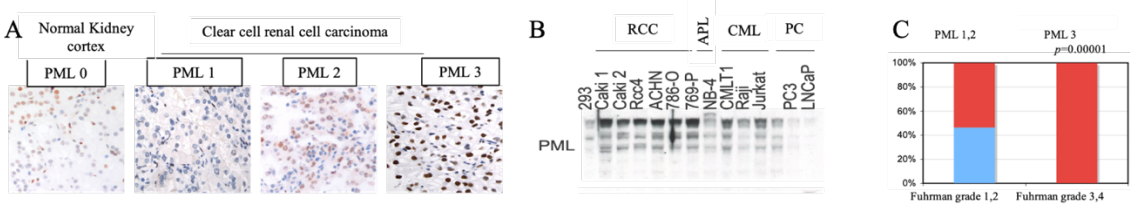


Figure 6. PML is overexpressed in ccRCC.
A. Immunohistochemistry results for PML expression in 5 human normal kidney cortexes and 36 ccRCC tissues. B. Western blot analysis of PML expression in cells lines of different origin (RCC, APL, CML, PC). 293: HEK-203T normal kidney cells; RCC: renal cell carcinoma; APL: acute promyelocytic leukemia; CML: chronic myeloid leukemia; PC: prostate cancer. C. Correlation analysis by Furnham grade's prediction.

1.5.2. The effect of PML silencing on ccRCC expansion in vitro and in vivo

To investigate the function of PML in ccRCC, *PML* was knocked down in three ccRCC cell lines (RCC4, Caki-1, A498) with specific *shRNA* constructs (*shPML#1* and *shPML#2*; Figure 7A, B).

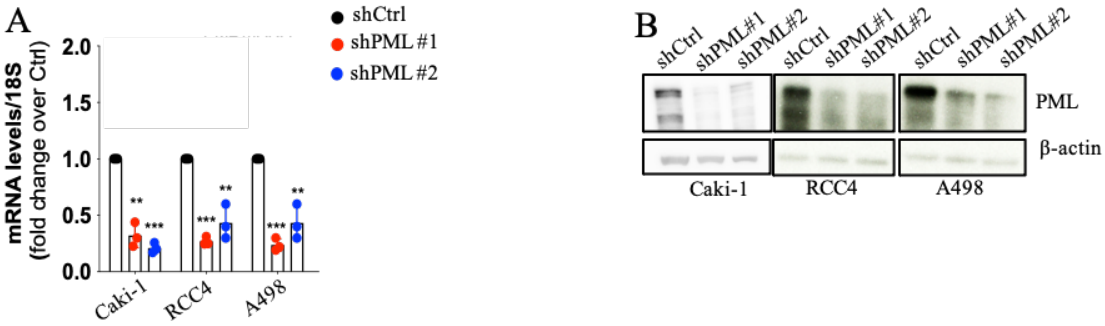


Figure 7. The efficiency of the Tet-On inducible system in silencing PML in ccRCC cell lines.
A. qRT-PCR showing mRNA expression levels in control (shCtrl) and PML-silenced (shPML) Caki-1, RCC4, A498 cell lines. B. Western blot analysis of PML expression in shCtrl and shPML Caki-1, RCC4, A498 cells. ß-actin was used as a loading control.

To test whether ccRCC rely on *PML* for *in vitro* expansion, a cell proliferation assay and focus forming assay were conducted. *PML* knockdown led to a significant decrease in cell proliferation and focus forming efficiency in all ccRCC cell lines (Figure 8A, B).

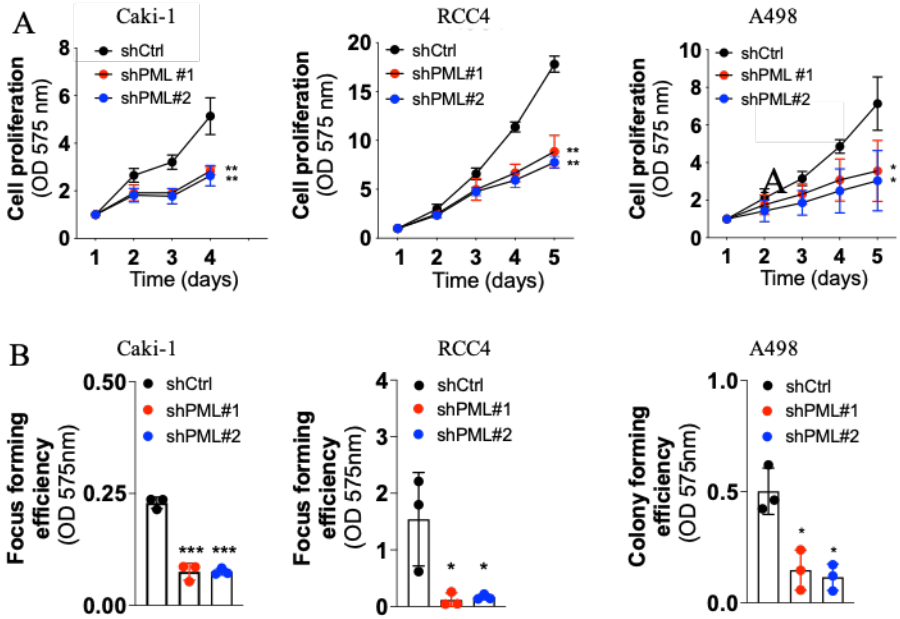


Figure 8. PML knockdown inhibits cell proliferation and survival capacity.
*A. Cell proliferation curves measured by crystal violet in shCtrl and shPML Caki-1, RCC4, A498. The values depict the ratio of optical density (OD) measured at 575 nm relative to day 1. B. Focus forming assay conducted in shCtrl and shPML Caki-1, RCC4, A498 over 14 days. Values were obtained by measuring OD at 575 nm. Statistics was performed using the Student's t-test (*p<0.05, **p<0.01, ***p<0.001).*

In order to test whether diminished cell proliferation was the consequence of cell cycle arrest, propidium iodide (PI) staining uptake assay was performed. This assay helped identify cell cycle distribution by FACS analysis. *PML* knockdown led to an increase of approximately 50 % of cells in G1 phase, indicative of cell cycle arrest in G0/G1 (Figure 9A, B, C).

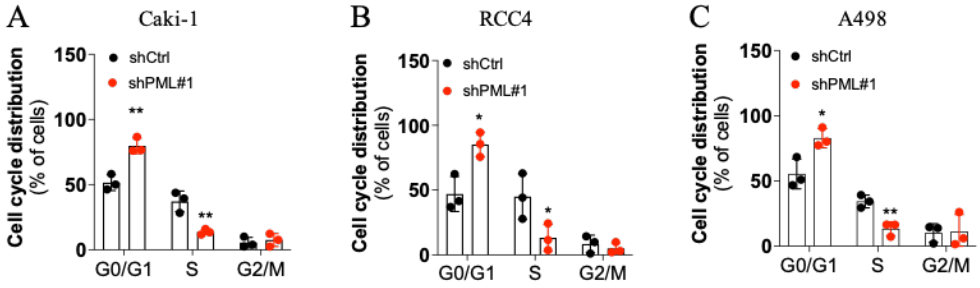


Figure 9. PML knockdown leads to cell cycle arrest in G0/G1 phase.
*FACS analysis of cell cycle distribution in cell cycle phases (% of cells) of shCtrl and shPML (A) Caki-1, (B) RCC4, (C) A498 at 96 hours. Statistics was performed using the Student's t-test (*p<0.05, **p<0.01, ***p<0.001).*

Taken together, these results suggest that PML is a driver of cell proliferation and cell cycle progression in ccRCC. Together with its increased expression and correlation with higher tumor grade, these observations point to an oncogenic function of PML in this disease.

Next, the effect of PML loss was evaluated *in vivo*. Immunocompromised mice were injected subcutaneously with inducible *shCtrl* and *shPML* ccRCC cells. Only Caki-1 and A498 were used since these cells had been previously reported to be engrafted in immunocompromised mice (Brodaczewska *et al*, 2016). After a period of three weeks following the administration of doxycycline, tumors originating from A498 and Caki-1 began to exhibit diminished *in vivo* growth upon *PML* silencing (Figure 10A). These findings provide clear evidence that *PML* silencing leads to a delay in *in vivo* tumor growth. To investigate whether the observed decrease in volume and weight resulting from *PML* depletion was associated with reduced cell proliferation, immunohistochemistry (IHC) analysis of Ki67 proliferation marker expression was conducted in *shCtrl* and *shPML* tumors. This analysis revealed a decrease in the number of actively proliferating cells in the *PML* silencing condition compared to the control (Figure 10B).

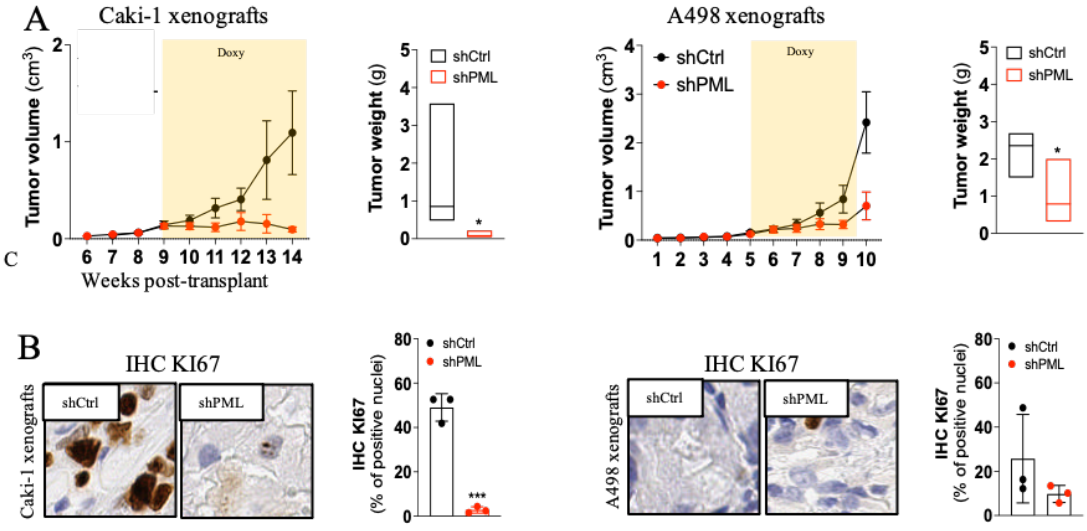


Figure 10. PML silencing causes tumor shrinkage in vivo.
*A. Growth curve analysis of tumors derived from Cak1-1 and A498 following administration of doxycycline. On the left side of each growth curve tumor weight is represented. B. Ki67 immunohistochemistry (IHC) in shCtrl and shPML Caki-1 and A498-derived tumors. Images were captured at 60x magnification. Data is presented as mean values with the standard error of the mean (SEM). Statistics was determined using Student's t-test (*p<0.05).*

1.5.3. The effect of PML silencing on p53 and HIF transcription factors in ccRCC

At the molecular level, cell cycle progression is controlled by checkpoints mediated by cyclins, CDKs and tumor suppressors such as p21 and p53 (Herranz & Gil, 2018). Given our discovery of PML's significant involvement in facilitating cell cycle advancement and cell proliferation in ccRCC cells, we sought to investigate the cause of such phenotype. Specifically, we hypothesized that cell cycle arrest at G1 phase was linked to the increased expression of p53 and p21 proteins. Notably, our observations revealed that *PML* silencing resulted in a marked up-regulation of both p53 and p21 (Figure 11A, B, C). These findings indicate that the inhibition of PML profoundly disrupts cell cycle progression by elevating the levels of p53 and p21 in ccRCC.

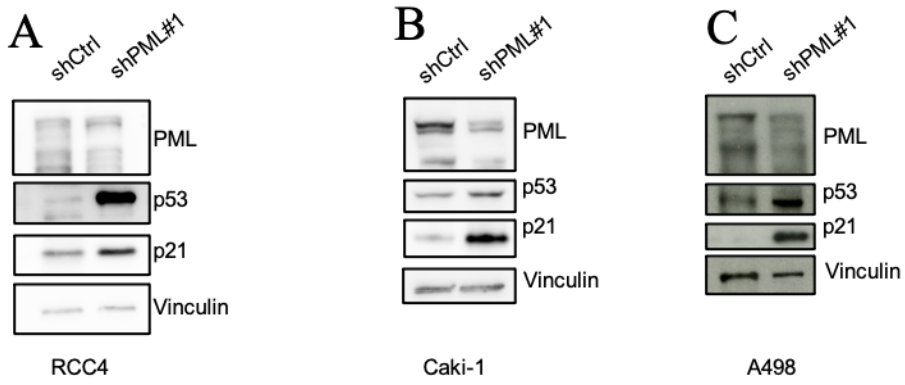


Figure 11. PML silencing causes p53 and p21 upregulation.
Western blot analysis of p53 and p21 expression in shCtrl and shPML (A)RCC4, (B)Caki-1, (C) A498 cell lines. Vinculin was used as a loading control.

Previous research has shown that PML collaboratively regulates a specific subset of HIF1α pro-metastatic target genes in TNBC, suggesting a potential physical association between PML and HIF1α at their regulatory regions (Ponente *et al*, 2017). Furthermore, we showed that PML promotes ccRCC proliferation, a function strongly associated with HIF2α in ccRCC (Biswas *et al*, 2010).

Therefore, in order to test whether PML regulates HIF1α and HIF2α expression in ccRCC, both mRNA and protein levels of HIF1α and HIF2α were measured upon *PML* silencing. Interestingly, we observed that *PML* silencing caused decreased HIF2α expression level both at *mRNA* and protein levels (Figure 12A), while HIF1α expression

increased (Figure 12B), indicating that PML regulates HIF1α and HIF2α in opposite manner in ccRCC.

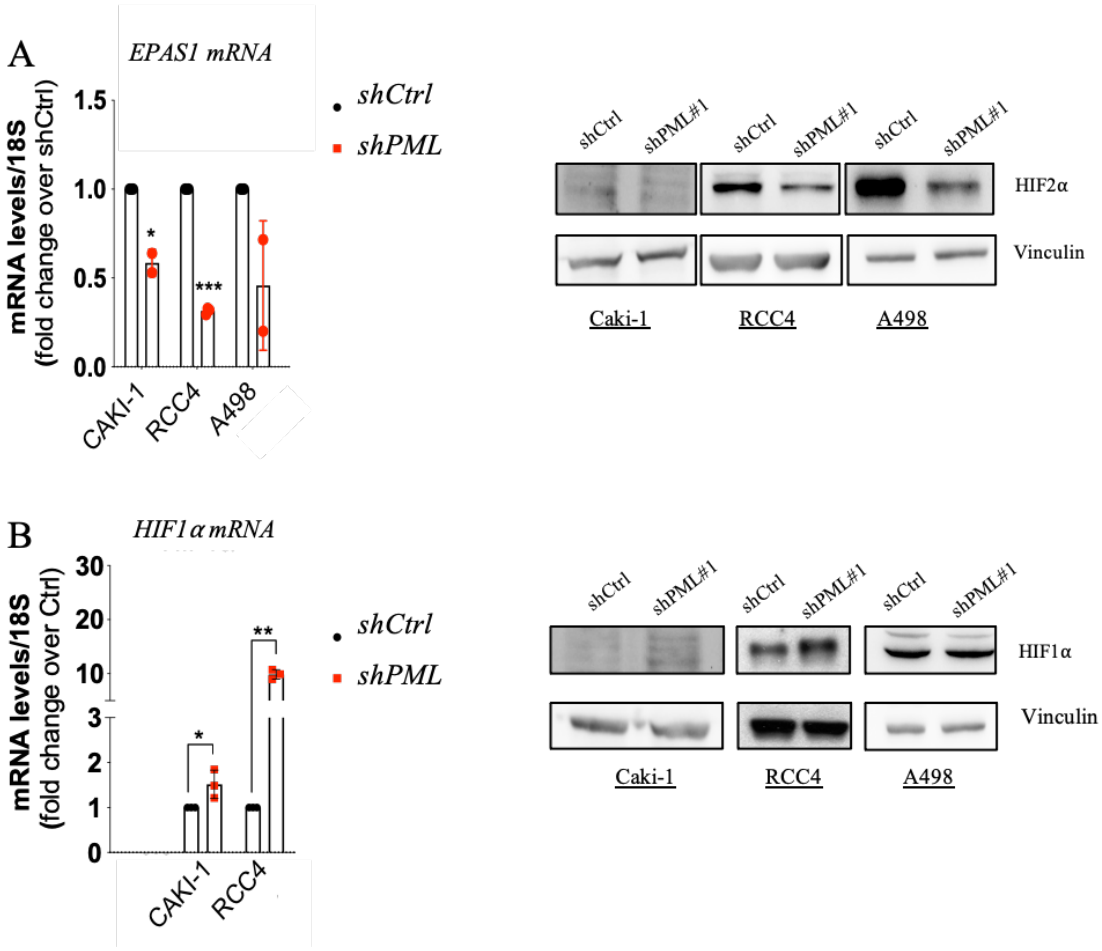


Figure 12.PML silencing causes HIF1α upregulation and HIF2α downregulation
A. qRT-PCR and Western blot analysis of EPAS1/HIF2α expression in shCtrl and shPML Caki-1, RCC4, A498 cell lines. B. qRT-PCR and Western blot analysis of HIF1α expression in shCtrl and shPML Caki-1, RCC4, A498 cells. Vinculin was used as a loading control in WB.

Chapter 2. AIM OF THE WORK

Until very recently, the role of PML in ccRCC has been a subject of contention. One published study suggested a tumor suppressive activity, while more recent studies aimed at identifying novel prognostic biomarkers in ccRCC revealed that PML is overexpressed in ccRCC and correlates with poorer survival outcomes. Our preliminary investigations align with these observations, indicating overexpression of PML in tumor tissues compared to normal kidney cortex and its association with higher tumor grades.

Consistent with these findings, our *in vitro* experiments demonstrated that *PML* knockdown impairs cell proliferation by regulating cell cycle progression. Inducing *PML* knockdown in ccRCC cells resulted in growth arrest, accompanied by the upregulation of tumor-suppressors p53 and p21. These observations prompted inquiries into whether PML's role in cell proliferation is sustained during tumor progression and whether the observed cell cycle arrest is indicative of a senescence phenotype. Furthermore, the molecular mechanisms underlying PML's function in this context remain to be elucidated, with a potential link to HIF regulation. Preliminary evidence suggesting that PML represses HIF1α expression and induces HIF2α expression raised the hypothesis that the HIF2α could serve as a direct link between PML expression, p53 upregulation, and enhanced cell proliferation. To address these questions, we have outlined the following research aims:

2.1. AIM 1. Define the function of PML in ccRCC progression;

2.2. AIM 2. Analyze the gene expression network upon *PML* silencing in ccRCC cells;

2.3. AIM 3. Explore the molecular mechanisms of PML-mediated control of proliferation.

Chapter 3. RESULTS

3.1. AIM 1. Define the function of PML in ccRCC progression

3.1.1. Bioinformatics analysis reveals PML overexpression in ccRCC

Previous results obtained in the laboratory of Dr. Bernardi showed that PML is overexpressed at the protein level in 56 specimens of ccRCC when compared to adjacent normal kidney tissue ("Preliminary data", Figure 6). However, these data contrast with a published report showing that PML is downregulated in ccRCC samples as opposed to normal kidney tissue (n=36) by immunohistochemistry (Lin *et al*, 2014).

Because divergent immunohistochemistry results may occur due to the use of different antibodies, we analyzed PML expression at the *mRNA* level in deposited datasets of ccRCC patients.

By interrogating the The Cancer Genome Atlas consortium (TCGA) from the University of Alabama at Birmingham CANcer data analysis portal (UALCAN), we observed that *mRNA* expression of *PML* is significantly increased in ccRCC tumor samples (Kidney Renal Clear Cell Carcinoma (KIRC) compared to normal tissue in (Figure 13A). Importantly, analysis of mass spectrometry-based proteomics data obtained from the Clinical Proteomic Tumor Analysis Consortium (CPTAC) available on UALCAN portal confirmed that PML protein expression is increased in ccRCC primary tumors compared to normal adjacent kidney tissue (Figure 13B). Therefore, these data confirm our previous immunohistochemical analysis with both *mRNA* data and an antibody-independent method to detect PML protein in tumor samples.

To assess whether PML overexpression may be caused by mutations that abolish its normal turn-over, we took advantage of the public cBioPortal database and found that *PML* is infrequently mutated in ccRCC tumor tissues (0.2% out of 445 tumor tissues cases). Taken together, these data indicate that PML in overexpressed in ccRCC via transcriptional upregulation.

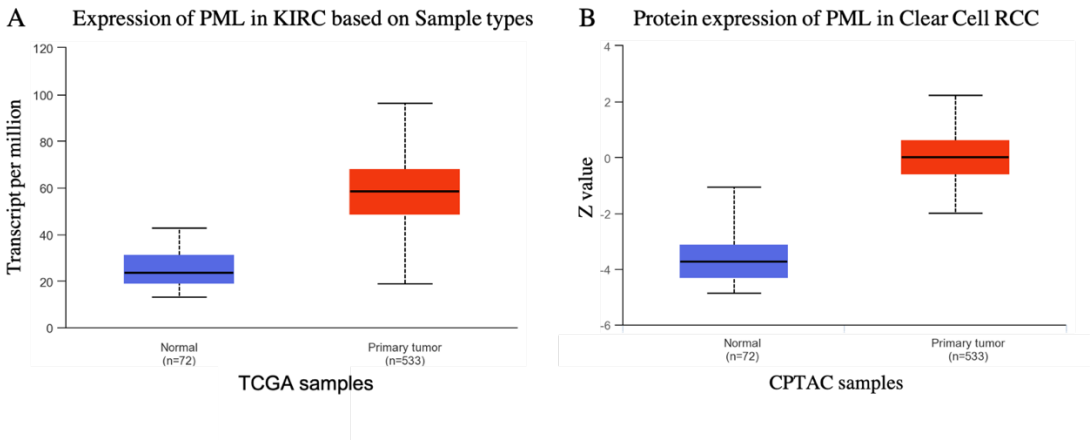


Figure 13.Bioinformatics analysis of PML mRNA and protein expression in ccRCC compared to adjacent normal tissue.
A. mRNA Expression of PML in KIRC based on TGCA samples. B. Protein expression levels of PML in ccRCC based on CPRAC samples. TCGA-KIRC and CPTAC *data is available on the UALCAN online database.*

Because *PML* has been described as either a tumor suppressor gene or an oncogene in different tumors contexts, we next took a general view of PML expression levels across a variety of tumor types. With this aim, we used the integrated database TNMplot, which contains RNA-seq data from TCGA, Therapeutically Applicable Research to Generate Effective Treatments (TARGET), and The Genotype-Tissue Expression (GTEx) repositories. This analysis confirmed previous literature by showing that depending on the tumor context, *PML* is either overexpressed or downregulated in the tumor counterpart with respect to normal adjacent tissue (Figure 14A, bold- and normal-lined boxes respectively). Of note, beside ccRCC, this analysis confirmed PML overexpression in ovarian cancer, where a pro-oncogenic function for PML was suggested (Liu *et al*, 2017) and other tumors such as esophagus, stomach and pancreas, where the function of PML has not been yet addressed fully. Moreover, it confirmed that PML is downregulated in lung cancer, where it was reported to act as a tumor suppressor (Kuo *et al*, 2014), and other tumors, such as prostate cancer (Kuo *et al*, 2014; Yuan *et al*, 2011; Wu *et al*, 2014; Kuwayama *et al*, 2009).

Importantly, analysis of *PML mRNA* expression in cancer cell lines of the Cell Line Encyclopedia revealed that *PML* overexpression is highest in renal cell carcinoma, adding further support to our preliminary data about an oncogenic function of PML in this tumor type (Figure 14B). Even though in ccRCC tumor samples PML expression was not higher than in other tumors (Figure 14A), we reasoned that cell lines represent the transformed

cell population, while tumor samples contain a mixture of tumor and stromal populations that may confound this analysis. In addition, tumor samples contain a mixture of patients at different tumor stages and undergoing different treatments, which may also account for increased variability and difference with cell line data. Nonetheless, these data confirmed that PML is overexpressed in ccRCC with respect to normal kidney tissue.

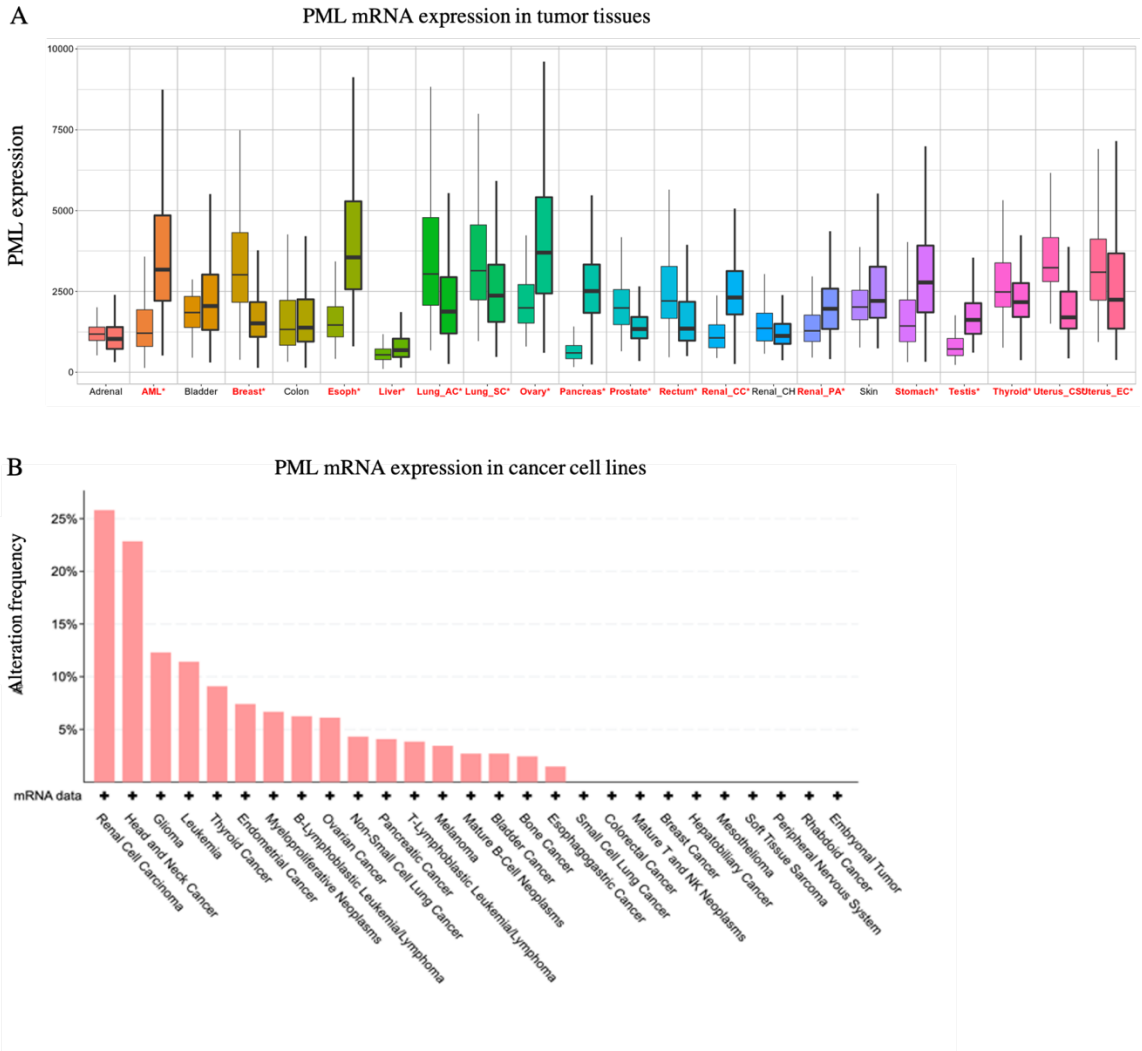


Figure 14.Comparative analysis of PML expression across tumor types.
A. Boxplot showing the range of PML mRNA expression across all tissues in both normal and tumor RNA-Seq datasets (TNMplot). For this analysis, TNMplot database was used. B. Alteration frequency of PML mRNA expression across different cell line in the cancer cell encyclopedia project (cBioPortal). Number of cell lines: Renal cell carcinoma; n=31, in red; Head and neck cancer; n=35; Glioma n=93; Leukemia n=48; Thyroid cancer; n=11; Endometrial cancer; n=27. Myeloproliferative neoplasms; n=15; B-Lymphoblastic Leukemia/Lymphoma; n=17. Ovarian cancer; n=64; NSCLC Non-small cell lung cancer; n=163; Pancreatic cancer; n=57;

T-Lymphoblastic Leukemia/Lymphoma; n=37; Melanoma n=106; Mature B-Cell neoplasia; n=112; Bladder n=44. Bone cancer; n=89; Esophagogastric cancer; n=84.

Finally, PML expression was correlated with survival data obtained from the publicly available datasets "Online consensus Survival analysis for KIRC" (OSkirc). Patients with ccRCC (KIRC) were stratified in high- and low-PML expression via *mRNA* analysis to measure survival. According to this analysis high PML expression correlates significantly with shorter overall survival (Figure 15). Therefore, elevated PML expression may serve as an indicator of an unfavorable prognosis in KIRC patients. Of note, after we produced this analysis, three independent publications implicated PML as a prognostic marker in ccRCC (Wang *et al*, 2023)(Wu *et al*, 2023)(Luo et al., 2023).

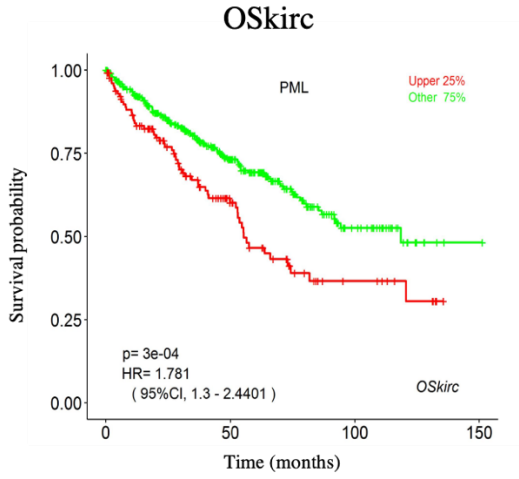


Figure 15.Survival probability of PML expression along time.
A. Kaplan Meier curve of overall survival of KIRC patients. A total of 629 KIRC patients from combined data sources (TCGA, GSE22541, GSE29609, and GSE3) were subjected to survival analysis with the patients split by "upper 25%" option. The KM curves of overall survival of KIRC patients were plotted along with the log-rank p-value and hazard ratio (HR).

To conclude this analysis, we also investigated the correlation between *PML mRNA* expression and the clinical characteristics of KIRC patients using UALCAN. PML expression showed no significant associations with patients age, race, or gender in samples of the TGCA dataset (Figure 16A, B, C), indicating that increased PML expression does not distinguish specific patients' categories.

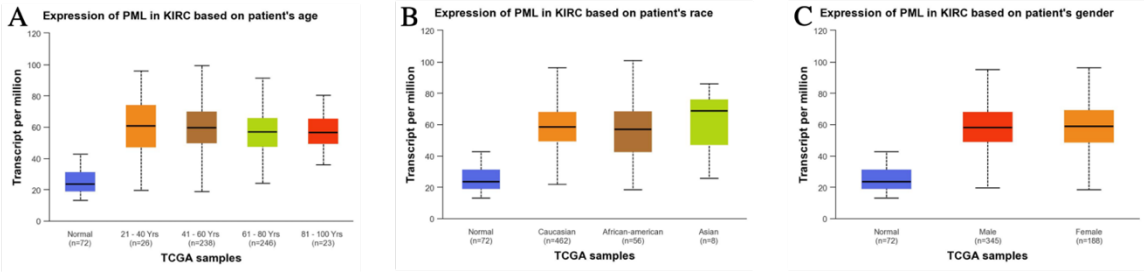


Figure 16.Correlation between PML expression and age, race and gender.
A. Boxplot representing mRNA expression of PML in KIRC based on patient's age. B. Boxplot representing mRNA expression of PML in KIRC based on patient's race. C. Boxplot representing mRNA expression of PML in KIRC based on patient's gender.

In summary, comprehensive analysis of PML expression in clear cell renal cell carcinoma (ccRCC) has provided significant confirmatory observations. Initial laboratory findings showed that PML is overexpressed at the protein level, as observed by immunohistochemistry and Western Blot analysis in ccRCC tumor samples and cell lines. These more recent bioinformatics studies corroborated these results by demonstrating elevated PML *mRNA* and protein expression in tumor samples through extensive data analysis. Notably, we found minimal *PML* mutations in ccRCC, suggesting that its overexpression is primarily driven by transcriptional upregulation.

3.1.2. Evaluating the effect of long PML silencing in RCC4 cells

In an effort to delineate the functional role of PML in ccRCC, in my laboratory it was recently observed that suppressing PML expression in ccRCC cell lines resulted in cell cycle arrest ("Preliminary data", Figure 8) accompanied by morphological changes typical of senescence, but not by β-galactosidase accumulation (data not shown). To understand if the proliferation arrest induced by *PML* knockdown is a stable phenotype, and to assess if prolonged *PML* inhibition may lead to β-galactosidase expression, we induced *PML* silencing in RCC4 with doxycycline exposure for 13 consecutive days by using a 3T3 passaging protocol where cells were replated every 3 days and doxycycline was continuously added to the culture medium. We chose the RCC4 cell line as it is the one that harbored the strongest phenotypes upon *PML* silencing. As control cells, to investigate whether PML's role in promoting cell proliferation was specific to ccRCC, we examined its impact on the proliferation of a breast cancer cell line, MDA-MB-231,

where PML has been identified as an oncogene in previous research (Arreal *et al*, 2020; Carracedo *et al*, 2012;Martín-Martín *et al*, 2016).

We first evaluated PML expression by Western Blot analysis upon 13 days in culture, and confirmed the efficacy of our *shRNA* induction protocol (Figure 17A). Importantly, in agreement with our earlier short-term silencing results, prolonged *PML* suppression led to accumulating reduction in cell proliferation compared to control cells (Figure 17B). These data confirmed that PML expression is necessary to maintain ccRCC cell proliferation and demonstrated that the phenotype is not reversed upon prolonged *in vitro* culture. One of the triplicates, independent experiments shown in Figure 17B was prolonged for up to a month in culture, and even in these conditions we did not detect reversal of the growth arrested phenotype, further showing that PML depletion induces a stable growth arrest in RCC4 cells (data not shown). To determine whether reduced cell proliferation was a result of cell death, we assessed the extent of apoptosis through trypan blue exclusion assay. There was no difference in the proportion of cell death population between dead and live cells, as indicated by the similar and low percentage of dead over live cells found in both conditions (approximately 0.5 %) (Figure 17C). The data on proliferation is even more significant when compared to the effect of *PML* silencing on MDA-MB-231 cells, where *PML* depletion with two independent *shRNAs* (Figure 17D) did not significantly affect cell proliferation (Figure 17E). Our results are consistent with published data where a moderate effect of *PML* silencing on MDA-MB-231 proliferation was reported (Arreal *et al*, 2020). However, because PML was reported to exert oncogenic functions in TNBC cells, we performed a focus forming assay to assess the ability of individual cells to form colonies upon *PML* silencing. In this setting, we observed decreased colony formation upon *PML* silencing, albeit significant only for *shPML* #1 (Figure 17F).

In conclusion, our data demonstrate that *PML* silencing causes reduced cell proliferation over a long period of time and that this phenotype is specifically relevant to ccRCC cells.

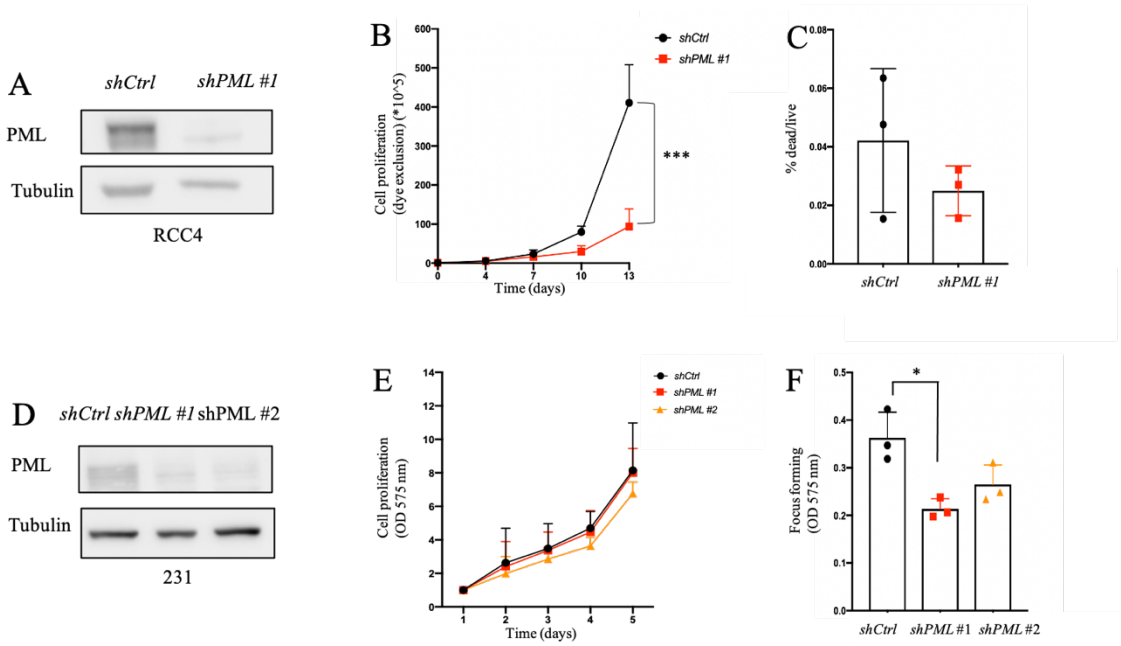


Figure 17. PML silencing drives stable growth arrest.
*A. Western blot showing PML expression in control RCC4 cells (shCtrl) and PML-silenced RCC4 cells (shPML). Tubulin was used as a loading control. B. Cell proliferation curve of shCtrl and shPML RCC4 performed using 3t3 protocol assay over 13 days. Values represent number of cells obtained by trypan blue dye exclusion assay. C. Barplot illustrating the percentage of dead RCC4 cells relative to live RCC4 cells at day 13. D. Western blot showing PML expression in control MDA-MB-231 cells (shCtrl) and PML-silenced MDA-MB-231 cells (shPML). E. Cell proliferation curve of shCtrl and shPML MDA-MB-231 cells over 5 days, expressed as optical density (OD)at 575 nm. F. Barplot illustrating focus forming efficiency of MDA-MB-231 cells expressed as optical density (OD)at 575 nm. Statistical significance was calculated using two-tailed, paired Student's t-test. *P<0.05, **P<0.01.*

3.1.3. The effect of PML silencing on senescence

Cell cycle arrest at the G0 phase, reduced proliferation, elevated levels of p53 and p21, and other senescence-like characteristics, such as changes in cell morphology (not shown), all indicate the presence of a senescence-like phenotype upon *PML* silencing. However, staining with the classical senescence marker senescence-associated β-GAL (SA-β-GAL) up to 4 days upon *PML* silencing did not lead to increased SA-β-GAL positive cells (not shown). Thus, to understand whether the observed phenotype indeed represents senescence and not an alternative state like quiescence, we examined SA-β-GAL positivity at longer time upon *PML* silencing (day 13) with a widely used histochemical test that measures hydrolysis of 5-bromo-4-chloro-3-indoyl-β-D-galactopyranoside (X-gal) by the β-GAL enzyme at pH 6.0. This reaction results in the formation of a dark blue, insoluble precipitate within the cultured cells. Remarkably,

strong SA-β-GAL staining was observed following *PML* silencing, in contrast to the control condition where the staining was less intense and less prevalent (Figure 18A). Quantitative analysis confirmed that RCC4 cells exhibited more pronounced labeling upon *PML* silencing compared to their respective control (Figure 18B).

In conclusion, with these experiments where PML depletion was prolonged in time, we were able to demonstrate that PML is essential to RCC4 cells propagation and its inhibition induces cellular senescence. We hypothesized that positivity for SA-β-GAL is not detected at earlier time points because it needs to accumulate over a specific threshold in the lysosomes of growth-arrested cells before being measurable with this assay.

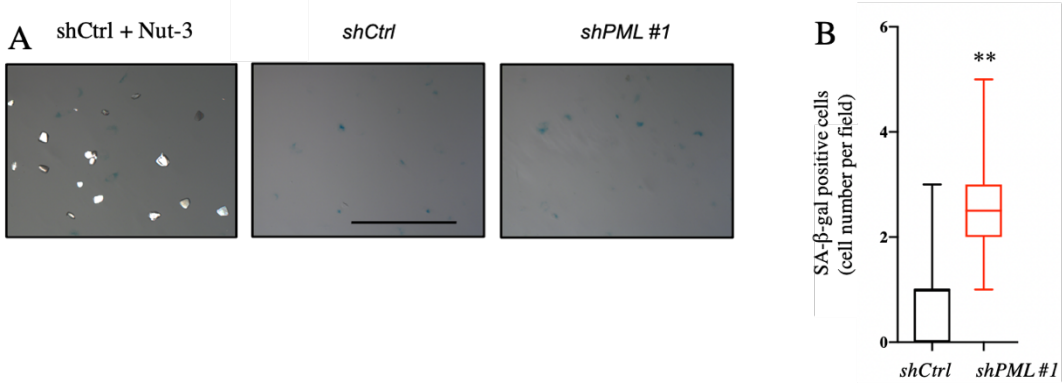


Figure 18. PML silencing cause senescence in vitro.
*A. SA-β-gal staining performed in control RCC4 cells (shCtrl) and PML-silenced RCC4 cells (shPML) 13 days after doxycycline (100 ng/ml) treatment (scale bar: 50 µm at 10x magnification). B. Boxplot showing quantification of SA-β-gal-stained cells in shCtrl and shPML. Statistical significance was calculated using two-tailed, unpaired Student's t-test. *P<0.05, **P<0.01.*

3.2. AIM 2. Global analysis of gene expression regulation upon PML silencing in ccRCC cells

3.2.1 Defining the effect of PML silencing on the RCC4 transcriptome

Our *in vitro* investigations have provided evidence of PML's involvement in the proliferation and progression ccRCC. This is a yet unreported function of the *PML* gene, which albeit acting as an oncogene in specific tumor contexts was never described as essential to promote tumor expansion. Thus, to elucidate the underlying molecular mechanisms connecting PML to the observed phenotypes, we conducted an unbiased experiment of RNA sequencing following *PML* knockdown in RCC4 cells. We chose this cell line for several reasons, including the wide characterization of PML-induced phenotypes that we have performed in the laboratory, as well as reported and publicly

available transcriptional changes occurring upon manipulation of HIF transcription factors (Arnaiz *et al*, 2021)(Smythies *et al*, 2019).

We found that *PML* knockdown resulted in differential expression of 2192 genes, of which 936 were upregulated (FC>1.5, padjvalue<0.05) and 1256 were downregulated (FC<1.5, padjvalue<0.05) (Figure 19).

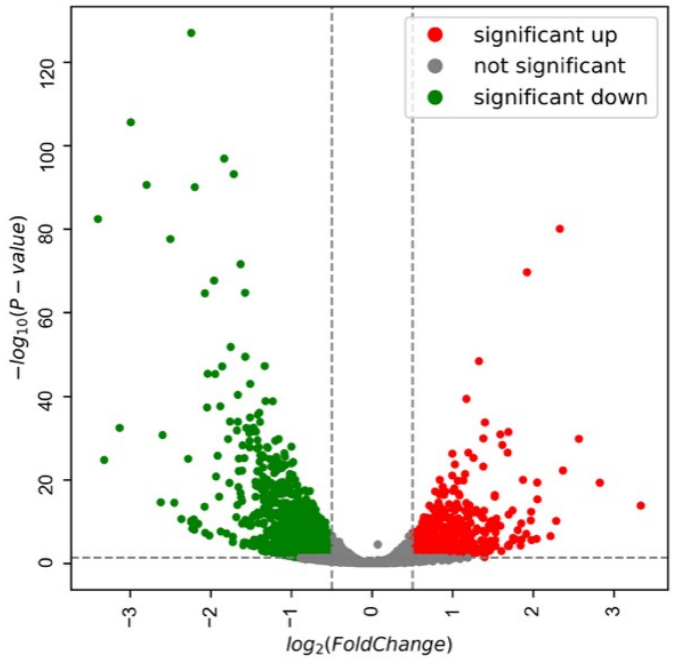


Figure 19. PML silencing induces altered mRNA expression of 2192 genes.
Volcano plot illustrating genes that are differentially expressed in PML-silenced RCC4 (shPML) relative to their control 96 hours after PML silencing. Each red dot represents a gene that is significantly upregulated upon PML silencing and each green dot is a gene that is downregulated upon PML silencing. The fold enrichment is calculated as the log2 of the fold change, with a cutoff value of 0.5 applied. Plot was constructed using Python.

To gain insights into cellular processes regulated by PML, we performed gene set enrichment analysis. In order to functionally annotate PML-regulated genes and identify pathways that are significantly enriched, we clustered the differentially expressed genes (DEGs) using the EnrichR online tool (Kuleshov *et al*, 2016). This tool employs statistical tests based on Fisher's exact test, applies a false discovery rate (FDR) correction of 0.05, and sets a p-value cutoff of 0.05. The Fold Enrichment metric is defined as the ratio of genes within our list belonging to a particular pathway compared to the corresponding ratio in the background, which consists of all protein-encoding genes in the genome. FDR

informs us about the likelihood of the observed enrichment happening by chance. To obtain a comprehensive overview of the broader biological processes and functions associated with our gene list, we merged information from four databases: WikiPathway, MSigDB_Hallmark, KEGG, REACTOME and Gene Ontologies. These databases are curated, ensuring that they encompass the most current data. After identifying significant gene families enriched within genes downregulated upon *PML* silencing, we grouped these families according to similarity and utilized a color code for visualization (Figure 20).

Our analysis revealed that the top 20 enriched pathways predominantly include processes related to cell cycle, DNA replication, mitosis and proliferation (Figure 20). This analysis aligns with the observed phenotype of cell cycle arrest and decreased proliferation induced by PML silencing both *in vitro* and *in vivo*. Embedded within these families, we found E2F target genes, genes linked to the G2/M and mitotic spindle checkpoints, again emphasizing a significant transcriptional alteration associated with the cell cycle.

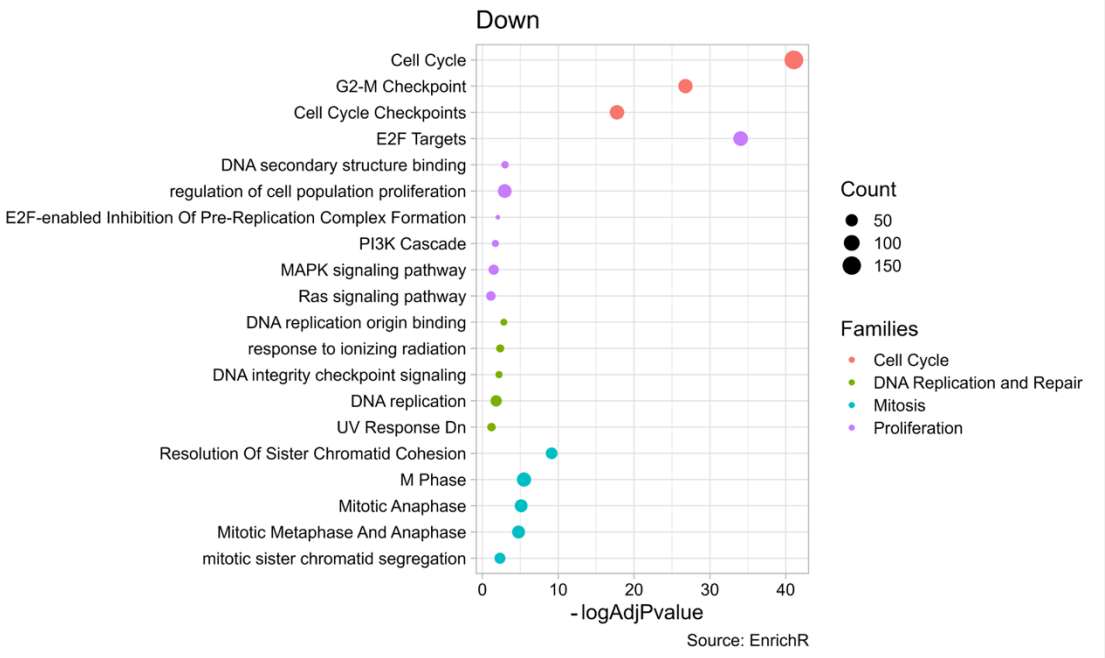


Figure 20. PML silencing causes downregulation of pathways related to cell cycle and proliferation.

Dotplot displaying the most significant enriched pathways and ontologies for genes downregulayed upon PML silencing in RCC4 relative to control. Functional enrichment analysis was performed using EnrichR. Databases used comprised of Reactome, KEGG, MSigDB_Hallmark, WikiPathway, and Gene Ontologies. Data was first filtered by P value < 0.1. Plots were constructed using ggplot2 library in R (https:// ggplot2.tidyverse.org/). Gene count refers to the number of genes positively regulated by PML and that are contained in the

pathway/ontology indicated. Each family is highlighted with a different color. Fold enrichment is calculated by the minus logarithm of the Adjusted P value.

We then analyzed the pathways that were most enriched within genes upregulated upon PML silencing. These were also grouped based on similarity of functions and revealed a more complex scenario and distinct functional groups. Specifically, we found that PML inhibits the expression of genes related to the following functions: cholesterol biosynthesis, extracellular matrix remodeling, inflammation and interferon signaling, mTORC pathway, senescence and TGF-beta pathway (Figure 21). It's worth highlighting that this contradicts previous findings in TNBC, where PML was observed to positively control the activation of proteins involved in ECM degradation, consequently amplifying the invasion capabilities of breast cancer cells (Ponente *et al*, 2017).

Some of these gene set terms, such as senescence and autophagy, lysosomes and p53 signaling are clearly in line with the senescence-like phenotype observed *in vitro* (Figure 21). Thus, this unbiased analysis confirmed that *PML* depletion induces senescence in RCC4 cells. Of note, RNA-sequencing was performed at 4 days upon induction of PML silencing, when SA-β-GAL is not detected via standard assays. However, the upregulation of genes linked to senescence confirms that the process is already initiated, and detection of SA-β-GAL may be related to low abundancy of this specific enzyme in RCC4 cells at this time point.

Besides induction of senescence genes, we found an enrichment in other gene sets that were already described as regulated by PML in different cell types. These include cholesterol biosynthesis and mTORC signaling. Published literature has already shown that PML suppresses cholesterol biosynthetic pathways in liver, white adipose tissue and skeletal muscle as well as in prostate cancer (Chen *et al*, 2018; Cheng *et al*, 2013). Our data thus confirm PML involvement in cholesterol biosynthesis also in RCC4 cells, albeit the functional consequence of this upregulation towards the phenotype induced by PML in this tumor context is currently unknown. We hypothesized that because RCC4 cells show expansion of lysosomes and degradative organelles (observed via immunofluorescence and electron microscopy, data not shown), increased membrane biosynthesis may be triggered to support lysosome expansion. However, this hypothesis remains to be validated.

Increased expression of genes related to PI3K-Akt-mTOR signaling can be also explained based on published literature indicating that PML inhibits Akt and mTORC1 signaling in other tumor contexts (Bernardi *et al*, 2011; Trotman *et al*, 2006). However, it is presently unclear how the upregulation of these pathways may contribute to the growth suppressive phenotype observed upon PML inhibition.

Finally, we noted that the upregulation of other pathways including extracellular matrix organization, responses to inflammatory cytokines and TFG-beta (Figure 21) may also appear counterintuitive, based on the oncogenic functions of PML in this tumor context. However, we reasoned that senescent cells often exhibit increased expression of genes related to cell mobility and migration and as part of the senescence-associated secretory phenotype (SASP), they release cytokines and chemokines into their microenvironment, promoting inflammation-mediated pathways (Krtolica *et al*, 2001; Coppé *et al*, 2008).

Other prominently enriched signaling pathways included with TNF signaling via NF-kB and KRAS signaling which have established connections with senescence (Figure 21) (Mijit *et al*, 2020; Pillai *et al*, 2017; Lee *et al*, 2022; Yu *et al*, 2015; Tyciakova *et al*, 2021; Flor *et al*, 2017).

Therefore, taken together the analysis of genes whose mRNA expression changed significantly upon *PML* silencing confirmed the phenotype of cell cycle arrest and senescence observed *in vitro.*

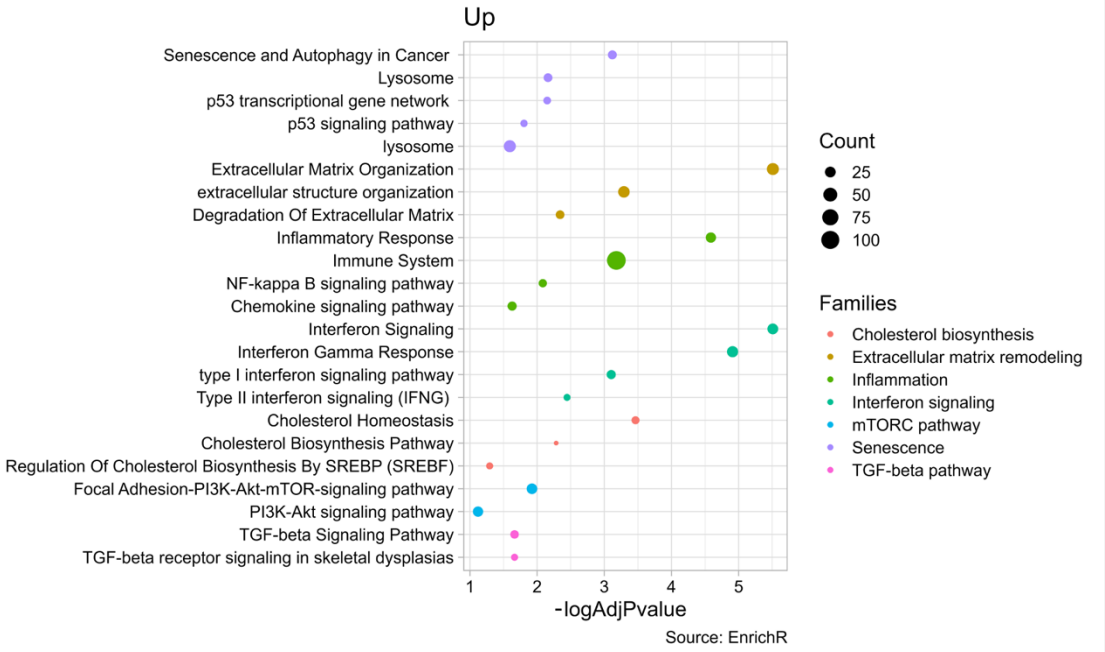


Figure 21. PML silencing causes upregulation of pathways related to senescence and inflammation

Dotplot displaying the most significant enriched pathways and ontologies for genes upregulated upon PML silencing in RCC4 relative to control. Functional enrichment analysis was performed using EnrichR, Databases used comprised of Reactome, KEGG, MSigDB_Hallmark, WikiPathway, and Gene Ontologies. Data was filtered using P value < 0.1. Plots were constructed using ggplot2 library in R (https:// ggplot2.tidyverse.org/). Gene count refers to the number of genes that are negatively regulated by PML and that are contained in the pathway/ontology indicated. Each family is highlighted with a different color. Fold enrichment is calculated by the minus logarithm of the Adjusted P value.

3.2.2. Comparisons of gene expression changes induced by PML silencing in RCC4 with other studies

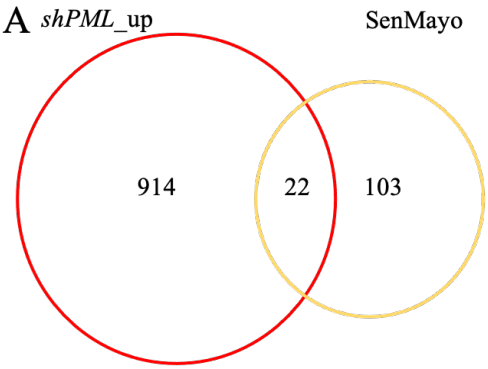
Our *in vitro* experiments, coupled with bioinformatics analysis of RNA sequencing data, have yielded substantiating evidence supporting the existence of a senescence phenotype regulated by the p53 pathway following *PML* silencing in RCC4. While the precise molecular indicators defining senescent cells remain to be meticulously delineated, there is a consensus within the scientific community regarding some discernible characteristics commonly associated with senescence. To discern the presence of classical senescence markers within our RNA sequencing data we searched the literature for broader and more analytic transcriptional and translational methods for identifying SASP. With this in mind we decided to overlap our list of upregulated genes with SenMayo, a transcriptomic-based dataset that identified 125 genes commonly regulated in a broader collection of senescence-associated signatures, not only from

fibroblasts but also from other primary, immortalized and cancer human cell lines and tissues (Saul *et al*, 2022). The SenMayo dataset primarily encompassed SASP factors, totaling 83 elements, alongside 20 transmembrane and 22 intracellular proteins. Moreover, cytokines and chemokines exhibited the highest degree of connectivity as regulators, as determined by the number of downstream proteins identified in the STRING analysis. After overlapping SenMayo with PML negatively-regulated genes we identified 22 common genes (Figure 22A). Importantly, most of these genes included metalloproteinases, such as MMP1, MMP9, MMP10 and cytokines, such as CXCL1, CXCL2, CXCL3, CXCL8 that were described in the study as SASP (Figure 22B, red-colored). These 22 genes are involved in pathways such as lipid, inflammatory response, TNF-alpha signaling via NF-kB, further demonstrating their known involvement in senescence program (Figure 22C).

Of note, overlap with SenMayo analysis further demonstrated that the transcriptional differences that we recorded upon *PML* silencing are not unique to epithelial ccRCC cells undergoing senescence but are common, at least in part, to different cell types.

Thus, this analysis confirmed that the phenotype of senescence observed *in vitro* is strongly underpinned by increased expression of senescence associated genes and most importantly SASP in *shPML* RCC4. These findings help us explain why gene signatures that are normally associated to tumor progression (cell migration/extracellular matrix remodeling) or tumor progression (immune signatures) are upregulated in conditions of suppressed growth conditions, as they probably relate to phenotypic features of senescent cells.

A



B 22 genes in common

Gene	log2FC	AdjPvalue	-logAdjPvalue
PLAT	2.37	6.4E-23	22.20
CTSB	0.89	4.5E-17	16.35
ITGA2	1.52	1.2E-16	15.92
ICAM1	0.67	1.1E-11	10.96
ANGPTL4	2.29	7.4E-11	10.13
C3	0.79	1.0E-09	9.00
IGFBP7	0.59	5.1E-09	8.29
PLAU	0.88	9.6E-08	7.02
TUBGCP2	0.61	1.1E-06	5.96
IL6ST	0.52	1.4E-06	5.87
MMP10	2.04	1.5E-06	5.83
FAS	0.71	1.5E-06	5.82
IL1B	1.43	1.9E-05	4.72
PTGES	1.69	6.8E-05	4.17
MMP9	1.17	2.8E-03	2.56
IL18	0.97	1.6E-02	1.81
SEMA3F	0.60	2.1E-02	1.68
CXCL1	0.68	2.6E-02	1.58
CXCL2	0.74	2.7E-02	1.57
CXCL3	1.02	3.2E-02	1.49
CXCL8	0.96	3.6E-02	1.45
MMP1	0.62	4.4E-02	1.36

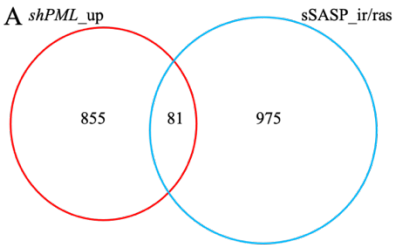
C Common pathways

Pathway/Ontology	Adjusted P-value	-logAdjPvalue
Lipid and atherosclerosis	9.55E-13	12.01992608
Rheumatoid arthritis	2.41E-12	11.61796072
Legionellosis	5.67E-12	11.24618595
Coagulation	2.71E-11	10.56649307
IL-17 signaling pathway	1.61E-10	9.793773676
NF-kappa B signaling pathway	2.65E-10	9.576438822
TNF-alpha Signaling via NF-kB	2.71E-10	9.566967423
Kaposi sarcoma-associated herpesvirus infection	3.05E-10	9.515017316
TNF signaling pathway	3.21E-10	9.493030662
Interleukin-10 Signaling R-HSA-6783783	7.66E-10	9.115880832

Figure 22. PML silencing causes upregulation of 22 senescence markers which are common to 15 transcriptomic studies of senescence.

A. Venn diagram showing overlapping genes between PML-negatively regulated genes and SenMayo gene set. B. Tables lists 22 genes found in A diplaying log2FC, Adjusted P value (AdjPvalue) and minus logarithm Adjusted P value (-logAdjPvalue) relative to differential expression of genes in shPML RCC4 compared to control RCC4 cells. Red: SASP. C. Table lists the most significant enriched term for the 22 common genes (-logPvalue>9).

To strengthen the concept that the SASP is an important signature of ccRCC cells upon PML suppression and to perform a comprehensive analysis of SASP proteins in our experimental conditions, we adopted a different approach by cross-referencing a published mass spectrometry-based quantification of SASP produced from fibroblasts or normal kidney cells exposed to different inducers of senescence (Basisty *et al*, 2020). We consulted the proteomic atlas of senescence-associated secretomes (SASP Atlas) to identify SASP components in our list of genes upregulated upon silencing of *PML*. Initially, we overlapped the list of SASP proteins elevated in human primary fibroblasts upon both irradiation and RAS with our list of genes upregulated in *shPML* RCC4. From the overlap we found 81 common soluble SASP factors (Figure 23A). Compared to the transcriptomic overlap discussed previously, this list included previously unidentified factors that were further interrogated for enriched pathways. This analysis highlighted that the top enriched pathways mostly related to ECM remodeling (Figure 23B).



B Common pathways

Pathway/Ontology	Adjusted P-value	logAdjPvalue
Extracellular Matrix Organization R-HSA-1474244	3.64E-14	13.43910753
Neutrophil Degranulation R-HSA-6798695	8.27E-10	9.082652692
Immune System R-HSA-168256	1.17E-07	6.931745464
Innate Immune System R-HSA-168249	3.29E-07	6.48273621
Interleukin-4 And Interleukin-13 Signaling R-HSA-6785807	8.63E-07	6.064126713
Laminin Interactions R-HSA-3000157	1.44E-06	5.841954959
ECM Proteoglycans R-HSA-3000178	4.17E-06	5.380122541
Signaling By Receptor Tyrosine Kinases R-HSA-9006934	4.17E-06	5.380122541
Assembly Of Collagen Fibrils And Other Multimeric Structures R-HSA-2022090	4.5E-06	5.346767055
Degradation Of Extracellular Matrix R-HSA-1474228	1.06E-05	4.976305006

Figure 23.. PML silencing causes upregulation of 81 soluble SASP which are related to inflammation and extracellular matrix organization.
A. Venn diagram showing overlapping of genes both negatively regulated by PML (our RNA sequencing) and defined as soluble SASP induced by ionizing radiation and expression of oncogene RAS (Basisty et al, 2020). B. Table lists pathways/ontologies enriched with the 81 genes found in A., along with Adjusted P value and minus logarithm P value (-logAdjPvalue) relative to differential expression of genes in shPML RCC4 compared to control RCC4 cells.

Taken together, these analyses strongly suggest that the senescence phenotype induced by *PML* silencing is accompanied by upregulation of SASP, and this might explain the counterintuitive upregulation of genes involved in cell migration and immune responses.

3.3. AIM 3. Explore the molecular mechanisms of PML-mediated control of proliferation

3.3.1. The role of p53 in cell proliferation in RCC4

So far, our data has demonstrated that PML acts as an oncogene in ccRCC, in fueling cell cycle progression and proliferation Moreover, we found that PML negatively regulates p53. Of note, ccRCC is a tumor type where p53 is rarely mutated, yet it is inhibited via poorly defined molecular mechanisms (Creighton *et al*, 2013; Amendolare *et al*, 2022) Therefore, we hypothesized that upregulation of p53 may be the main driver of cell cycle arrest. To test whether loss of p53 function was able to rescue the defect in cell proliferation in *shPML* RCC4 cells, we infected RCC4 cells with a retrovirus carrying a dominant negative p53 mutant (p53DD). This mutant was generated in the laboratory of Moshe Oren and has been widely used to inhibit wild-type p53 function (Chappell *et al*, 2012; Pires *et al*, 2013; Heyne *et al*, 2008). Similar to the long-term culture assays previously used to determine whether cell cycle arrest upon PML suppression is stable (Figure 17B), cell proliferation was assessed every third day until day 13 in RCC4 cells carrying *PML shRNA* with or without expression of p53DD (Figure 24A). Long induction of p53DD alone did not modify the proliferation rate of RCC4 cells (Figure 24A), supporting the view that wild-type p53 is not active in ccRCC cells, however it was sufficient to rescue proliferation in conditions of PML suppression, as demonstrated by measurements of cell number taken at the endo of the experiment (Figure 24B).

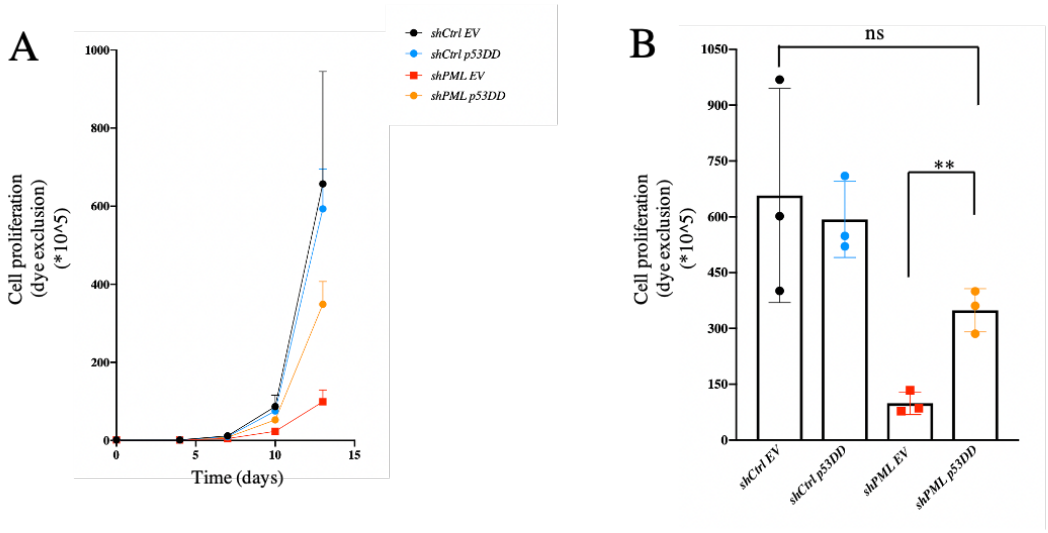


Figure 24. Loss of p53 function rescues proliferation.
*A. Cell proliferation curve of control RCC4 cells (shCtrl) and PML-silenced RCC4 (shPML) over 13 days performed using the 3t3 protocol. Data is expressed as number of cells * 10^5 counted by using the trypan blue dye exclusion assay. B. Boxoplot illustrating cell proliferation expressed as number of cells * 10^5 13 days after doxycycline-induced PML silencing. Statistical significance was calculated using two tailed, paired Student's t-test. *P<0.05, **P<0.01.*

This finding demonstrates a major role of p53 in mediating cell cycle regulation in *shPML* RCC4 and led us to begin investigate possible mechanisms of p53 regulation by PML. Understanding how PML may suppress p53 expression and function in the context of ccRCC is not an easy task, given the large amount of literature indicating that in pre-cancerous cells PML rather activates p53 and facilitates p53-induced senescence in apparent contradiction with our observations in ccRCC (Liebl & Hofmann, 2022). However, senescence has been described as a stress-responsive mechanism that cells utilize upon both expression or removal of oncogenes. For example, the *c-MYC* gene leads to oncogene-induced senescence when overexpressed in untransformed cells (Zindy *et al*, 1998) and oncogene removal-induced senescence when inhibited in fully transformed cancerous cells (Wu *et al*, 2007). Of note, both groups described these mechanisms as mediated by p53. Thus, we reasoned that p53-induced senescence upon PML inhibition may be caused by removal of proliferative, oncogenic forces stimulated by PML, thus leading to a form of oncogene removal-induced senescence. To identify which oncogenic pathway may lead to p53 activation when inhibited upon PML suppression we turned to HIF2α, a major oncogene in ccRCC (Schödel *et al*, 2016; Cuvillier, 2017) whose expression we had found to be positively regulated by PML

("Preliminary data", Figure 12A). Moreover, available literature showed that HIF2a suppresses p53 (Das *et al*, 2012; Bertout *et al*, 2009) thus providing a possible mechanism of p53 reactivation by *PML* downregulation.

3.3.2. The role of PML in the regulation of HIF2α-induced genes

We have observed that PML regulates HIF1α and HIF2α in an opposite manner, by leading to increased and decreased expression respectively (preliminary data). To understand whether regulation of HIFs expression by PML lead to functional consequences, we first measured expression of a few bona fide HIF1α or HIF2α target genes via RT-qPCR. We assessed the expression levels of a limited subset of target genes regulated by HIF1α, specifically those linked to glycolysis, and gene regulated by HIF2 encompassing those associated with proliferation (CD1, NDRG1) and self-renewal (Oct4, SOX2) (Forristal *et al*, 2010; Cho *et al*, 2016) In agreement with PML negatively regulating HIF1α and positively regulating HIF2α, we observed that HIF1α-target genes were upregulated upon *PML* silencing and HIF2α-target genes were suppressed (Figure 25AB).

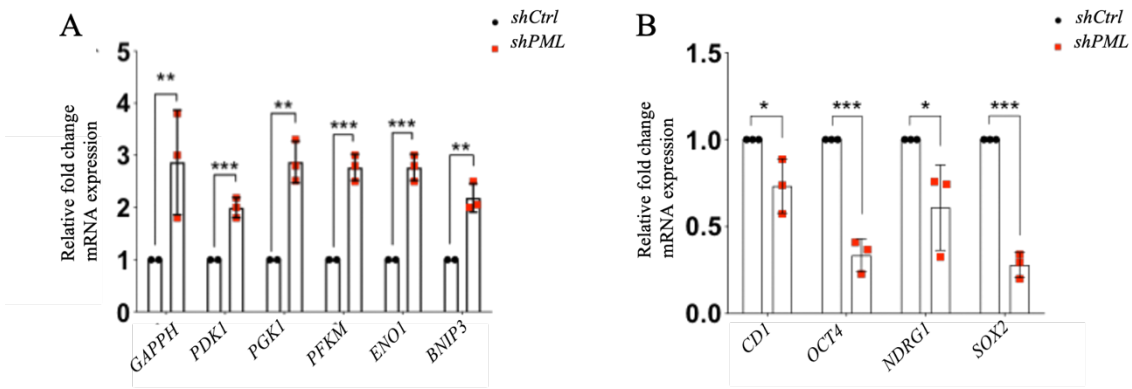


Figure 25. PML negatively regulates HIF1α -target genes and positively regulates HIF2α -target genes.
*Quantitative real time PCR (qrt-PCR) of mRNA expression levels of HIF1α-target genes (A) and HIF2α-target genes (B) in PML-silenced RCC4 cells (shPML) compared to control RCC4 cells (shctrl) 96 hours after doxycycline-induced PML silencing. Statistical significance was calculated using two-tailed, paired Student's t-test. *P<0.05, **P<0.01.*

On this basis, we decided to delve deeper into the functional interaction between PML and HIF2α. To determine whether PML shares co-regulated sets of genes with HIF2α, we compared the PML-regulated transcriptome with publicly available transcriptomic and ChIP sequencing data of HIF2α. First, we overlapped our list of downregulated genes (i.e., positively regulated by PML), with genes downregulated upon treatment of tumourgraft/patient-derived xenograft platform with the HIF2α inhibitor PT2399 (Chen *et al*, 2016). Of note, about half of the genes regulated upon HIF2α inhibition overlapped with genes positively regulated by PML (Figure 26A), and they were enriched for cell cycle pathways (Figure 26B). Moreover, some of these genes, involved in cell cycle control, DNA replication and DNA damage, exhibited high co-expression values when we compared their expression with PML in TCGA-KIRC dataset in cBioPortal (Figure 26C) (Fuchs *et al*, 2016).

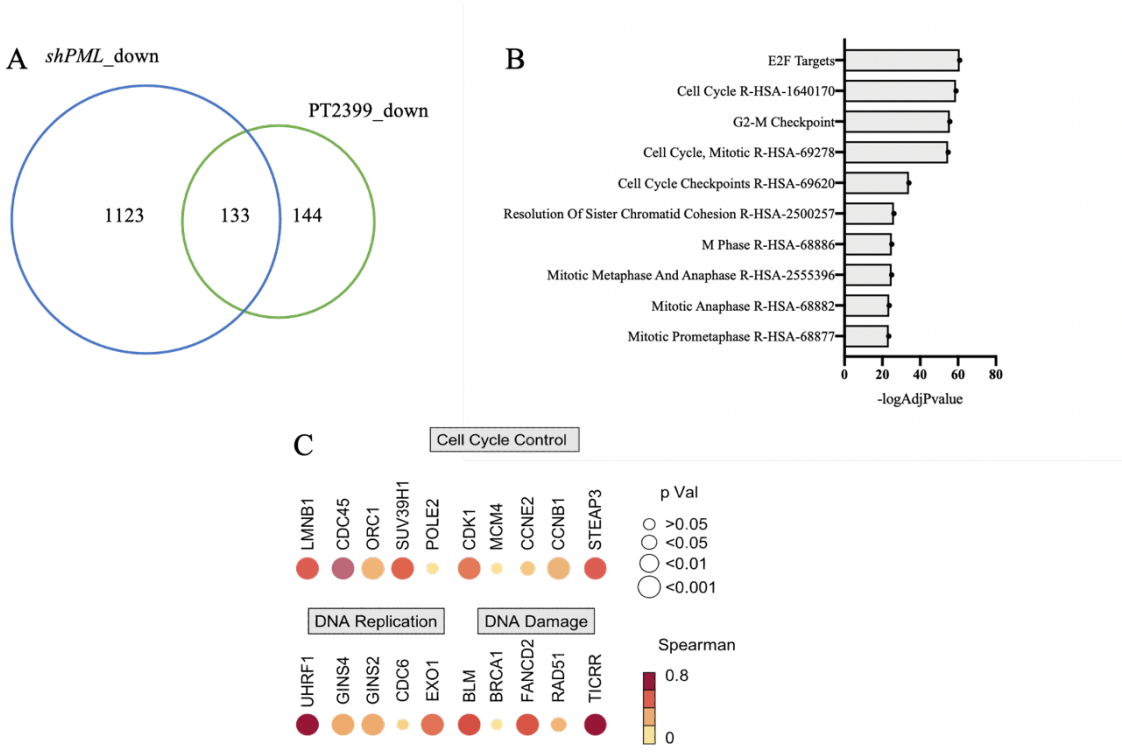


Figure 26. PML and HIF2α co-regulate genes that are involved in cell cycle and DNA replication in vivo

A. Venn diagram of overlapping genes that are both positively regulated by PML (our study) and downregulated upon treatment with PT2399 (Chen *et al*, 2016). *B. Barplot showing the pathways/ontologies enriched with genes identified in the overlap described above. C. Correlation analysis between some of the genes found by the overlap described above and PML in TCGA-KIRC dataset. Correlation analysis was performed on the CBioPortal online tool.*

Based on these results, we decided to further characterize the functional interaction between PML and HIF2α by overlapping PML-regulated genes with both transcriptomic and ChIP sequencing data available for HIF2α in other cell lines. These analyses will help us identify genes or pathways co-regulated by both PML and HIF2α. Patel and colleagues recently published a first ever characterization of *bona fide* early response HIF2α target genes by performing RNA sequencing on an HIF2α knock-out clone derived from the ccRCC 786-M1A cell line (Patel *et al*, 2022). By overlapping genes positively regulated by PML with genes that are repressed upon HIF2α knock-out 32 h after doxycycline removal we found an overlap of 137 genes (Figure 27A). These genes were enriched in terms linked to cell cycle, DNA replication and E2F targets (Figure 27B), further suggesting that PML and HIF2α co-regulate genes involved in cell cycle. Intriguingly, mass spectrometry analysis performed on HIF2α immunoprecipitates in the same study (Patel *et al*, 2022) identified PML as a HIF2α interactor, suggesting a physical and functional relationship between these proteins.

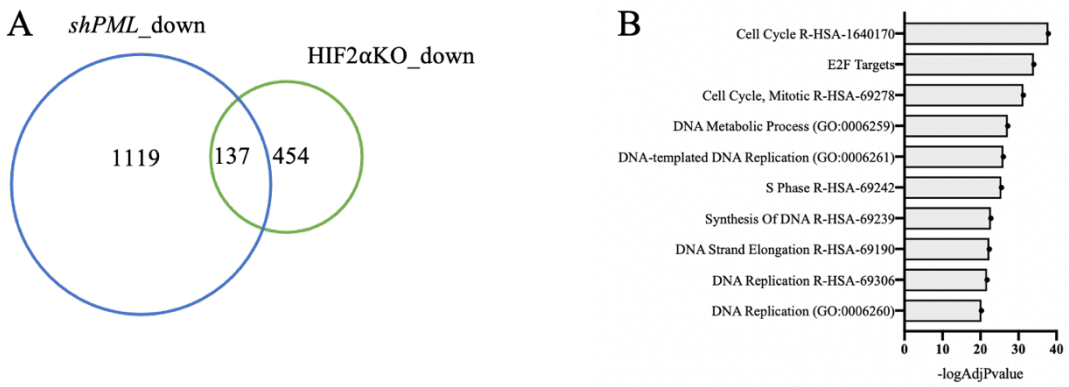


Figure 27. PML and HIF2α co-regulate genes that are involved in cell cycle and DNA replication in vitro.
A. Venn diagram of overlapping genes that are positively regulated by both PML (our study) and HIF2α (Patel et al, 2022). B. Barplot showing the top 10 most enriched pathways for genes identified to be co-regulated by both PML and HIF2α in ccRCC.

Next, in order to identify specifically those genes that are bound directly by HIF2α we compared the PML-regulated transcriptome with HIF2α ChIP-sequencing data available in RCC4 cells (Smythies *et al*, 2019). However, we found only few genes in common

(Figure 28). We reasoned that the little overlap between genes positively regulated by PML and bound by HIF2α may be due to the fact that HIF2α preferentially binds enhancers regions (Smythies *et al*, 2019), which escape precise gene mapping in ChIP-sequencing data in the absence of 3D chromatin analysis. Along these lines, despite the very important function of HIF2α in this tumor, only 249 genes were mapped as *bona fide* HIF2α targets in this study (Smythies *et al*, 2019). Therefore, potential regulatory relationships between HIF2α and other genes may be hindered by lack of proper mapping of physical chromatin loops between promoter-enhancer and enhancer-enhancer. Enrichment analysis of the few genes was not significant due to the few genes overlapping, each playing diverse functions by being involved in a range of cellular processes, including metabolism, development, signal transduction, and cellular structure (data not shown). Therefore, we hypothesize that PML regulates HIF2α-target genes promoting cell cycle progression through HIF2α binding to yet unidentified enhancers.

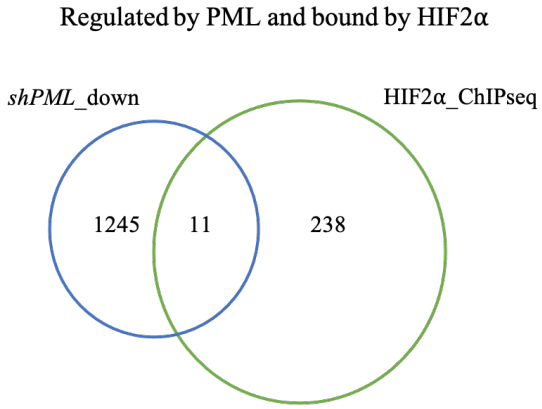


Figure 28.PML regulates few genes that are bound by HIF2α.
Venn diagram of the overlapping genes that are both positively regulated by PML (our study) and bound by HIF2α (Smythies et al, 2019).

3.3.3. HIF2α rescue experiments in RCC4 cells upon PML silencing

The identification of genes involved in cell cycle progression that are co-regulated by both HIF2α and PML, together with evidence of HIF2α being positively regulated by PML ("Preliminary data", Figure 12A), prompted us to test whether PML promotes cell proliferation and suppresses p53 activity via HIF2α. To do this, we developed overexpression systems to induce HIF2α expression in RCC4 cells upon *PML* silencing,

a condition where we previously observed decreased HIF2α levels ("Preliminary data", 12A). We first used a constitutive system to express high levels of HIF2α via retroviral-mediated infection of wild-type RCC4 cells with a plasmid containing shRNA against HIF2α. The latter was then transduced with lentiviral vectors carrying inducible control or PML specific *shRNAs*. RCC4 cells were infected with an empty vector (RCC4-EV) or a vector carrying a mutant HA-HIF2α that is not subjected to proteasomal degradation (RCC4-H2). First, to validate the system, cells were immunoblotted with anti-HA and anti-HIF2α antibodies to confirm overexpression (Figure 29A). Secondly, we assessed whether HIF2α overexpression induced any changes in cell proliferation in RCC4. We did not observe any difference in cell proliferation upon HIF2α activation, which is coherent with RCC4 cells being *VHL* mutant and expressing high baseline levels of HIF2α (Figure 29B). To understand whether exogenously expressed HIF2α could rescue the growth arrest induced by PML suppression, we infected RCC4-EV and RCC4-HIF2α with lentiviral vectors carrying either a control shRNA (*shCtrl*) or a PML-specific *shRNA* (*shPML*) using the TetON system. However, cell proliferation assays suggested that PML was not silenced in this system, as we did not observe a proliferation defect (Figure 29C). This is likely due to the fact that both viral vectors were carrying the same antibiotic resistance cassette.

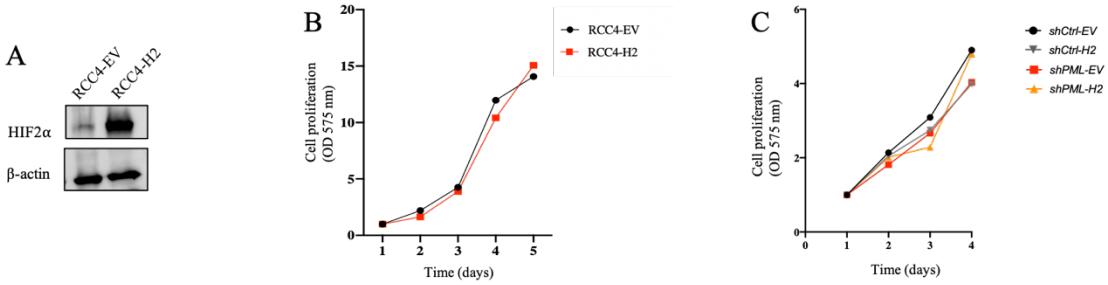


Figure 29. Retroviral-mediated infection of wild-type RCC4 cells with two plasmids expressing a mutant HA-HIF2α and shRNAs against PML failed to provide an HIF2α overexpression system.

A. Western blot analysis of HIF2α protein levels in RCC4 cells expressing an empty vector (RCC4-EV) and RCC4 cells expressing a plasmid carrying a mutant HA-HIF2α (RCC4-H2). B. Cell proliferation curve of RCC4-EV and RCC4-H2 over 5 days performed by crystal violet staining. Data is expressed as optical density at 575 nm. C.. Cell proliferation curve of shCtrl-EV, shCtrl-H2, shPML-EV, shPML-H2 over 4 days performed by crystal violet staining. Data is expressed as optical density at 575 nm. Statistical analysis used two-tailed, paired Student's T-test.

Because we failed to subclone PML and control *shRNAs* in a lentiviral vector carrying a different antibiotic resistance gene (data not shown), to attempt to answer our question we decided to use a different strategy.

To induce HIF2α overexpression in RCC4 cells with a second approach, we took advantage of a recently published method where protein overexpression can be induced by inducing alternative splicing of a transduced construct with LMI070 (Figure 30A) (Smythies *et al*, 2019). A stable HIF2α mutant was synthesized and cloned in a bidirectional lentiviral vector, which was then used to transduce RCC4 *wt* cells. Infection efficiency was measured by flow cytometry using an antibody against the aNGFR APC and cells were sorted by magnetic selection of transduced cells expressing CD271. Then, similar to the non-inducible system described above, RCC4 cells were infected with either a lentiviral vector carrying either *shCtrl* or *shPML*. Validation of the system was confirmed by Western Blot, where cells carrying HA-HIF2α expressed a HIF2α protein with higher molecular weight compared with the respective empty vectors (Figure 30B). Importantly, *PML* silencing was maintained in this system. Consistent with the previous model, HIF2α overexpression did not affect cell proliferation in shCtrl RCC4 cells (Figure 30C). However, overexpression of HIF2α not only did not rescue the defect in proliferation caused by *PML* silencing, but led to further decrease of cell proliferation in shPML cells (Figure 30C). We currently do not have an explanation for these findings. We hypothesized that RCC4 cells with reduced PML expression and higher p53 activity may be sensitized to the toxic effect of the drug used to induce HIF2α splicing and expression in this system. Consistently, we observed increased cell death upon PML suppression and HIF2α induction (data not shown). Alternatively, increased expression of exogenous HIF2α in a cellular system where the protein is already stabilized due to *VHL* mutations may lead to toxic effects that are particularly evident when the PML-dependent stress responsive system is removed.

In conclusion, although these experiments did not exclude that PML may utilize HIF2α to induce proliferation in ccRCC cells, they suggest that the growth arrest induced by PML depletion does not depend on suppression of HIF2α expression.

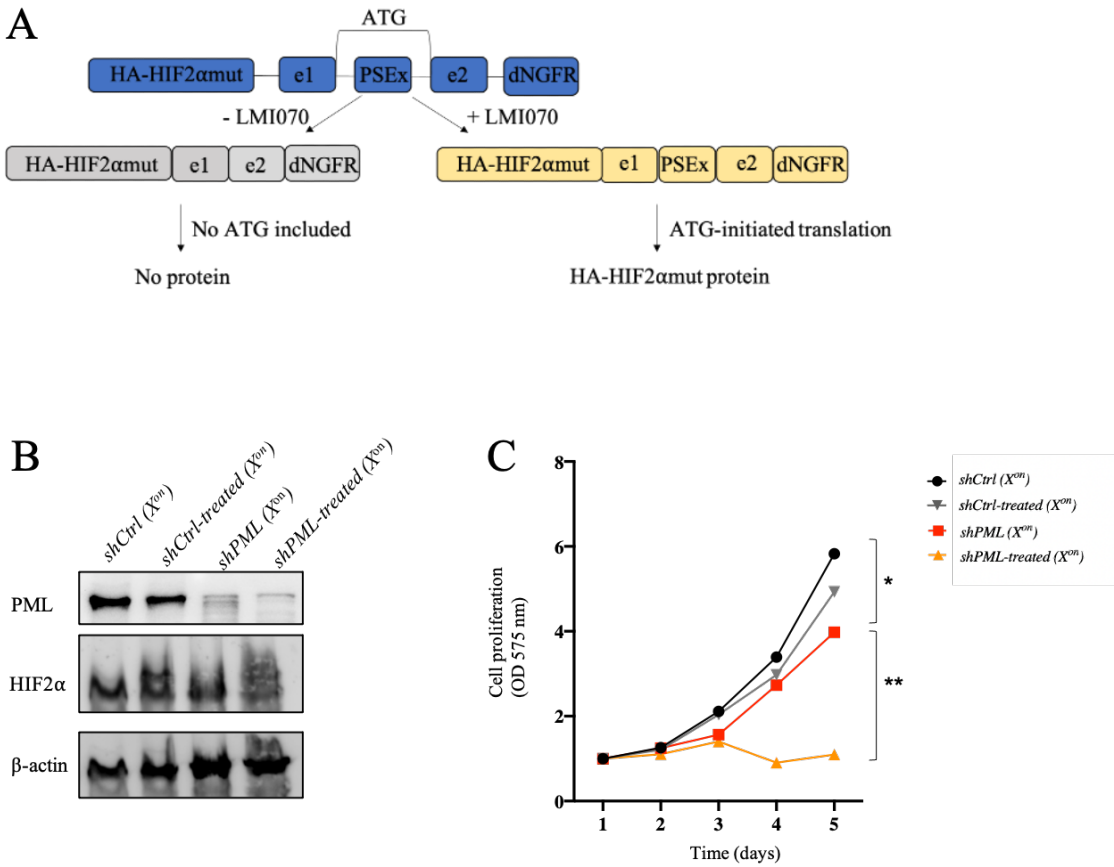


Figure 30. HIF2α overexpression does not rescue proliferation.
*A. Western blot analysis of HIF2α and PML protein levels upon LMI070-induced expression of exogenous HIF2α. β-actin was used as a loading control. B. Cell proliferation curve of shCtrl RCC4 and shPML RCC4 treated with LMI070 or treated with DMSO (controls) to induce or not, respectively, ATG-initiated translation of HIF2α a mRNA. Statistical analysis used two-tailed paired Student's T-test. *P<0.05, **P<0.01.*

To further investigate this aspect, we assessed the impact of *EPAS1* (HIF2α) gene silencing on cell proliferation in RCC4 and A498 cell lines. A498 cells were included in this study due to their specific overexpression of only HIF2α and not HIF1α. Both RCC4 and A498 cells were transduced with shRNA targeting *EPAS1 (shEPAS1*), and transduction effectiveness was verified (Figure 31A). However, HIF2α silencing had no discernible effect on cell proliferation in either RCC4 or A498 cells (Figure 31 C, D). To further validate these observations, we examined whether prolonged exposure to HIF2α would have any impact on cell proliferation; First we tested whether HIF2α inhibition was maintained at day 16 of infection by Western blot (Figure 31E).

However, even after prolonged HIF2α inhibition proliferation remained unaffected (Figure 31F).

These observations are in line with published literature, which indicates that silencing of HIF2α does not impact cell proliferation in ccRCC RCC4 cells (Arnaiz *et al*, 2021; Wallace *et al*, 2016). When analyzed in comparison to our data on PML, these experiments suggest that suppression of PML may have a more relevant effect than HIF2α suppression. However, our data have compared the effect of PML and HIF2α only *in vitro*, and more detailed analysis of *in vivo* effects, will need to be performed to reach this conclusion.

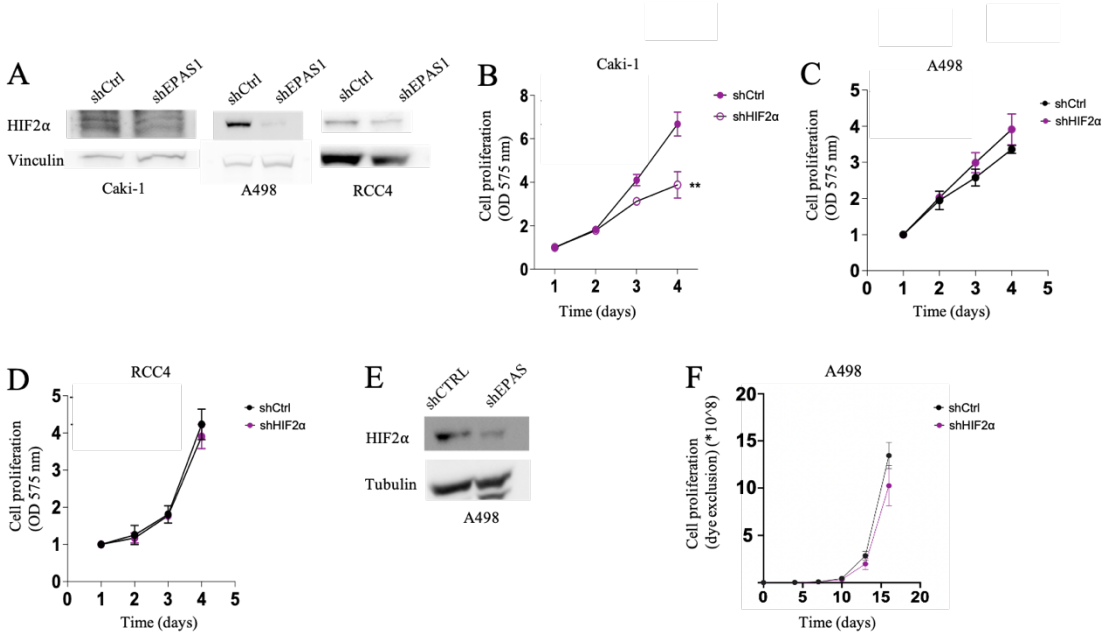


Figure 31. HIF2α silencing does not affect cell proliferation in RCC4 and A498.
*A. Western blot analysis of HIF2α protein levels in RCC4 cells expressing a scramble plasmid (shCtrl) or expressing a plasmid carrying a mutant HA-HIF2α shRNA against HIF2α (shEPAS1). B, C, D. Cell proliferation curve of RCC4, Caki-1 and A498 expressing either shCtrl or shEPAS1 over 5 days performed by crystal violet staining. Data is expressed as optical density at 575 nm. E. Western blot analysis of HIF2α protein levels in A498 cells expressing a scramble plasmid (shCtrl) or expressing a plasmid carrying a mutant HA-HIF2α shRNA against HIF2α (shEPAS1) at day 16 of proliferation curve. F. Cell proliferation curve of A498 expressing either shCtrl or shEPAS1 over 16 days performed by crystal violet staining. Data is expressed as optical density at 575 nm. Statistical analysis used two-tailed paired Student's T-test. *P<0.05, **P<0.01.*

In summary, the lack of rescue upon HIF2α overexpressing in RCC4 cells following PML silencing and the lack of significant effects on cell proliferation in RCC4 and A498 cells upon *EPAS1* silencing suggest that HIF2α alone is not sufficient to mediate cell

proliferation in ccRCC and is likely not implicated in phenotypes induced by PML depletion.

3.3.4. The effect of arsenic trioxide on ccRCC in vitro

Many studies showed that HIF2α inhibition, either via genetic or pharmacologic strategies, does not affect cell proliferation *in vitro.* Because our results showed that PML silencing causes cell cycle arrest, we aimed at testing the effect of pharmacological inhibition of PML on ccRCC proliferation by conducting experiments using arsenic trioxide *in vitro* and *ex vivo*, using RCC4 cells and PDX-derived cells models (XP258). With the idea of constructing a cellular system where we could test the cooperativity of PML inhibition and additional compounds, we introduced the Luciferase gene into RCC4 and XP258 cells. We then set up an experimental procedure on 96-well plate where luciferase activity is measured as a proxy of cell numbers. Luciferase expression is measured at seeding time (time 0) and at day 2, when treatment with different concentrations of arsenic trioxide is started for 72 hours (day 5). Treatment with ATO at all concentrations reduced significantly the proliferation of RCC4 and XP258 PDX-derived cells (Figure 32A, B). In RCC4 cells we observed a drastic effect of ATO at all doses (Figure 32A), including doses much lower than the standard concentration of 1μM that is used for leukemia cells. On the contrary, proliferation in XP258 xenographs was reduced in a dose-dependent manner (Figure 32B). Importantly, this assay enabled us to verify whether arsenic trioxide also induced cell death. Indeed, 72 hours after treatment with ATO RCC4 cells were less numerous than at the day of treatment, indicating cell death upon treatment (Figure 32A). On the contrary, although less than controls XP258 PDX-derived cells kept growing upon treatment with ATO, suggesting that ATO slowed cell proliferation without affecting cell death (Figure 32B).

Taken together these results indicate that ATO mimics *PML* silencing and promotes cytostatic and cytotoxic effects in ccRCC cell models.

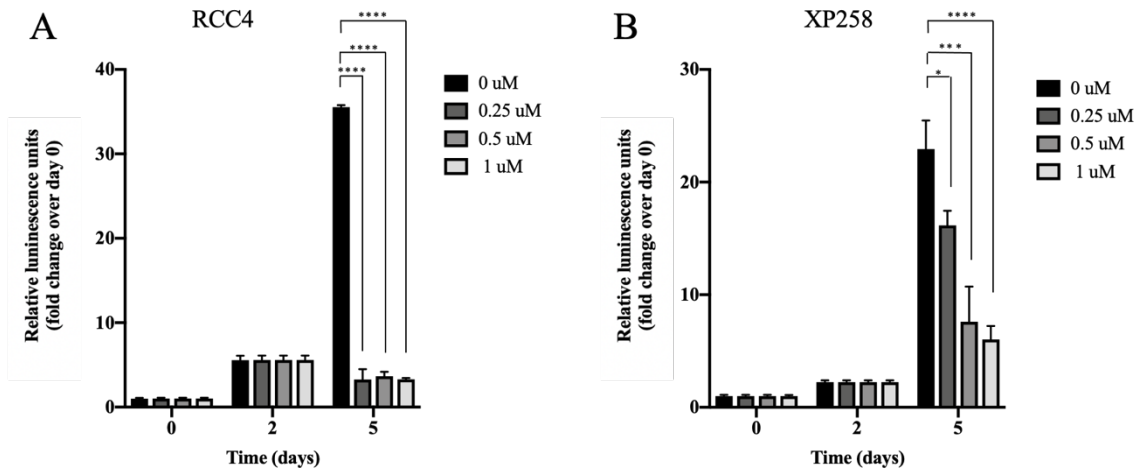


Figure 32.Arsenic trioxide (ATO) treatment inhibits cell growth in ccRCC
*Barplot showing the effect of ATO in RCC4 (A) and XP258 (B) cells 72 hours after treatment. Statistics was performed using the Student's t-test (*p<0.05, **p<0.01, ***p<0.001, ****p<0.0001).*

3.3.5. The identification of putative transcription factors regulating pathways downstream of PML

In our pursuit to identify PML-mediated mechanisms of senescence suppression and increased proliferation, we decided to investigate transcription factors that exhibit enriched binding to genes either upregulated or downregulated upon PML silencing. To gain a more comprehensive view of the regulatory landscape, we leveraged multiple publicly available gene set libraries, such as ChEA, ENCODE TRRUST, TRANSFAC and JASPAR that contain information about transcriptional regulatory relationships explore in the literature, available ChIP-sequencing data of transcription factors and predictions of binding motifs and regulatory elements associated with the genes(Lachmann *et al*, 2010; Khan *et al*, 2018; Han *et al*, 2015; Wingender *et al*, 2000) After following removal of duplicates, epigenetic factors and proteins that do not act directly as transcription factors, we compiled a list of 33 transcription factors exhibiting significant enrichment in genes positively regulated by PML ("DOWN"). We then grouped these TFs into two major superfamilies based on the major role they play, these being cell cycle and cell proliferation (Figure 33). It's worth highlighting that certain member of the E2F family, specifically E2F1, E2F4, and E2F6, manifested the most statistically significant enrichment and the highest count of genes among all the transcription factors examined (indicated by arrows in Figure 33). Interestingly, previous

research has shown that PML plays a role in the regulation of E2F-induced senescence in prostate cancer, whereby it facilitates the recruitment of E2F1-3 to the PML nuclear bodies, thereby promoting their interaction with the Rb protein (Vernier *et al*, 2011). These data appear in contradiction to our current data, where we find PML rather inhibiting senescence. However, it is worth noting that other E2F transcription factors, such as E2F4 and E2F6 have been described as transcriptional repressors rather than activators (Dyson, 1998; Takahashi *et al*, 2000; Cam *et al*, 2004). Moreover, a more recent work has shed light on an intriguing mechanism wherein PML's binding to the promoter of the TBX2 TF requires the presence of a functional E2F4/p130 repressor complex (Martin *et al*, 2012). This study, conducted in WI38 fibroblasts, demonstrated that PML physically interacts with E2F4, thereby accounting for the TBX2-mediated inhibition of senescence.

Additionally, it is worth highlighting MYC in the PML-positively regulated genes (Figure 33, arrow). Consistently with the identification of MYC as a TF that together with PML regulates proliferative genes, in TNBC PML inhibition is associated with cell growth arrest (Arreal *et al*, 2020). Moreover, in the same study PML inhibition leads to decreased MYC protein and mRNA levels, suggesting that MYC is also downstream of PML. Of note, PML and MYC can colocalize and physically interact (Cairo *et al*, 2005). A relationship between PML and p53 has been well established with studies showing a high positive correlation between these two proteins in other contexts and their expression negatively correlate with patient survival in acute myeloid leukemia (Gao *et al*, 2021). Despite this, a recent study demonstrated that c-MYC can negatively regulate p53 by long non coding RNA MILIP-dependent polySUMOylation of p53 and degradation (Feng *et al*, 2020). Moreover, in MEFs c-MYC activity was shown to be enhanced by HIF2a further fueling HIF2-mediated transformation. All together these studies are consistent with the HIF2a enhanced activity in ccRCC and the identification of MYC as a positive regulator factor together with PML of genes related to cell cycle.

Finally, the Ying Yang (YY1) zinc finger protein was identified among the transcription factors that bound genes positively regulated by PML and exhibiting high gene count (Figure 33, arrow). In this particular case, ChIP sequencing of YY1 was performed in HEK-293T human kidney embryo, making it interesting for our study due to the tissue similarity compared to the other transcription factors (Schmitges *et al*, 2016). Knockdown

of YY1 reduces cell proliferation in two renal cell carcinoma cell lines as measured by MTT assays (Weng *et al*, 2014). Moreover, two studies have described the role of YY1 in inhibiting p53 activity, by promoting MDM2- dependent ubiquitination and p-300-dependent stabilization (Grönroos *et al*, 2004; Sui *et al*, 2004).

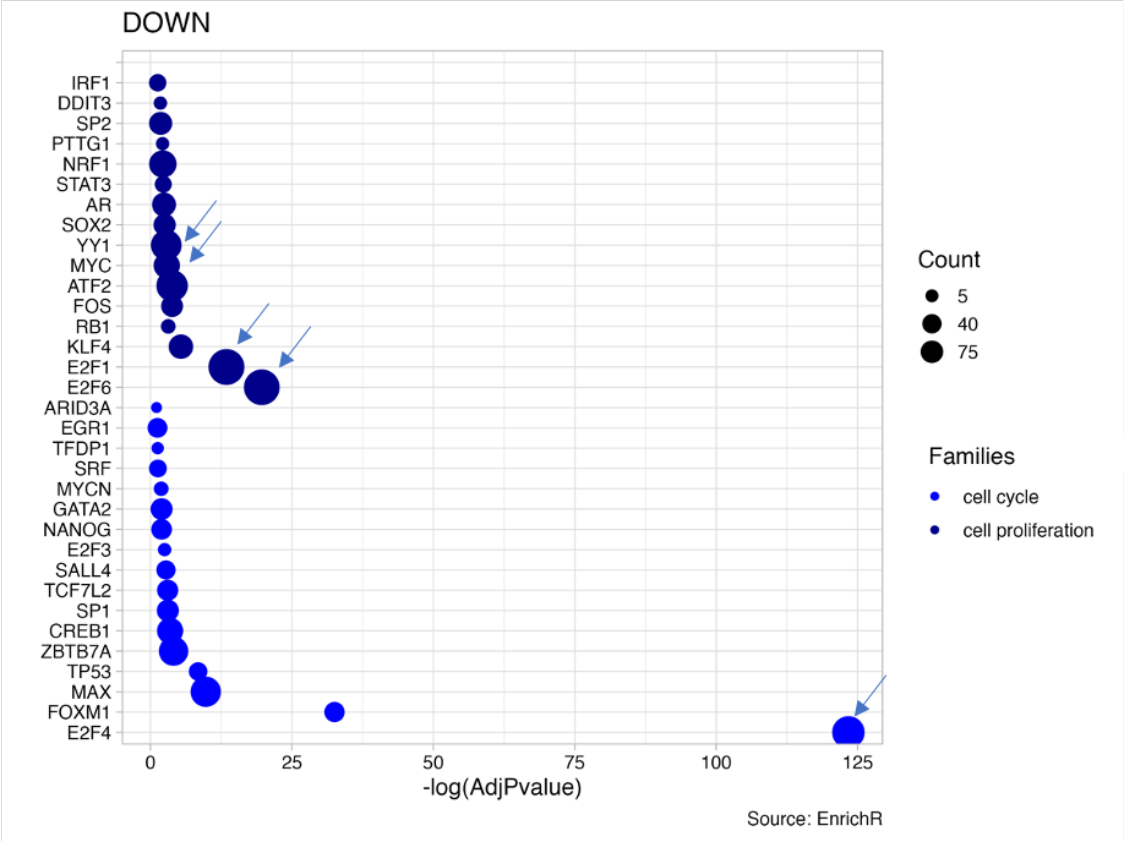


Figure 33.33 transcription factors have been identified in multiple different cellular contexts as transcriptional regulators of PML-activated genes in RCC4.
Dotplot of integrated analysis of Transcriptional Regulatory Networks from other cellular contexts concerning genes that are positively regulated by PML in RCC4. Data and sources tools used include: ENCODE and ChEA Consensus TFs from ChIP-X; TRRUST; TRANSFAC and JASPAR PWMs. Data was filtered using an adjusted P-value < 0.1. Count refers to genes from the input list (PML regulated in RCC4) contained in each transcriptional factor network. TFs are grouped into color-coded families.

We then performed the same analysis for the genes negatively regulated by PML ("UP") and by using the same criteria described above, we formulated obtained a list of 33 TFs, implicated in metabolism, senescence and inflammation (Figure 34). We found that the TFs that displayed the highest enrichment were RELA, NFKB1, NFKB1A and BCL3

(Figure 34, see arrows). PML was previously known to be a negative regulator of the activity of the RELA in U2OS and other cell lines, for the maintenance of energy balance and functional mitochondria (Wu *et al*, 2003). Interestingly these TFs were also the ones with the highest enrichment for genes overlapping with the SenMayo (Figure 22, "Chapter 3.2.2."), thus senescence-associated TFs.

Of note among the metabolism family of TFs, we found that two regulators of the fatty acid oxidation, PPARG (one constituent of the PPAR family) and USF1, were the most enriched (figure 34, see arrows). The involvement of PML in the PPAR signaling activation has already been explored in TNBC, where PML was found to induce activation of PPAR signaling (Carracedo *et al*, 2012). Interestingly, our findings suggest a distinct role for PML in RCC compared to TNBC.

Interestingly, within the "senescence" family of transcription factors, our analysis identified two members of the SP1 family, SP1 and SP3, which were high in fold enrichment as well as gene count (figure 34, see arrows). Intriguingly, previous research has demonstrated a physical interaction between SP1 and PML, which results in the disruption of SP1 binding to DNA (Vallian *et al*, 1998). Later, studies have demonstrated their physical interaction inside the PML NBs is facilitated by SUMOylation of SP1 by PML (Li *et al*, 2014). Therefore, PML regulates SP1-bound genes via sequestration of SP1 into PML NBs. Interestingly, SP1 and p53 share many consensus sequences at GC-boxes on DNA, suggesting SP1 and p53 might co-operate or compete in the transcription regulation of downstream genes, such as *CDKN1A/P21* gene (Koutsodontis *et al*, 2001; Levine & Oren, 2009). Moreover, SP1 overexpression increases p53 protein levels in various cancer lines (Chuang *et al*, 2009).

Moreover, older studies have emphasized the crucial role of SP1 in orchestrating cell growth and regulating DHFR expression as cell progress through cell cycle after serum stimulation of quiescent cells (Noé *et al*, 1997). Additionally, a thorough examination of the DHFR promoter has unveiled that the Sp1 sites, rather than the E2F site, mediate its transcriptional activity during the late G1/S phase of the cell cycle (Swick & Azizkhan, 1997). Collectively, these investigations underscore the significance of SP1 in governing cell growth and cell cycle progression.

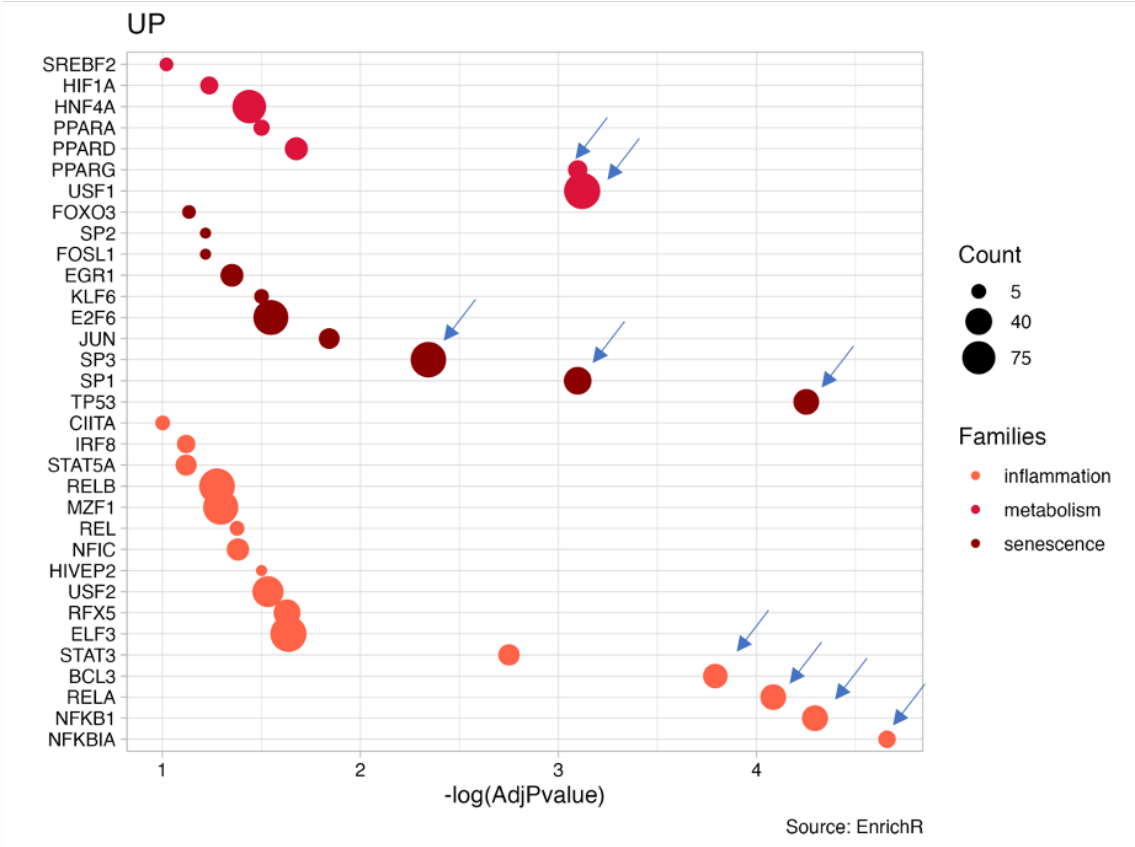


Figure 34. 33 transcription factors have been identified in multiple different cellular contexts as transcriptional regulators of PML-repressed genes in RCC4.
Dotplot of integrated analysis of Transcriptional Regulatory Networks from other cellular contexts concerning genes that are negatively regulated by PML in RCC4 (input list). Data and sources tools used include: ENCODE and ChEA Consensus TFs from ChIP-X; TRRUST; TRANSFAC and JASPAR PWMs. Data was filtered using an adjusted P-value < 0.1. Count refers to genes from the input list contained in each transcriptional factor network. TFs are grouped into color-coded families.

In light of these findings, we hypotheses that SP1 could be one of the candidate transcriptions factors that by physically interacting with PML it can regulate expression of genes involved in senescence in ccRCC. To characterize the spatial association between PML-NBs and SP1 protein in RCC4 *wt* we performed colocalization studies via double immunofluorescence. We found that on average RCC4 cells express 21 PML-NBs and that the majority of these cells (approximately 40 %) harbor 3 out of 21 PML-NBs that are found in close proximity to SP1 (figure 35).

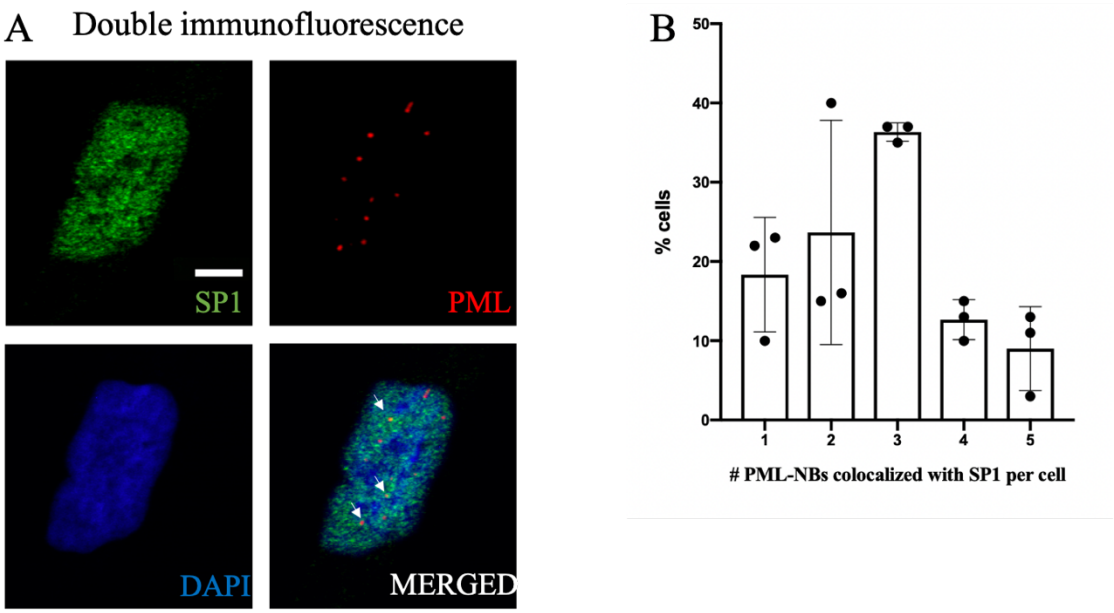


Figure 35. PML and SP1 colocalize in ccRCC RCC4 cells.
A. Double immunofluorescence analyzing localization of SP1 (green) and PML (red) proteins in RCC4 wt cells (63X magnification; Scale bar: 5 μm. Nuclei were stained with DAPI (blue). Images shown are representative of one Z-stack. B. Histogram showing percentage of cells harboring PML-NBs colocalization with SP1 in each cell.

Chapter 4. DISCUSSION

PML was initially described as a tumor-suppressive gene in cancer. However, recent insights suggested a more complex role dependent on tissue context, with PML exhibiting both oncogenic and tumor-suppressive roles. PML overexpression has been widely investigated in TNBC, where its expression was found, among other activities, to promote metastasis via HIF1α-mediated regulation of downstream genes (Ponente *et al*, 2017).

In the context of renal cancer, few studies have been published on the role of PML, and they are conflicting. In a *TSC2* inactivating model of papillary renal cell carcinoma PML depletion was found to accelerate tumor progression (Bernardi *et al*, 2011). In addition, one study suggested that PML could play tumor suppressive functions also in ccRCC, being stabilized by the tumor suppressive phosphatase SCP1 (Lin *et al*, 2014). However, this study fell short of describing phenotypes mediated by PML suppression per se, and analyzed the effect of PML silencing only upon SCP1 genetic manipulation. In addition, by performing PML immunohistochemistry on a small number of ccRCC specimens, the study reported PML downregulation with respect to normal adjacent kidney (Lin *et al*, 2014). Following this report a series of more recent studies aiming to identify prognostic biomarkers in ccRCC, identified PML as overexpressed in ccRCC (Li *et al*, 2019a; Luo *et al*, 2023; Wu *et al*, 2023; Wang *et al*, 2023). These findings challenged earlier categorizations and prompted a deeper exploration of PML's role in this specific cancer type. In line with these last studies, preliminary data obtained in my laboratory has recently uncovered an unprecedented role of PML in promoting ccRCC proliferation *in vitro* and *in vivo*. By using an inducible model of PML silencing, the laboratory has demonstrated important phenotypes mediated by *PML* in ccRCC, which I have described in the preliminary data. Specifically, PML i) promotes proliferation; ii) blocks p53 and p21 activation; iii) regulates HIF1α and HIF2α with distinct outputs.

On this basis, we hypothesized that discrepancies on the expression of PML in ccRCC may stem from patient selection or use of specific antibodies in immunohistochemical studies. Thus, my first aim was to better define the expression levels of PML by using available RNA sequencing and proteomic data from ccRCC patients. Through applied bioinformatics and extensive analyses, I found elevated PML expression in ccRCC at both mRNA and protein levels, both in tumor specimens as well as in ccRCC cell lines.

Because these data were obtained by analyzing mass spectrometry data, they provide antibody-independent validation of the recently published overexpression of PML mRNA, thus confirming that PML is highly expressed in ccRCC. Importantly, PML expression correlated with decreased survival, further suggesting an oncogenic function. This unbiased analysis also revealed PML overexpression in tumor tissues where PML's role had not been described before, these being AML, esophagus, stomach and pancreas, expanding the usefulness of this analyses to other tumor tissues.

I next moved to a functional validation of PML's functions in ccRCC. Preliminary data performed in the laboratory was suggestive of a strong senescence-like phenotype (dictated by p53 activation and cell cycle arrest). However, work performed in the laboratory had failed to provide strong evidence of senescence after short-term induction of *PML* silencing due to the lack of positive staining by one of the most classical senescent markers, SA-beta-galactosidase (data not shown). We thus speculated that longer PML silencing may be necessary to induce a conventional senescence phenotype. By performing long-term *PML* silencing I demonstrated that ccRCC cell become positive to SA-beta-galactosidase. In addition, I found that cell proliferation is kept repressed long-term, meaning that this phenotype is stable over time.

Following these findings, my second aim was to better characterize the plethora of functions regulated by PML. Functional enrichment analysis of genes positively regulated by PML revealed an overrepresentation of gene families associated with cell cycle progression and proliferation, in agreement with the growth-arrested phenotype in PML-depleted cells. Interestingly, genes suppressed by PML were enriched in diverse gene families associated with four major biological processes: senescence, extracellular matrix organization, inflammation/interferon signaling, and cholesterol biosynthesis. It is noteworthy that all these processes have been previously reported to be regulated by PML, albeit in different cellular systems and sometimes in opposite direction. For instance, our data align with reports of PML inhibiting cholesterol biosynthesis in prostate cancer (Chen *et al*, 2018), albeit the functional consequences of this regulation in ccRCC remains to be investigated. However, our observations are in apparent contrast with published data, where PML was shown to promote the expression of extracellular matrix remodeling factors in TNBC, stimulate inflammation/interferon signaling in various cell

types, and induce p53-dependent senescence upon oncogenic insults (Fracassi *et al*, 2023; El Bougrini *et al*, 2011).

With respect with the upregulation of p53-dependent and senescence gene networks upon *PML* silencing, it is worth noting that recent data has revealed that in tumor types where PML performs oncogenic functions, such as TNBC and glioblastoma, PML removal also leads to senescence (Ponente *et al*, 2017; Amodeo *et al*, 2017), which is in agreement with our observations.

While the specific molecular determinants of this senescence phenotype remain to be fully characterized, I decided to employ a broader approach to explore the senescent phenotype induced by *PML* loss in ccRCC. Notably, the overlap with the SenMayo dataset indicated that the observed enrichment of inflammatory pathways within the upregulated gene sets upon *PML* silencing in RCC4 cells is in line with the secretome of senescent cells, known as the senescence-associated secretory phenotype (SASP), and includes proteins promoting extracellular matrix remodeling, inflammatory cytokines, and chemokines. To ascertain whether the gene families linked to extracellular matrix remodeling and inflammation upregulated in RCC4 cells with low PML levels belonged to a SASP, I overlapped all genes negatively regulated by PML with a SASPome profiled in fibroblasts subjected to different types of senescence inducers. This analysis yielded a substantial overlap identifying 81 common soluble SASP factors. This emphasized the role of SASP, particularly in influencing ECM remodeling, as a crucial aspect of the cellular response in ccRCC cells when PML is suppressed and allowed us to reconcile the apparent contradiction of our observations. In other words, we currently believe that the inflammatory and matrix-remodelling genes that are upregulated in ccRCC cells upon PML silencing belong to a SASP program. The functional consequences of this regulation will have to be validated with dedicated experiments.

In the third aim, I sought to investigate the mechanisms linking PML to the control of cell proliferation. Published literature indicates that PML may promote cell proliferation by regulating the transcriptional activity of oncogenic transcription factors like MYC, HIF1α, SOX9, and STAT3 (Carracedo *et al*, 2012; Martín-Martín *et al*, 2016; Ponente *et al*, 2017; Liu *et al*, 2017). Moreover, in TNBC, the growth arrest induced by PML silencing is accompanied by decreased levels of MYC and PIM1 (Arreal *et al*, 2020).

However, because our preliminary data showed that PML positively regulates HIF2α, which is a known oncogene in ccRCC, we decided to test the hypothesis that the proliferative function of PML is mediated by HIF2α. This hypothesis was validated by a gene expression overlap of genes involved in cell cycle and mitosis as co-regulated by both PML and HIF2α. However, I found that neither overexpression nor silencing of HIF2α had an effect on RCC4 cell proliferation. Of note, these results are in line with published literature obtained in the same cell line, RCC4 cells (Arnaiz *et al*, 2021), and suggests that PML is a stronger regulator of proliferation *in vitro* than HIF2α, or that compensatory mechanisms are activated upon HIF2α depletion. In addition, I found that HIF2α overexpression was not able to revert the decrease in proliferation induced by PML silencing. In summary these data suggest that PML may regulate ccRCC proliferation via HIF2α-independent mechanisms. In line with this hypothesis, use of the HIF2α small molecule inhibitor PT2399 on ccRCC cells *in vitro* failed to induce growth arrest, while treatment with the PML inhibitors ATO slowed down ccRCC expansion.
Finally, to gain insights into the transcription factors that may be modulated by PML in this tumor context, my analysis of transcription factors enrichment in genes regulated by PML highlighted a regulatory network involving both positive and negative regulators, emphasizing the complexity of PML's role in ccRCC. SP1 emerged as a potential candidate transcription factor, as it in other contexts it was shown be essential for p53 activity and because the colocalization studies I showed suggesting a spatial association with PML-NBs.

4.1. Future perspectives

Further functional studies are needed to determine SP1 regulation by PML as well as co-immunoprecipitation studies to determine any physical interaction between these proteins. It would be interesting to then test any physical association and spatial interaction that may exist between p53 and SP1 in ccRCC and whether this is PML regulated. In addition, our preliminary observations suggest a complex interplay between PML and various transcription factors in the regulation of senescence, proliferation, and cell cycle progression, highlighting the need for further research to understand these mechanisms fully.

Finally, the data obtained with ATO treatment open the doors to new therapeutic implications and the model used will be used next for studies in combination with other drugs that will allow expansion of the therapeutic potential of ATO in ccRCC-

Chapter 5. MATERIALS AND METHODS

5.1 Applied bioinformatics analysis

For analysis of PML expression the following datasets in the UALCAN web tool were used: CPTAC-KIRC (proteomic) and TCGA-KIRC (transcriptomic).(Chandrashekar *et al*, 2017)(online source: https://ualcan.path.uab.edu). *PML* mRNA abundance in cancer cell lines was queried in the Cancer Cell Line Encyclopedia dataset using cBioPortal (Cerami *et al*, 2012; Gao *et al*, 2013), (online source: https://www.cbioportal.org). For PML expression across different tumor types, the TNMplot.com tool was used (Bartha & Győrffy, 2021) (https://tnmplot.com/analysis/). For survival analysis the OSkirc tool was used (Xie *et al*, 2019) (https://bioinfo.henu.edu.cn/KIRC/KIRCList.jsp).

5.2. Senescence-associated β-Galactosidase staining

For SA-β-Gal assay, 2.5 x 10^5 of RCC4 cells were plated on 100 mm petri-dish and PML silencing was induced with doxycycline 100 ng/ml the day after. Doxycycline-containing medium was replaced every 48 h and cells were split and counted every 72 h, each time re-plating 300,000 cells. At day 13 (T20 post-transduction), cells were split and 2 x 10^4 cells were plated in 12-well plate on 13 mm coverslip. The day after cells were fixed with 4% PFA solution and left in PBS 1X at 4°C until use. β-galactosidase accumulation was detected by using the senescence β-galactosidase staining kit (Cell Signaling Technology #9860). For each condition 12 images were taken with the Zeiss Axio Imager M2 microscope using a 10X objective magnification. Cells were evaluated positive or not for β-galactosidase based on the intensity (bluer) and size of the staining (bigger).

5.3. RNA extraction and RNA sequencing

For RNA sequencing upon PML silencing, RCC4 cells expressing shCtrl or shPML#1 were treated with doxycycline (100 ng/ml) for 96 hours. Two biological replicates with independent lentiviral infections were used. The processing of each sample involved the following steps: (i) total RNA isolation using the QIAGEN RNeasy Plus Micro Kit, following the manufacturer's guidelines; (ii) RNA treatment with DNAse I (Sigma, D5307), following the manufacturer's instructions; (iii) assessment of RNA quality using a 2100 Bioanalyzer (Agilent) to select RNA with a RIN above 9. The TruSeq stranded

mRNA protocol was employed for 50/30 library preparation, starting with 100 ng of total RNA. Libraries were barcoded, pooled, and sequenced on an Illumina Nova-Seq 6000 sequencing system. In each run, RNA sequencing experiments produced 30 million single-end reads, each 100 nucleotides long. After trimming low-quality reads with Trimmomatic (version 0.39), sequences were aligned to the human reference genome GRCh38 using the STAR aligner (Dobin *et al*, 2013).The number of reads per gene (gene counts) was determined using FeatureCount (Liao *et al*, 2014) based on the latest Gencode release for RNA sequencing (Harrow *et al*, 2012). Differential gene expression analysis was conducted in R/BioConductor (Harrow *et al*, 2012) using the DESeq2 package (version 1.30.1) (Love *et al*, 2014). The Python library "matplotlib.pyplot" was utilized for generating the volcano plot. A significance threshold of 0.05, adjusting the P-value by False Discovery Rate (FDR), was applied to identify differentially expressed genes. A log2 Fold Change (log2FC) cut-off of 0.5 was implemented to distinguish upregulated (log2FC > 0.5) and downregulated (log2FC < -0.5) genes.

5.4. Functional enrichment analysis

Functional enrichment analyses of differentially expressed genes upon PML silencing compared to controls were performed using the EnrichR tool (64). Enrich R uses the Fisher's exact test for enrichment analysis, and it calculates adjusted p-values to account for multiple testing using methods such as the Benjamini-Hochberg procedure (also known as the false discovery rate or FDR adjustment). The adjusted p-value (often denoted as FDR or q-value) represents the corrected significance level for each gene set or pathway. A lower adjusted p-value indicates stronger evidence of enrichment. Reactome, KEGG, MSigDB_Hallmark, WikiPathway, and Gene Ontologies, were used as reference databases. Functional enrichment anlaysis of transcriptional regulation was performed using EnrichR and the following databases: ENCODE and ChEA Consensus TFs from ChIP-X; TRRUST Transcription Factors 2019 and TRANSFAC and JASPAR PWMs. For all analysis, Significant pathways were filtered by adjusted P-value < 0.1. ggplot2 in R (https:// ggplot2.tidyverse.org/) was used for plots.

5.5. Cell culture

Human ccRCC cell lines RCC4 [European Collection of Authenticated Cell Lines (EACC) number 03112702], and TNBC cells MDA-MB-231 (ATCC number: HTB-26) and MDA-MB-468 (ATCC number: HTB-132) were cultured in DMEM (Euroclone ECM0103L). ccRCC cells Caki-1 (ATCC number: HTB-46) were cultured in RPMI. ccRCC A498 cells (ATCC number: HTB-44) were cultured in MEM (Life Technologies 11095-080) supplemented with MEM Non-Essential Amino Acids (1 %, Life Technologies 11140050) and pyruvate (1%). XP258 PDX-derived cells (Chen *et al*, 2016) were maintained in MEM (Life Technologies 11095-080) supplemented with MEM Non-Essential Amino Acids (1%, Life Technologies 11140050), EGF (10 ng/ml, Life Technology 13247-051), and Hydrocortisone (0.4 μm/ml, Merck H0396). For lentiviral production, HEK293T (ATCC number: CRL-11268) cells were grown in IMDM. For retroviral production, Phoenix-AMPHO (ATCC number: CRL-3213) cells were cultured in DMEM (ECB1072L). All culture media were supplemented with heat-inactivated (10 % FBS, Euroclone ECS5000L) and (1% P/S, Euroclone ECB 3001). They were *Mycoplasma* tested periodically and maintained in a humidified incubator containing CO2 (5%) and O2 (20 %).

5.6. Western Blotting

For Western blot, cells were pre-treated with doxycycline (100 ng/ml) for 72 h and then re-plated until the day after, so that a confluence of approximately 70% was reached. Then pellets were lysed using RIPA buffer, containing Tris-HCl pH8 (50 mM), NaCl (150 mM), NP-40 (1 %), deoxycholate (0.5 %), SDS (0.1 %) for 20 minutes. Cell lysates were centrifuged at 13,000 rpm for 10 min and protein-containing supernatant was collected and quantification was performed using the Bradford Protein Assay at 595 nm. Prior to loading, samples were denatured using 4x laemmli buffer (BioRad) and boiled for 5 minuets at 95 °C, spined for 1 minutes at maximum speed and resolved by SDS-PAGE on a 7.5/12 % gradient hand-made gel. Proteins were transferred to PDVF membranes by using a Trans-Blot® Turbo™ Transfer System (BioRad). Subsequently, membranes were washed in milliQ H_2O and proteins were stained and visualized using Ponceau S dye. Once the dye was removed, membranes were blocked for 1 hour at room temperature in phosphate-buffer saline with a 0.1 % Tween® 20 (TPBS) and bovine serum

albumin (BSA, 5 %). Membranes were incubated at 4 °C overnight with primary antibodies (table 1) diluted in TPBS with BSA (1 %) The day after, membranes were washed three times 10 minutes each in TPBS then incubated at room temperature for 1 hour with secondary anti-mouse or anti-rabbit HRP- conjugated antibodies (table 1) diluted in TPBS with BSA (1 %). After washing the membrane three times in TPBS, proteins were detected through the Clarity™ Wester ECL Substrate (BioRad) chemiluminescent imaging system.

5.7. Cell Proliferation and focus forming assay

For short-term cell proliferation assays, triplicates of MDA-MB-231 cells (1.5×10^4), RCC4, and A498 cells (5×10^3 each), as well as Caki-1 cells (1×10^4), were seeded on 12-well plates, with one plate assigned to each time point. After 24 hours, one plate was fixed with 4% PFA in PBS and stained using a 0.1% crystal violet solution (98 ml distilled water, 2 ml methanol, and 0.1 g Crystal Violet), designated as Day 1. The remaining cells were treated with 100 mg/ml doxycycline to induce PML silencing, with media changes every 48 hours. Crystal violet was solubilized with 10% acetic acid in dH_2O, and cell proliferation was assessed by measuring absorbance at λ 575 nm, expressed as OD575. Data was presented as OD575 fold change over Day 1.

For long-term cell proliferation assays a 3T3 protocol was used. On day 0, 2.5×10^5 of RCC4 cells, were seeded on a 100 mm culture dish (Corning™ Costar®). The following day, we administered doxycycline at a concentration of 100 ng/ml to the cells. On day 4, which corresponds to 72 hours after the doxycycline treatment, we detached the cells using trypsin, collected them, and conducted a cell count using the trypan blue dye exclusion method. Subsequently, we replated 3×10^5 of these counted cells onto 100 mm culture dishes and treated them once again with doxycycline at 100 ng/ml. We continued to follow the procedure described for day 4 for two weeks. Consequently, every 72 hours, we recorded the total cell count and multiplied it by the proliferation rate factor. For simplicity, we scaled down each recorded number to 10^5 on the graphs. For cell proliferation of p53DD RCC4 cells, 1.4×10^4 cells were plated on 12-well well plates (Corning™ Costar®) and PML silencing was induced with 100 ng/ml doxycycline the day after. 72 h after induction cells were split and 1.8×10^4 cells were plated for each condition. From this point, cells were split and counted every 72 hours using the trypan blue dye

exclusion method. Medium was replaced every 48 hours with the addition of doxycycline to keep on PML silencing.

5.8. Focus forming assay

In focus-forming assays, triplicates of MDA-MB-231 cells (4 x 10^3) were plated on a 6-well plate and allowed to form colonies over a period of 10 days. Subsequently, the cells were fixed with 4% PFA in PBS and stained using a 0.1% Crystal Violet Staining Solution. To assess colony formation efficiency, Crystal Violet was solubilized with 10% acetic acid in dH_2O. The evaluation involved measuring the absorbance of Crystal Violet at λ 575 nm and expressing the results as OD575 absorbance values.

5.9. Lentivirus production and cell transduction

For generation of third-generation lentivirus stocks published protocols were used (Dull *et al*, 1998; Follenzi *et al*, 2000)with some modifications. 8 x 10^6 HEK-293T cells were seeded on a p150 mm Petri dish and cultured in IMDM medium with FBS (10 %) and P/S (1 %). For transfection, the calcium phosphate method was used. Briefly, HEK-293T cells were transiently transfected with the packaging plasmid pMDLg/pRRE, Rev-expressing pCMV-Rev and VSV-G envelop -encoding pMD2.VSV-G plasmids and shRNA-carring vectors. For PML silencing, 32 g of shRNA-carrying vectors harboring Tet-pLKO-puro plasmid expressing shPML #1 (Sigma-Aldrich TRCN 0000003867) and the pLKO-puro empty vector, the latter used as a control. For shPML#2 (TRCN0000003868) Tet-pLKO-puro (Addgene #21915) was linearized with AgeI and EcoRI restriction enzymes and ligating annealed shPML oligos (TRCN0000003868). Selection of positive closed was verified by diagnostic digestions with the XhoI restriction enzyme. These plasmids were a generous gift from Arkaitz Carracedo (Martín-Martín *et al*, 2016). The next day medium was replaced and lentivirus was collected, repeating this procedure another time for the second harvest. Lentiviral particles underwent concentration by ultracentrifugation at 20,000 rpm for 2.20 hours and conserved in PBS at -80°C. For lentiviral transduction, ccRCC cells were seeded so that 70-80 % confluence was reached the next day. For *PML* silencing, cells were infected along with addition of polybrene (8 μg/ml) with lentiviral particles harboring the plasmids. Different concentration of puromycin (Merck P8833) were used to select

transduced cells: 1 ug/ml for RCC4, XP258 and MDA-MB-231 cells and 2 ug/ml for Caki-1 and A498 cells.

5.10. Retrovirus production and cell transduction

For retrovirus production, the protocol from de Lange (https://delangelab.org/protocols) was used. Briefly, 2 x 10^6 phoenix-AMPHO packaging cells were seeded the day before transfection. The next day phoenix cells reached a confluence of 40-50 % and were transfected with and 20 μg of DNA (Qiagen prep purified) using the calcium phosphate precipitation method. Medium was changed 20 hours after transfection and ccRCC cells were seeded late on that same day, such that the day after the cell density would be 40 %. Three rounds of infections were performed, the first occurring no later than 48 hours after transfection, followed by the last two every 24 hours. Different concentration of puromycin (Merck P8833) were used to select transduced cells: 1 ug/ml for RCC4, XP258 and MDA-MB-231 cells and 2 ug/ml for Caki-1 and A498 cells. For HIF2α overexpression using the constitutive system, 10g of the pBABE-puro-HA-HIF2α P405A/P531A vector (Qiagen prep purified), which was donated by W. Kaelin (Kondo *et al*, 2003), was used. For HIF2α overexpression using the inducible system, the HIF2α mutant sequence (P405A/P531, (Kondo *et al*, 2003) from the plasmid pBABE-puro-HA-HIF2α P405A/P531A was modified as follow: i) removal of the first methionine; ii) removal of the BamHI site (GGA → GGC); iii) substitution of the first HIF2α methionine with a leucine (ATG → CTT). This sequence was synthesized by GenScript in the X^{on} LM1070-inducible construct (Monteys *et al*, 2021). The resulting sequence was subcloned (AgeI-SalI) in a bidirectional lentiviral vector (BdLV) transfer plasmid #1954_hPGK.mCD19inactive.WPRE_mhCMV.dNGFR.SV40PA to obtain plasmid ##3567_hPGK.Xon.HA. HIF2αmut.WPRE_mhCMV.dNGFR.SV40PA. Transduction was checked by flow cytometry by AAD, αNGFR APC (1.100, Miltenyi Biotec, 130- 113-418), FACS Canto II. For selection of NGFR positive cells magnetic selection of transduced cells with CD271 MicroBead Kit, human (Miltenyi Biotec, 130-099-023) was performed. For p53 loss of function, Phoenix-AMPHO cells were transfected with pBABE-puro empty vector (Addgene #1764) or pBaBE-puro-p53DD (R175H) (generated by O. Moshe). For HIF2α silencing, pLKO.1-puro with HIF2α shRNAs (TRCN0000003805) were purchased from Sigma MISSION®.

To produce retroviral particles, we transfected Phoenix-AMPHO cells with either the pBABE-puro Empty vector (Addgene #1764) or pBABE-puro-p53DD (constructed by O. Moshe), following the de Lange laboratory's established protocol (accessible at https://delangelab.org/protocols). (Shaulian *et al*, 1992; Eliyahu *et al*, 1989).

5.11. Quantitative real time (qRT) PCR

Total RNA was isolated from RCC4 cells using the RNeasy mini kit (Qiagen). Subsequently, 1 µg of RNA underwent reverse transcription into cDNA, employing the Advantage RT-for-PCR Kit (Clontech) with random-hexamers primers. The PCR reaction was conducted on a 7900 Fast Real-time PCR System (Applied Biosystems) under standard cycling conditions. Gene expression analysis utilized Taqman probes (PML HS00971694_m1, 18S Hs03003631_g) obtained from Applied Biosystems. Relative expression was determined using the comparative threshold cycle method (2-ΔΔCt), and the results are presented as the fold change in (2-ΔΔCt) relative to the respective *shCtrl.*

5.12. Generation of cancer cell lines expressing luciferase and treatment with ATO

To generate RCC4 and XP258 expressing luciferase, 7 x 10^4 of cells were seeded on 6-well plates (Corning™ Costar®) in the late afternoon so that the morning after they attained 70 % confluence and were ready for infection. Each of the 5 wells were transduced with 1 ml of viral supernatant containing a third-generation lentiviral vector carrying the luciferase gene pLenti PGL V5 luc neo (w623-2) (addgene, plasmid #21471) (Campeau *et al*, 2009). Polybrene (8 µg/ml) was added during transduction. The viral supernatant was generously given by Oronzina Botrugno (Oronza A. Botrugno *et al*, 2019) (PhD, Ospedale San Raffaele). After 3 hours incubation the medium was replaced with fresh medium, and again after 18 hours. 24 hours after medium replacement cells underwent antibiotic selection with G418 (geneticin) (0.6 mg/ml).

For cell proliferation assay, 300 of RCC4 cells and 250 of XP258 cells were seeded on 96-well white plates (Thermo Scientific™ 265302) on day 0, treated with arsenic trioxide (0.25 µM, 0.5 µM, 1 µM) on day 2 and left for 72 hours prior to assessment. Medium was changed every 48 hours. To measure cell proliferation cells were incubated for 10 minutes

in the dark with Pierce™ D-Luciferin, Monosodium Salt (Thermo Scientific™, Cat# number 88291) and luciferase activity was measured on the microplate reader 'Mithras LB 940' (Berthold Technologies). Measures were taken at day 0 (time of plating), day 2 (time of treatment with ATO) and day 5 (end of curve). Data was expressed as relative luciferase units and fold change over day 0.

5.13. Immunofluorescence

For double immunofluorescence, RCC4 cells were pre-treated with doxycycline (100 ng/ml) for 72 hours, then 1.2 x 10^4 cells were re-plated on glass slides inside well from a 12-well plate (Corning™ Costar®). The day after cells were fixed with PFA (4 %) for 10 minutes, permeabilized with Triton X-100 (1 %) for 5 minutes and washed three times with PBS (1X). Once moved into a humidified chamber, blocking was performed using BSA (3 %) and goat serum (10 %) diluted in PBS (1 X) for 1 hour at room temperature. Subsequently, cells were quickly washed three times in PBS (1X) prior to incubation with primary antibodies (table 1) diluted in PBS 1X containing BSA (0.2 %) and goat serum (1 %) for 1 hour at room temperature. Cells were quickly washed three times in PBS (1X) containing Tween®20 (0.02 %) prior to incubation with fluorophore-conjugated secondary antibodies (1:500; table 1) diluted in PBS 1X containing Tween®20 (0.02 %) for 1 hour at room temperature. Cells were quickly washed three time in PBS (1X), nuclei were counterstained with DAPI (1X) for 5 minutes and mounted in hand-made Mowiol. Three biological replicates were performed and 30 cells per replicate was evaluated. Images were captured using Leica TCS SP5 X (Leica Bioystems) confocal microscope employing a 63X objective. Z-step size was set to 0.69 uM.

5.14. Statistical analysis

Unless explicitly mentioned in the figure captions, every experiment detailed in this research was conducted through a minimum of three distinct experiments or biological replicates. To evaluate statistical significance between two groups, the two-tailed Student's t-test was employed, and a confidence level of 0.05 was considered as the threshold for statistical significance. Statistical analyses were performed using GraphPad Prism version 8.1.1 for macOS, a software developed by GraphPad Software in San Diego, California, USA (www.graphpad.com).

5.15. Reagents and treatments

To initiate PML silencing, cells were exposed to doxycycline (100 ng/µl). The doxycycline monohydrate used in this experiment was obtained from Merck (D1822-500MG). To inhibit *PML in vitro*, cells were treated with arsenic trioxide (ATO) at concentrations of 0.25 µM, 0.5 µM and 1 µM. ATO was purchased from Merck (A1010). For SA-β-Gal positive control, cells were treated with Nutlin-3 (10 nM) for 6 days. Nutlin-3 was purchased by Merck (N6287). To induce expression of HIF2α protein in the X^{on} inducible system, cells were treated with LMI070 (25 nM). LMI070 was purchased from Selleckchem (Cat# S6642). For luciferase expression cells were incubated with Pierce™ D-Luciferin, Monosodium Salt (Thermo Scientific™, Cat# number 88291).

5.16. List of antibodies

Antibody	Species	Dilution	Application
PML (NB100-59787)	R	1:1,000	WB, IF
HIF2α (D9E3) #7096	R	1:500	WB, IF
SP1	M	1:50	IF
Vinculin (7F9): sc-73614	M	1:10,000	WB
Tubulin (ab15246)	R	1:10,000	WB
β-actin (AC-15): sc-69879	M	1:10,000	WB
AlexaFluor™ 488 A32732	M	1:500	IF
AlexaFluor™ 546 A32731	R	1:500	IF

Table 1. List of antibodies.

Chapter 5. REFERENCES

Ades L, Guerci A, Raffoux E, Sanz M, Chevallier P, Lapusan S, Recher C, Thomas X, Rayon C, Castaigne S, *et al* (2009) Very Long Term Outcome of Acute Promyelocytic Leukemia After Treatment with All Trans Retinoic Acid and Chemotherapy: The European APL Group Experience. *Blood* 114: 2088–2088

Alexander KA, Yu R, Skuli N, Coffey NJ, Nguyen S, Huang H, Dardani IP, Good AL, Lim J, Li C, *et al* (2023) Nuclear speckles regulate HIF-2a programs and correlate with patient survival in kidney cancer. *BioRxiv*

Amendolare A, Marzano F, Petruzzella V, Vacca RA, Guerrini L, Pesole G, Sbisà E & Tullo A (2022) The Underestimated Role of the p53 Pathway in Renal Cancer. *Cancers* 14: 1–15

Amodeo V, A D, Betts J, Bartesaghi S, Zhang Y, Richard-Londt A, Ellis M, Roshani R, Vouri M, Galavotti S, *et al* (2017) A PML/Slit Axis Controls Physiological Cell Migration and Cancer Invasion in the CNS. *Cell Rep* 20: 411–426

An WG, Kanekal M, Simon MC, Maltepe E, Blagosklonny M V. & Neckers LM (1998) Stabilization of wild-type p53 by hypoxia-inducible factor 1α. *Nature* 392: 405–408

Arnaiz E, Miar A, Bridges E, Prasad N, Hatch SB, Ebner D, Lawrie CH & Harris AL (2021) Differential effects of HIF2α antagonist and HIF2α silencing in renal cancer and sensitivity to repurposed drugs. *BMC Cancer* 21: 1–12

Arreal L, Piva M, Fernández S, Revandkar A, Schaub- Clerigué A, Villanueva J, Zabala-Letona A, Pujana M, Astobiza I, Cortazar AR, *et al* (2020) Targeting PML in triple negative breast cancer elicits growth suppression and senescence. *Cell Death Differ* 27: 1186–1199

Atkins MB & Tannir NM (2018) Current and emerging therapies for first-line treatment of metastatic clear cell renal cell carcinoma. *Cancer Treat Rev* 70: 127–137

Banani SF, Rice AM, Peeples WB, Lin Y, Jain S, Parker R & Rosen MK (2016) Compositional Control of Phase-Separated Cellular Bodies. *Cell* 166: 651–663

Bartha Á & Győrffy B (2021) TNMplot.com: A Web Tool for the Comparison of Gene Expression in Normal, Tumor and Metastatic Tissues. *Int J Mol Sci* 22: 2622

Basisty N, Kale A, Jeon OH, Kuehnemann C, Payne T, Rao C, Holtz A, Shah S, Sharma V, Ferrucci L, *et al* (2020) A proteomic atlas of senescence-associated secretomes

for aging biomarker development. *PLoS Biol* 18: 1–26

Bernardi R & Pandolfi PP (2007) Structure, dynamics and functions of promyelocytic leukaemia nuclear bodies. *Nat Rev Mol Cell Biol* 8: 1006–1016

Bernardi R, Papa A, Egia A, Coltella N, Teruya-Feldstein J, Signoretti S & Pandolfi PP (2011) Pml represses tumour progression through inhibition of mTOR. *EMBO Mol Med* 3: 249–257

Bernardi R, Scaglioni PP, Bergmann S, Horn HF, Vousden KH & Pandolfi PP (2004) PML regulates p53 stability by sequestering Mdm2 to the nucleolus. *Nat Cell Biol* 6: 665–672

Bertout JA, Majmundar AJ, Gordan JD, Lam JC, Ditsworth D, Keith B, Brown EJ, Nathanson KL & Simon MC (2009) HIF2α inhibition promotes p53 pathway activity, tumor cell death, and radiation responses. *Proc Natl Acad Sci U S A* 106: 14391–14396

Biswas S, Troy H, Leek R, Chung Y-L, Li J, Raval RR, Turley H, Gatter K, Pezzella F, Griffiths JR, *et al* (2010) Effects of HIF-1 and HIF2 on Growth and Metabolism of Clear-Cell Renal Cell Carcinoma 786-0 Xenografts. *J Oncol* 2010: 1–14

Boisvert F-M, Hendzel MJ & Bazett-Jones DP (2000) Promyelocytic Leukemia (Pml) Nuclear Bodies Are Protein Structures That Do Not Accumulate RNA. *J Cell Biol* 148: 283–292

El Bougrini J, Dianoux L & Chelbi-Alix MK (2011) PML positively regulates interferon gamma signaling. *Biochimie* 93: 389–398

Brodaczewska KK, Szczylik C, Fiedorowicz M, Porta C & Czarnecka AM (2016) Choosing the right cell line for renal cell cancer research. *Mol Cancer* 15: 1–15

Brugarolas J (2014) Molecular Genetics of Clear-Cell Renal Cell Carcinoma. *J Clin Oncol* 32: 1968–1976

Cabaj A, Moszyńska A, Charzyńska A, Bartoszewski R & Dąbrowski M (2022) Functional and HRE motifs count analysis of induction of selected hypoxia-responsive genes by HIF-1 and HIF-2 in human umbilical endothelial cells. *Cell Signal* 90: 110209

Cairo S, De Falco F, Pizzo M, Salomoni P, Pandolfi PP & Meroni G (2005) PML interacts with Myc, and Myc target gene expression is altered in PML-null fibroblasts. *Oncogene* 24: 2195–2203

Cam H, Balciunaite E, Blais A, Spektor A, Scarpulla RC, Young R, Kluger Y & Dynlacht BD (2004) A common set of gene regulatory networks links metabolism and growth inhibition. *Mol Cell* 16: 399–411

Campeau E, Ruhl VE, Rodier F, Smith CL, Rahmberg BL, Fuss JO, Campisi J, Yaswen P, Cooper PK & Kaufman PD (2009) A Versatile Viral System for Expression and Depletion of Proteins in Mammalian Cells. *PLoS One* 4: e6529

Cardote TAF, Gadd MS & Ciulli A (2017) Crystal Structure of the Cul2-Rbx1-EloBC-VHL Ubiquitin Ligase Complex. *Structure* 25: 901-911.e3

Carracedo A, Weiss D, Leliaert AK, Bhasin M, De Boer VCJ, Laurent G, Adams AC, Sundvall M, Song SJ, Ito K, *et al* (2012) A metabolic prosurvival role for PML in breast cancer. *J Clin Invest* 122: 3088–3100

Cerami E, Gao J, Dogrusoz U, Gross BE, Sumer SO, Aksoy BA, Jacobsen A, Byrne CJ, Heuer ML, Larsson E, *et al* (2012) The cBio Cancer Genomics Portal: An Open Platform for Exploring Multidimensional Cancer Genomics Data. *Cancer Discov* 2: 401–404

Chandrashekar DS, Bashel B, Balasubramanya SAH, Creighton CJ, Ponce-Rodriguez I, Chakravarthi BVSK & Varambally S (2017) UALCAN: A Portal for Facilitating Tumor Subgroup Gene Expression and Survival Analyses. *Neoplasia* 19: 649–658

Chappell WH, Lehmann BD, Terrian DM, Abrams SL, Steelman LS & McCubrey JA (2012) p53 expression controls prostate cancer sensitivity to chemotherapy and the MDM2 inhibitor Nutlin-3. *Cell Cycle* 11: 4579–4588

Chelbi-Alix MK, Pelicano L, Quignon F, Koken MH, Venturini L, Stadler M, Pavlovic J, Degos L & de Thé H (1995) Induction of the PML protein by interferons in normal and APL cells. *Leukemia* 9: 2027–33

Chen D, Li M, Luo J & Gu W (2003) Direct Interactions between HIF-1α and Mdm2 Modulate p53 Function. *J Biol Chem* 278: 13595–13598

Chen M, Zhang J, Sampieri K, Clohessy JG, Mendez L, Gonzalez-Billalabeitia E, Liu X-S, Lee Y-R, Fung J, Katon JM, *et al* (2018) An aberrant SREBP-dependent lipogenic program promotes metastatic prostate cancer. *Nat Genet* 50: 206–218

Chen W, Hill H, Christie A, Kim MS, Holloman E, Pavia-Jimenez A, Homayoun F, Ma Y, Patel N, Yell P, *et al* (2016) Targeting renal cell carcinoma with a HIF-2 antagonist. *Nature* 539: 112–117

Chen X, Pan X, Zhang W, Guo H, Cheng S, He Q, Yang B & Ding L (2020) Epigenetic strategies synergize with PD-L1/PD-1 targeted cancer immunotherapies to enhance antitumor responses. *Acta Pharm Sin B* 10: 723–733

Cheng X, Guo S, Liu Y, Chu H, Hakimi P, Berger NA, Hanson RW & Kao HY (2013) Ablation of promyelocytic leukemia protein (PML) re-patterns energy balance and protects mice from obesity induced by a western diet. *J Biol Chem* 288: 29746–29759

Cheng X, Liu Y, Chu H & Kao H-Y (2012) Promyelocytic Leukemia Protein (PML) Regulates Endothelial Cell Network Formation and Migration in Response to Tumor Necrosis Factor α (TNFα) and Interferon α (IFNα). *J Biol Chem* 287: 23356–23367

Cho H, Du X, Rizzi JP, Liberzon E, Chakraborty AA, Gao W, Carvo I, Signoretti S, Bruick RK, Josey JA, *et al* (2016) On-target efficacy of a HIF-2α antagonist in preclinical kidney cancer models. *Nature* 539: 107–111

Choueiri TK & Motzer RJ (2017) Systemic Therapy for Metastatic Renal-Cell Carcinoma. *N Engl J Med* 376: 354–366

Chuang JY, Wu CH, Lai MD, Chang WC & Hung JJ (2009) Overexpression of Sp1 leads to p53-dependent apoptosis in cancer cells. *Int J Cancer* 125: 2066–2076

Comprehensive molecular characterization of clear cell renal cell carcinoma (2013) *Nature* 499: 43–49

Condemine W, Takahashi Y, Le Bras M & de Thé H (2007) A nucleolar targeting signal in PML-I addresses PML to nucleolar caps in stressed or senescent cells. *J Cell Sci* 120: 3219–3227

Condemine W, Takahashi Y, Zhu J, Puvion-Dutilleul F, Guegan S, Janin A & De Thé H (2006) Characterization of endogenous human promyelocytic leukemia isoforms. *Cancer Res* 66: 6192–6198

Coppé JP, Patil CK, Rodier F, Sun Y, Muñoz DP, Goldstein J, Nelson PS, Desprez PY & Campisi J (2008) Senescence-associated secretory phenotypes reveal cell-nonautonomous functions of oncogenic RAS and the p53 tumor suppressor. *PLoS Biol* 6

Corpet A, Kleijwegt C, Roubille S, Juillard F, Jacquet K, Texier P & Lomonte P (2020) PML nuclear bodies and chromatin dynamics: catch me if you can! *Nucleic Acids Res* 48: 11890–11912

Courtney KD, Infante JR, Lam ET, Figlin RA, Rini BI, Brugarolas J, Zojwalla NJ, Lowe AM, Wang K, Wallace EM, *et al* (2018) Phase I Dose-Escalation Trial of PT2385, a First-in-Class Hypoxia-Inducible Factor-2α Antagonist in Patients With Previously Treated Advanced Clear Cell Renal Cell Carcinoma. *J Clin Oncol* 36: 867–874

Creighton CJ, Morgan M, Gunaratne PH, Wheeler DA, Gibbs RA, Robertson G, Chu A, Beroukhim R, Cibulskis K, Signoretti S, *et al* (2013) Comprehensivemolecular characterization of clear cell renal cell carcinoma. *Nature* 499: 43–49

Creutzig U, Zimmermann M, Dworzak M, Urban C, Henze G, Kremens B, Lakomek M, Bourquin JP, Stary J & Reinhardt D (2010) Favourable outcome of patients with childhood acute promyelocytic leukaemia after treatment with reduced cumulative anthracycline doses. *Br J Haematol* 149: 399–409

Di Croce L (2005) Chromatin modifying activity of leukaemia associated fusion proteins. *Hum Mol Genet* 14: 77–84

Cuvillier O (2017) The therapeutic potential of HIF-2 antagonism in renal cell carcinoma. *Transl Androl Urol* 6: 131–133

D'Orazi G, Cecchinelli B, Bruno T, Manni I, Higashimoto Y, Saito S, Gostissa M, Coen S, Marchetti A, Del Sal G, *et al* (2002) Homeodomain-interacting protein kinase-2 phosphorylates p53 at Ser 46 and mediates apoptosis. *Nat Cell Biol* 4: 11–19

Das B, Bayat-Mokhtari R, Tsui M, Lotfi S, Tsuchida R, Felsher DW & Yeger H (2012) HIF-2α suppresses p53 to enhance the stemness and regenerative potential of human embryonic stem cells. *Stem Cells* 30: 1685–1695

Delbarre E & Janicki SM (2021) Modulation of H3.3 chromatin assembly by PML: A way to regulate epigenetic inheritance. *BioEssays* 43

Dellaire G & Bazett-Jones DP (2004) PML nuclear bodies: dynamic sensors of DNA damage and cellular stress. *BioEssays* 26: 963–977

Dellaire G, Ching RW, Dehghani H, Ren Y & Bazett-Jones DP (2006) The number of PML nuclear bodies increases in early S phase by a fission mechanism. *J Cell Sci* 119: 1026–1033

Dobin A, Davis CA, Schlesinger F, Drenkow J, Zaleski C, Jha S, Batut P, Chaisson M & Gingeras TR (2013) STAR: ultrafast universal RNA-seq aligner. *Bioinformatics* 29: 15–21

Dror N, Rave-Harel N, Burchert A, Azriel A, Tamura T, Tailor P, Neubauer A, Ozato K & Levi B-Z (2007) Interferon Regulatory Factor-8 Is Indispensable for the Expression of Promyelocytic Leukemia and the Formation of Nuclear Bodies in Myeloid Cells. *J Biol Chem* 282: 5633–5640

Dull T, Zufferey R, Kelly M, Mandel RJ, Nguyen M, Trono D & Naldini L (1998) A Third-Generation Lentivirus Vector with a Conditional Packaging System. *J Virol* 72: 8463–8471

Dyson N (1998) The regulation of E2F by pRB-family proteins. *Genes Dev* 12: 2245–2262

Eliyahu D, Michalovitz D, Eliyahu S, Pinhasi-Kimhi O & Oren M (1989) Wild-type p53 can inhibit oncogene-mediated focus formation. *Proc Natl Acad Sci* 86: 8763–8767

Eskiw CH, Dellaire G & Bazett-Jones DP (2004) Chromatin Contributes to Structural Integrity of Promyelocytic Leukemia Bodies through a SUMO-1-independent Mechanism. *J Biol Chem* 279: 9577–9585

Fenaux P, Chastang C, Chomienne C, Castaigne S, Sanz M, Link H, Löwenberg B, Fey M, Archim-Baud E & Degos L (1995) Treatment of Newly Diagnosed Acute Promyelocytic Leukemia (APL) by All Transretinoic Acid (ATRA) Combined with Chemotherapy: The European Experience. *Leuk Lymphoma* 16: 431–437

Feng YC, Liu XY, Teng L, Ji Q, Wu Y, Li JM, Gao W, Zhang YY, La T, Tabatabaee H, *et al* (2020) c-Myc inactivation of p53 through the pan-cancer lncRNA MILIP drives cancer pathogenesis. *Nat Commun* 11: 4980

Ferbeyre G, de Stanchina E, Querido E, Baptiste N, Prives C & Lowe SW (2000) PML is induced by oncogenic ras and promotes premature senescence. *Genes Dev* 14: 2015–27

Fitzmaurice C, Allen C, Barber RM, Barregard L, Bhutta ZA, Brenner H, Dicker DJ, Chimed-Orchir O, Dandona R, Dandona L, *et al* (2017) Global, Regional, and National Cancer Incidence, Mortality, Years of Life Lost, Years Lived With Disability, and Disability-Adjusted Life-years for 32 Cancer Groups, 1990 to 2015. *JAMA Oncol* 3: 524

Flor AC, Wolfgeher D, Wu D & Kron SJ (2017) A signature of enhanced lipid metabolism, lipid peroxidation and aldehyde stress in therapy-induced senescence. *Cell Death Discov* 3: 1–12

Follenzi A, Ailles LE, Bakovic S, Geuna M & Naldini L (2000) Gene transfer by lentiviral vectors is limited by nuclear translocation and rescued by HIV-1 pol sequences. *Nat Genet* 25: 217–222

Forristal CE, Wright KL, Hanley NA, Oreffo ROC & Houghton FD (2010) Hypoxia inducible factors regulate pluripotency and proliferation in human embryonic stem cells cultured at reduced oxygen tensions. *REPRODUCTION* 139: 85–97

Fracassi C, Ugge' M, Abdelhalim M, Zapparoli E, Simoni M, Magliulo D, Mazza D, Lazarevic D, Morelli MJ, Collas P, *et al* (2023) PML modulates epigenetic composition of chromatin to regulate expression of pro-metastatic genes in triple-negative breast cancer. *Nucleic Acids Res* 51: 11024–11039

Frew IJ & Moch H (2015) A Clearer View of the Molecular Complexity of Clear Cell Renal Cell Carcinoma. *Annu Rev Pathol Mech Dis* 10: 263–289

Fuchs SBA, Lieder I, Stelzer G, Mazor Y, Buzhor E, Kaplan S, Bogoch Y, Plaschkes I, Shitrit A, Rappaport N, *et al* (2016) GeneAnalytics: An Integrative Gene Set Analysis Tool for Next Generation Sequencing, RNAseq and Microarray Data. *Omi A J Integr Biol* 20: 139–151

Gao C, Cheng X, Lam M, Liu Y, Liu Q, Chang K-S & Kao H-Y (2008a) Signal-dependent Regulation of Transcription by Histone Deacetylase 7 Involves Recruitment to Promyelocytic Leukemia Protein Nuclear Bodies. *Mol Biol Cell* 19: 3020–3027

Gao C, Ho C-C, Reineke E, Lam M, Cheng X, Stanya KJ, Liu Y, Chakraborty S, Shih H-M & Kao H-Y (2008b) Histone Deacetylase 7 Promotes PML Sumoylation and Is Essential for PML Nuclear Body Formation. *Mol Cell Biol* 28: 5658–5667

Gao J, Aksoy BA, Dogrusoz U, Dresdner G, Gross B, Sumer SO, Sun Y, Jacobsen A, Sinha R, Larsson E, *et al* (2013) Integrative Analysis of Complex Cancer Genomics and Clinical Profiles Using the cBioPortal. *Sci Signal* 6

Gao L, Saeed A, Golem S, Zhang D, Woodroof J, McGuirk J, Ganguly S, Abhyankar S, Lin TL & Cui W (2021) High-level MYC expression associates with poor survival in patients with acute myeloid leukemia and collaborates with overexpressed p53 in leukemic transformation in patients with myelodysplastic syndrome. *Int J Lab Hematol* 43: 99–109

Geng Y, Monajembashi S, Shao A, Cui D, He W, Chen Z, Hemmerich P & Tang J (2012)

Contribution of the C-terminal regions of promyelocytic leukemia protein (PML) isoforms II and V to PML nuclear body formation. *J Biol Chem* 287: 30729–30742

Geoffroy M-C, Jaffray EG, Walker KJ & Hay RT (2010) Arsenic-Induced SUMO-Dependent Recruitment of RNF4 into PML Nuclear Bodies. *Mol Biol Cell* 21: 4227–4239

Gerlinger M, Rowan AJ, Horswell S, Larkin J, Endesfelder D, Gronroos E, Martinez P, Matthews N, Stewart A, Tarpey P, *et al* (2012) Intratumor Heterogeneity and Branched Evolution Revealed by Multiregion Sequencing. *N Engl J Med* 366: 883–892

Gordan JD, Bertout JA, Hu C-J, Diehl JA & Simon MC (2007) HIF-2α Promotes Hypoxic Cell Proliferation by Enhancing c-Myc Transcriptional Activity. *Cancer Cell* 11: 335–347

Gordan JD, Lal P, Dondeti VR, Letrero R, Parekh KN, Oquendo CE, Greenberg RA, Flaherty KT, Rathmell WK, Keith B, *et al* (2008) HIF-α Effects on c-Myc Distinguish Two Subtypes of Sporadic VHL-Deficient Clear Cell Renal Carcinoma. *Cancer Cell* 14: 435–446

Gossage L, Eisen T & Maher ER (2015) VHL, the story of a tumour suppressor gene. *Nat Rev Cancer* 15: 55–64

Gottifredi V & Prives C (2001) P53 and PML: new partners in tumor suppression. *Trends Cell Biol* 11: 184–187

Greenman C, Stephens P, Smith R, Dalgliesh GL, Hunter C, Bignell G, Davies H, Teague J, Butler A, Stevens C, *et al* (2007) Patterns of somatic mutation in human cancer genomes. *Nature* 446: 153–158

Grönroos E, Terentiev AA, Punga T & Ericsson J (2004) YY1 inhibits the activation of the p53 tumor suppressor in response to genotoxic stress. *Proc Natl Acad Sci U S A* 101: 12165–12170

Guo S, Cheng X, Lim J-H, Liu Y & Kao H-Y (2014) Control of antioxidative response by the tumor suppressor protein PML through regulating Nrf2 activity. *Mol Biol Cell* 25: 2485–2498

Gurrieri C, Capodieci P, Bernardi R, Scaglioni PP, Nafa K, Rush LJ, Verbel DA, Cordon-Cardo C & Pandolfi PP (2004) Loss of the Tumor Suppressor PML in Human Cancers of Multiple Histologic Origins. *JNCI J Natl Cancer Inst* 96: 269–279

Haase V (2009) The VHL Tumor Suppressor: Master Regulator of HIF. *Curr Pharm Des* 15: 3895–3903

Hagen T, Taylor CT, Lam F & Moncada S (2003) Redistribution of Intracellular Oxygen in Hypoxia by Nitric Oxide: Effect on HIF1α. *Science (80-)* 302: 1975–1978

Han H, Shim H, Shin D, Shim JE, Ko Y, Shin J, Kim H, Cho A, Kim E, Lee T, *et al* (2015) TRRUST: A reference database of human transcriptional regulatory interactions. *Sci Rep* 5: 1–11

Harrow J, Frankish A, Gonzalez JM, Tapanari E, Diekhans M, Kokocinski F, Aken BL, Barrell D, Zadissa A, Searle S, *et al* (2012) GENCODE: The reference human genome annotation for The ENCODE Project. *Genome Res* 22: 1760–1774

Herranz N & Gil J (2018) Mechanisms and functions of cellular senescence. *J Clin Invest* 128: 1238–1246

Heyne K, Schmitt K, Mueller D, Armbruester V, Mestres P & Roemer K (2008) Resistance of mitochondrial p53 to dominant inhibition. *Mol Cancer* 7: 1–17

Hofmann TG, Möller A, Sirma H, Zentgraf H, Taya Y, Dröge W, Will H & Schmitz ML (2002) Regulation of p53 activity by its interaction with homeodomain-interacting protein kinase-2. *Nat Cell Biol* 4: 1–10

Hoischen C, Monajembashi S, Weisshart K & Hemmerich P (2018) Multimodal Light Microscopy Approaches to Reveal Structural and Functional Properties of Promyelocytic Leukemia Nuclear Bodies. *Front Oncol* 8

Hsu K-S, Guan B-J, Cheng X, Guan D, Lam M, Hatzoglou M & Kao H-Y (2016) Translational control of PML contributes to TNFα-induced apoptosis of MCF7 breast cancer cells and decreased angiogenesis in HUVECs. *Cell Death Differ* 23: 469–483

Hsu KS & Kao HY (2018) PML: Regulation and multifaceted function beyond tumor suppression. *Cell Biosci* 8: 1–21

Hu C-J, Wang L-Y, Chodosh LA, Keith B & Simon MC (2003) Differential Roles of Hypoxia-Inducible Factor 1α (HIF-1α) and HIF-2α in Hypoxic Gene Regulation. *Mol Cell Biol* 23: 9361–9374

Huang LE, Gu J, Schau M & Bunn HF (1998) Regulation of hypoxia-inducible factor 1α is mediated by an O 2 -dependent degradation domain via the ubiquitin-proteasome pathway. *Proc Natl Acad Sci* 95: 7987–7992

Huber KE, Carey LA & Wazer DE (2009) Breast Cancer Molecular Subtypes in Patients With Locally Advanced Disease: Impact on Prognosis, Patterns of Recurrence, and Response to Therapy. *Semin Radiat Oncol* 19: 204–210

Hudes G, Carducci M, Tomczak P, Dutcher J, Figlin R, Kapoor A, Staroslawska E, Sosman J, McDermott D, Bodrogi I, *et al* (2007) Temsirolimus, Interferon Alfa, or Both for Advanced Renal-Cell Carcinoma. *N Engl J Med* 356: 2271–2281

Ito K, Bernardi R, Morotti A, Matsuoka S, Saglio G, Ikeda Y, Rosenblatt J, Avigan DE, Teruya-Feldstein J & Pandolfi PP (2008a) PML targeting eradicates quiescent leukaemia-initiating cells. *Nature* 453: 1072–1078

Ito K, Carracedo A, Weiss D, Arai F, Ala U, Avigan DE, Schafer ZT, Evans RM, Suda T, Lee C-H, *et al* (2012) A PML–PPAR-δ pathway for fatty acid oxidation regulates hematopoietic stem cell maintenance. *Nat Med* 18: 1350–1358

Ivan M, Kondo K, Yang H, Kim W, Valiando J, Ohh M, Salic A, Asara JM, Lane WS & Kaelin Jr. WG (2001) HIFα Targeted for VHL-Mediated Destruction by Proline Hydroxylation: Implications for O 2 Sensing. *Science (80-)* 292: 464–468

Ivanschitz L, Takahashi Y, Jollivet F, Ayrault O, Le Bras M & de Thé H (2015) PML IV/ARF interaction enhances p53 SUMO-1 conjugation, activation, and senescence. *Proc Natl Acad Sci* 112: 14278–14283

Ivanschitz L, De Thé H & Le Bras M (2013) PML, SUMOylation, and Senescence. *Front Oncol* 3

Jensen K, Shiels C & Freemont PS (2001) PML protein isoforms and the RBCC/TRIM motif. *Oncogene* 20: 7223–7233

Kakizuka a, Miller WH, Umesono K, Warrell RP, Dmitrovsky E, Evans RM & Jolla L (1991) Putative Transcription Factor , PML. *Cell* 66: 663–674

Kalinowski L, Janaszak-Jasiecka A, Siekierzycka A, Bartoszewska S, Woźniak M, Lejnowski D, Collawn JF & Bartoszewski R (2016) Posttranscriptional and transcriptional regulation of endothelial nitric-oxide synthase during hypoxia: the role of microRNAs. *Cell Mol Biol Lett* 21: 16

Kamitani T, Kito K, Nguyen HP, Wada H, Fukuda-Kamitani T & Yeh ETH (1998) Identification of Three Major Sentrinization Sites in PML. *J Biol Chem* 273: 26675–26682

Keith B, Johnson RS & Simon MC (2012) HIF1α and HIF2α: sibling rivalry in hypoxic

tumour growth and progression. *Nat Rev Cancer* 12: 9–22

Key J, Scheuermann TH, Anderson PC, Daggett V & Gardner KH (2009) Principles of Ligand Binding within a Completely Buried Cavity in HIF2α PAS-B. *J Am Chem Soc* 131: 17647–17654

Khan A, Fornes O, Stigliani A, Gheorghe M, Lee R Van Der, Bessy A, Ch J & Kulkarni R (2018) Erratum: JASPAR 2018: Update of the open-access database of transcription factor binding profiles and its web framework (Nucleic Acids Research (2017) DOI: 10.1093/nar/gkx1126). *Nucleic Acids Res* 46: D1284

Khan MM, Nomura T, Kim H, Kaul SC, Wadhwa R, Shinagawa T, Ichikawa-Iwata E, Zhong S, Pandolfi PP & Ishii S (2001) Role of PML and PML-RARα in Mad-Mediated Transcriptional Repression. *Mol Cell* 7: 1233–1243

Kim MK, Yang S, Lee K-H, Um J-H, Liu M, Kang H, Park SJ & Chung JH (2011) Promyelocytic leukemia inhibits adipogenesis, and loss of promyelocytic leukemia results in fat accumulation in mice. *Am J Physiol Metab* 301: E1130–E1142

Koh MY & Powis G (2012) Passing the baton: the HIF switch. *Trends Biochem Sci* 37: 364–372

Kondo K, Kim WY, Lechpammer M & Kaelin WG (2003) Inhibition of HIF2α Is Sufficient to Suppress pVHL-Defective Tumor Growth. *PLoS Biol* 1: e83

Kondo K, Klco J, Nakamura E, Lechpammer M & Kaelin WG (2002) Inhibition of HIF is necessary for tumor suppression by the von Hippel-Lindau protein. *Cancer Cell* 1: 237–246

Koshiji M, Kageyama Y, Pete EA, Horikawa I, Barrett JC & Huang LE (2004) HIF-1α induces cell cycle arrest by functionally counteracting Myc. *EMBO J* 23: 1949–1956

Koutsodontis G, Tentes I, Papakosta P, Moustakas A & Kardassis D (2001) Sp1 Plays a Critical Role in the Transcriptional Activation of the Human Cyclin-dependent Kinase Inhibitor p21WAF1/Cip1 Gene by the p53 Tumor Suppressor Protein. *J Biol Chem* 276: 29116–29125

Krtolica A, Parrinello S, Lockett S, Desprez PY & Campisi J (2001) Senescent fibroblasts promote epithelial cell growth and tumorigenesis: A link between cancer and aging. *Proc Natl Acad Sci U S A* 98: 12072–12077

Kuleshov M V., Jones MR, Rouillard AD, Fernandez NF, Duan Q, Wang Z, Koplev S, Jenkins SL, Jagodnik KM, Lachmann A, *et al* (2016) Enrichr: a comprehensive gene

set enrichment analysis web server 2016 update. *Nucleic Acids Res* 44: W90–W97

Kuo HY, Huang YS, Tseng CH, Chen YC, Chang YW, Shih HM & Wu CW (2014) PML represses lung cancer metastasis by suppressing the nuclear EGFR-mediated transcriptional activation of MMP2. *Cell Cycle* 13: 3132–3142

Kuwayama K, Matsuzaki K, Mizobuchi Y, Mure H, Kitazato KT, Kageji T, Nakao M & Nagahiro S (2009) Promyelocytic leukemia protein induces apoptosis due to caspase-8 activation via the repression of NFκB activation in glioblastoma. *Neuro Oncol* 11: 132–141

Lachmann A, Xu H, Krishnan J, Berger SI, Mazloom AR & Ma'ayan A (2010) ChEA: Transcription factor regulation inferred from integrating genome-wide ChIP-X experiments. *Bioinformatics* 26: 2438–2444

Lallemand-Breitenbach V, Jeanne M, Benhenda S, Nasr R, Lei M, Peres L, Zhou J, Zhu J, Raught B & de Thé H (2008) Arsenic degrades PML or PML–RARα through a SUMO-triggered RNF4/ubiquitin-mediated pathway. *Nat Cell Biol* 10: 547–555

Lee KA, Flores RR, Jang IH, Saathoff A & Robbins PD (2022) Immune Senescence, Immunosenescence and Aging. *Front Aging* 3: 1–7

Levine AJ & Oren M (2009) The first 30 years of p53: Growing ever more complex. *Nat Rev Cancer* 9: 749–758

Li J, Guo L, Chai L & Ai Z (2019a) Comprehensive Analysis of Driver Genes in Personal Genomes of Clear Cell Renal Cell Carcinoma. *Technol Cancer Res Treat* 18: 153303381983096

Li J, Zou WX & Chang KS (2014) Inhibition of Sp1 functions by its sequestration into PML nuclear bodies. *PLoS One* 9

Li W, Ferguson BJ, Khaled WT, Tevendale M, Stingl J, Poli V, Rich T, Salomoni P & Watson CJ (2009) PML depletion disrupts normal mammary gland development and skews the composition of the mammary luminal cell progenitor pool. *Proc Natl Acad Sci* 106: 4725–4730

Li Y, Lih T-SM, Dhanasekaran SM, Mannan R, Chen L, Cieslik M, Wu Y, Lu RJ-H, Clark DJ, Kołodziejczak I, *et al* (2023) Histopathologic and proteogenomic heterogeneity reveals features of clear cell renal cell carcinoma aggressiveness. *Cancer Cell* 41: 139-163.e17

Li Y, Ma X, Chen Z, Wu H, Wang P, Wu W, Cheng N, Zeng L, Zhang H, Cai X, *et al*

(2019b) B1 oligomerization regulates PML nuclear body biogenesis and leukemogenesis. *Nat Commun* 10

Liao Y, Smyth GK & Shi W (2014) featureCounts: an efficient general purpose program for assigning sequence reads to genomic features. *Bioinformatics* 30: 923–930

Liebl MC & Hofmann TG (2022) Regulating the p53 Tumor Suppressor Network at PML Biomolecular Condensates. *Cancers (Basel)* 14

Lin H-K, Bergmann S & Pandolfi PP (2004) Cytoplasmic PML Function in TGF-β Signaling. *Blood* 104: 481–481

Lin Y-C, Lu L-T, Chen H-Y, Duan X, Lin X, Feng X-H, Tang M-J & Chen R-H (2014) SCP Phosphatases Suppress Renal Cell Carcinoma by Stabilizing PML and Inhibiting mTOR/HIF Signaling. *Cancer Res* 74: 6935–6946

Liu S-B, Shen Z-F, Guo Y-J, Cao L-X & Xu Y (2017) PML silencing inhibits cell proliferation and induces DNA damage in cultured ovarian cancer cells. *Biomed Reports* 7: 29–35

Ljungberg B, Campbell SC, Cho HY, Jacqmin D, Lee JE, Weikert S & Kiemeney LA (2011) The Epidemiology of Renal Cell Carcinoma. *Eur Urol* 60: 615–621

Love MI, Huber W & Anders S (2014) Moderated estimation of fold change and dispersion for RNA-seq data with DESeq2. *Genome Biol* 15: 550

Lunardi A, Gaboli M, Giorgio M, Rivi R, Bygrave A, Antoniou M, Drabek D, Dzierzak E, Fagioli M, Salmena L, *et al* (2011) A Role for PML in Innate Immunity. *Genes Cancer* 2: 10–9

Luo G, Wang L, Zheng Z, Gao B & Lei C (2023) Cuproptosis-Related Ferroptosis genes for Predicting Prognosis in kidney renal clear cell carcinoma. *Eur J Med Res* 28: 1–11

Magliulo D & Bernardi R (2018) HIF-α factors as potential therapeutic targets in leukemia. *Expert Opin Ther Targets* 22: 917–928

Mandriota SJ, Turner KJ, Davies DR, Murray PG, Morgan N V, Sowter HM, Wykoff CC, Maher ER, Harris AL, Ratcliffe PJ, *et al* (2002) HIF activation identifies early lesions in VHL kidneys. *Cancer Cell* 1: 459–468

Martín-Martín N, Piva M, Urosevic J, Aldaz P, Sutherland JD, Fernández-Ruiz S, Arreal L, Torrano V, Cortazar AR, Planet E, *et al* (2016) Stratification and therapeutic potential of PML in metastatic breast cancer. *Nat Commun* 7

Martin N, Benhamed M, Nacerddine K, Demarque MD, Van Lohuizen M, Dejean A & Bischof O (2012) Physical and functional interaction between PML and TBX2 in the establishment of cellular senescence. *EMBO J* 31: 95–109

Matt S & Hofmann TG (2018) Crosstalk between p53 modifiers at PML bodies. *Mol Cell Oncol* 5: e1074335

Maul GG & Everett RD (1994) The nuclear location of PML, a cellular member of the C3HC4 zinc-binding domain protein family, is rearranged during herpes simplex virus infection by the C3HC4 viral protein ICP0. *J Gen Virol* 75: 1223–1233

McNally BA, Trgovcich J, Maul GG, Liu Y & Zheng P (2008) A Role for Cytoplasmic PML in Cellular Resistance to Viral Infection. *PLoS One* 3: e2277

Metallo CM, Gameiro PA, Bell EL, Mattaini KR, Yang J, Hiller K, Jewell CM, Johnson ZR, Irvine DJ, Guarente L, *et al* (2012) Reductive glutamine metabolism by IDH1 mediates lipogenesis under hypoxia. *Nature* 481: 380–384

Mijit M, Caracciolo V, Melillo A, Amicarelli F & Giordano A (2020) Role of p53 in the regulation of cellular senescence. *Biomolecules* 10: 1–16

Missiroli S, Bonora M, Patergnani S, Poletti F, Perrone M, Gafà R, Magri E, Raimondi A, Lanza G, Tacchetti C, *et al* (2016) PML at Mitochondria-Associated Membranes Is Critical for the Repression of Autophagy and Cancer Development. *Cell Rep* 16: 2415–2427

Motzer RJ, Escudier B, Oudard S, Hutson TE, Porta C, Bracarda S, Grünwald V, Thompson JA, Figlin RA, Hollaender N, *et al* (2008) Efficacy of everolimus in advanced renal cell carcinoma: a double-blind, randomised, placebo-controlled phase III trial. *Lancet* 372: 449–456

Nisole S, Maroui MA, Mascle XH, Aubry M & Chelbi-Alix MK (2013) Differential roles of PML isoforms. *Front Oncol* 3 MAY: 1–17

Niu C, Yan H, Yu T, Sun HP, Liu JX, Xiu-Song L, Wu W, Zhang FQ, Chen Y, Zhou L, *et al* (1999) Studies on treatment of acute promyelocytic leukemia with arsenic trioxide: Remission induction, follow-up, and molecular monitoring in 11 newly diagnosed and 47 relapsed acute promyelocytic leukemia patients. *Blood* 94: 3315–3324

Noé V, Chen C, Alemany C, Nicolás M, Caragol I, Chasin LA & Ciudad CJ (1997) Cell-growth regulation of the hamster dihydrofolate reductase gene promoter by

transcription factor Sp1. *Eur J Biochem* 249: 13–20

Ohh M, Park CW, Ivan M, Hoffman MA, Kim T-Y, Huang LE, Pavletich N, Chau V & Kaelin WG (2000) Ubiquitination of hypoxia-inducible factor requires direct binding to the β-domain of the von Hippel–Lindau protein. *Nat Cell Biol* 2: 423–427

Oronza A. Botrugno, Silvia Bianchessi, Desirée Zambroni, Michela Frenquelli, Daniela Belloni, Lucia Bongiovanni, Stefania Girlanda, Simona Di Terlizzi, Marina Ferrarini, Elisabetta Ferrero, *et al* (2019) ATR addiction in multiple myeloma: synthetic lethal approaches exploiting established therapies. *Haematologica* 105: 2440–2447

P. PK, Bischof O, Purbey PK, Notani D, Urlaub H, Dejean A & Galande S (2007) Functional interaction between PML and SATB1 regulates chromatin-loop architecture and transcription of the MHC class I locus. *Nat Cell Biol* 9: 45–56

Pan Y, Oprysko PR, Asham AM, Koch CJ & Simon MC (2004) p53 cannot be induced by hypoxia alone but responds to the hypoxic microenvironment. *Oncogene* 23: 4975–4983

Patel SA, Hirosue S, Rodrigues P, Vojtasova E, Richardson EK, Ge J, Syafruddin SE, Speed A, Papachristou EK, Baker D, *et al* (2022) The renal lineage factor PAX8 controls oncogenic signalling in kidney cancer. *Nature* 606: 999–1006

Peña-Llopis S, Vega-Rubín-de-Celis S, Liao A, Leng N, Pavía-Jiménez A, Wang S, Yamasaki T, Zhrebker L, Sivanand S, Spence P, *et al* (2012) BAP1 loss defines a new class of renal cell carcinoma. *Nat Genet* 44: 751–759

Pillai RK, Mur FM, Reig JA, Tchkonia T, Kirkland JL & Schwartz S (2017) Aging-V9I11-101328. 9: 10–12

Pires MM, Hopkins BD, Saal LH & Parsons RE (2013) Alterations of EGFR, p53 and PTEN that mimic changes found in basal-like breast cancer promote transformation of human mammary epithelial cells. *Cancer Biol Ther* 14: 246–253

Ponente M, Campanini L, Cuttano R, Piunti A, Delledonne GA, Coltella N, Valsecchi R, Villa A, Cavallaro U, Pattini L, *et al* (2017) PML promotes metastasis of triple-negative breast cancer through transcriptional regulation of HIF1A target genes. *JCI Insight* 2: 1–15

Powles T, Plimack ER, Soulières D, Waddell T, Stus V, Gafanov R, Nosov D, Pouliot F, Melichar B, Vynnychenko I, *et al* (2020) Pembrolizumab plus axitinib versus

sunitinib monotherapy as first-line treatment of advanced renal cell carcinoma (KEYNOTE-426): extended follow-up from a randomised, open-label, phase 3 trial. *Lancet Oncol* 21: 1563–1573

Previati M, Missiroli S, Perrone M, Caroccia N, Paliotto F, Milani D & Giorgi C (2018) Functions and dys-functions of promyelocytic leukemia protein PML. *Rend Lincei Sci Fis e Nat* 29: 411–420

Raval RR, Lau KW, Tran MGB, Sowter HM, Mandriota SJ, Li J-L, Pugh CW, Maxwell PH, Harris AL & Ratcliffe PJ (2005) Contrasting properties of hypoxia-inducible factor 1 (HIF-1) and HIF-2 in von Hippel-Lindau-associated renal cell carcinoma. *Mol Cell Biol* 25: 5675–86

Regad T, Bellodi C, Nicotera P & Salomoni P (2009) The tumor suppressor Pml regulates cell fate in the developing neocortex. *Nat Neurosci* 12: 132–140

Rini BI, Campbell SC & Escudier B (2009) Renal cell carcinoma. *Lancet* 373: 1119–1132

Roberts AM, Watson IR, Evans AJ, Foster DA, Irwin MS & Ohh M (2009) Suppression of hypoxia-inducible factor 2α restores p53 activity via Hdm2 and reverses chemoresistance of renal carcinoma cells. *Cancer Res* 69: 9056–9064

Rogers JL, Bayeh L, Scheuermann TH, Longgood J, Key J, Naidoo J, Melito L, Shokri C, Frantz DE, Bruick RK, *et al* (2013) Development of Inhibitors of the PAS-B Domain of the HIF-2α Transcription Factor. *J Med Chem* 56: 1739–1747

Sahin U, Ferhi O, Jeanne M, Benhenda S, Berthier C, Jollivet F, Niwa-Kawakita M, Faklaris O, Setterblad N, de Thé H, *et al* (2014) Oxidative stress–induced assembly of PML nuclear bodies controls sumoylation of partner proteins. *J Cell Biol* 204: 931–945

Salama R, Masson N, Simpson P, Sciesielski LK, Sun M, Tian Y-M, Ratcliffe PJ & Mole DR (2015) Heterogeneous Effects of Direct Hypoxia Pathway Activation in Kidney Cancer. *PLoS One* 10: e0134645

Sato Y, Yoshizato T, Shiraishi Y, Maekawa S, Okuno Y, Kamura T, Shimamura T, Sato-Otsubo A, Nagae G, Suzuki H, *et al* (2013) Integrated molecular analysis of clear-cell renal cell carcinoma. *Nat Genet* 45: 860–867

Saul D, Kosinsky RL, Atkinson EJ, Doolittle ML, Zhang X, LeBrasseur NK, Pignolo RJ, Robbins PD, Niedernhofer LJ, Ikeno Y, *et al* (2022) A new gene set identifies

senescent cells and predicts senescence-associated pathways across tissues. *Nat Commun* 13

Scaglioni PP, Rabellino A, Yung TM, Bernardi R, Choi S, Konstantinidou G, Nardella C, Cheng K & Pandolfi PP (2012) Translation-dependent mechanisms lead to PML upregulation and mediate oncogenic K-RAS-induced cellular senescence. *EMBO Mol Med* 4: 594–602

Scheuermann TH, Tomchick DR, Machius M, Guo Y, Bruick RK & Gardner KH (2009) Artificial ligand binding within the HIF2α PAS-B domain of the HIF2 transcription factor. *Proc Natl Acad Sci* 106: 450–455

Schmitges FW, Radovani E, Najafabadi HS, Barazandeh M, Campitelli LF, Yin Y, Jolma A, Zhong G, Guo H, Kanagalingam T, *et al* (2016) Multiparameter functional diversity of human C2H2 zinc finger proteins. *Genome Res* 26: 1742–1752

Schödel J, Grampp S, Maher ER, Moch H, Ratcliffe PJ, Russo P & Mole DR (2016) Hypoxia, Hypoxia-inducible Transcription Factors, and Renal Cancer. *Eur Urol* 69: 646–657

Schofield CJ & Ratcliffe PJ (2004) Oxygen sensing by HIF hydroxylases. *Nat Rev Mol Cell Biol* 5: 343–354

Scortegagna M, Ding K, Oktay Y, Gaur A, Thurmond F, Yan L-J, Marck BT, Matsumoto AM, Shelton JM, Richardson JA, *et al* (2003) Multiple organ pathology, metabolic abnormalities and impaired homeostasis of reactive oxygen species in Epas1−/− mice. *Nat Genet* 35: 331–340

Seeler J-S & Dejean A (2017) SUMO and the robustness of cancer. *Nat Rev Cancer* 17: 184–197

Semenza GL (2003) Targeting HIF-1 for cancer therapy. *Nat Rev Cancer* 3: 721–732

Serocki M, Bartoszewska S, Janaszak-Jasiecka A, Ochocka RJ, Collawn JF & Bartoszewski R (2018) miRNAs regulate the HIF switch during hypoxia: a novel therapeutic target. *Angiogenesis* 21: 183–202

Shaulian E, Zauberman A, Ginsberg D & Oren M (1992) Identification of a Minimal Transforming Domain of p53: Negative Dominance through Abrogation of Sequence-Specific DNA Binding. *Mol Cell Biol* 12: 5581–5592

Shen C, Beroukhim R, Schumacher SE, Zhou J, Chang M, Signoretti S & Kaelin WG (2011) Genetic and Functional Studies Implicate HIF1 α as a 14q Kidney Cancer

Suppressor Gene. *Cancer Discov* 1: 222–235

Shuch B, Amin A, Armstrong AJ, Eble JN, Ficarra V, Lopez-Beltran A, Martignoni G, Rini BI & Kutikov A (2015) Understanding Pathologic Variants of Renal Cell Carcinoma: Distilling Therapeutic Opportunities from Biologic Complexity. *Eur Urol* 67: 85–97

Smythies JA, Sun M, Masson N, Salama R, Simpson PD, Murray E, Neumann V, Cockman ME, Choudhry H, Ratcliffe PJ, *et al* (2019) Inherent DNA -binding specificities of the HIF -1α and HIF -2α transcription factors in chromatin . *EMBO Rep* 20: 1–17

Stadler M, Chelbi-Alix MK, Koken MH, Venturini L, Lee C, Saïb A, Quignon F, Pelicano L, Guillemin MC & Schindler C (1995) Transcriptional induction of the PML growth suppressor gene by interferons is mediated through an ISRE and a GAS element. *Oncogene* 11: 2565–73

de Stanchina E, Querido E, Narita M, Davuluri R V, Pandolfi PP, Ferbeyre G & Lowe SW (2004) PML Is a Direct p53 Target that Modulates p53 Effector Functions. *Mol Cell* 13: 523–535

Stransky LA, Vigeant SM, Huang B, West D, Denize T, Walton E, Signoretti S & Kaelin WG (2022) Sensitivity of VHL mutant kidney cancers to HIF2 inhibitors does not require an intact p53 pathway. *Proc Natl Acad Sci U S A* 119

Sui G, Affar EB, Shi Y, Brignone C, Wall NR, Yin P, Donohoe M, Luke MP, Calvo D, Grossman SR, *et al* (2004) Yin Yang 1 is a negative regulator of p53. *Cell* 117: 859–872

Swick G & Azizkhan JC (1997) ⇣ Community Help ⇣ save. 3800808

Takahashi Y, Rayman JB & Dynlacht BD (2000) Analysis of promoter binding by the E2F and pRB families in vivo: Distinct E2F proteins mediate activation and repression. *Genes Dev* 14: 804–816

Tatham MH, Geoffroy MC, Shen L, Plechanovova A, Hattersley N, Jaffray EG, Palvimo JJ & Hay RT (2008) RNF4 is a poly-SUMO-specific E3 ubiquitin ligase required for arsenic-induced PML degradation. *Nat Cell Biol* 10: 538–546

de Thé H, Le Bras M & Lallemand-Breitenbach V (2012) Acute promyelocytic leukemia, arsenic, and PML bodies. *J Cell Biol* 198: 11–21

De Thé H, Chomienne C, Lanotte M, Degos L & Dejean A (1990) The t(15;17)

translocation of acute promyelocytic leukaemia fuses the retinoic acid receptor α gene to a novel transcribed locus. *Nature* 347: 558–561

de Thé H, Lavau C, Marchio A, Chomienne C, Degos L & Dejean A (1991) The PML-RARα fusion mRNA generated by the t(15;17) translocation in acute promyelocytic leukemia encodes a functionally altered RAR. *Cell* 66: 675–684

Triner D & Shah YM (2016) Hypoxia-inducible factors: a central link between inflammation and cancer. *J Clin Invest* 126: 3689–3698

Trotman LC, Alimonti A, Scaglioni PP, Koutcher JA, Cordon-Cardo C & Pandolfi PP (2006) Identification of a tumour suppressor network opposing nuclear Akt function. *Nature* 441: 523–527

Tyciakova S, Valova V, Svitkova B & Matuskova M (2021) Overexpression of TNFα induces senescence, autophagy and mitochondrial dysfunctions in melanoma cells. *BMC Cancer* 21: 1–13

Uggè M, Simoni M, Fracassi C & Bernardi R (2022) PML isoforms: a molecular basis for PML pleiotropic functions. *Trends Biochem Sci* 47: 609–619

Vallian S, Chin K-V & Chang K-S (1998) The Promyelocytic Leukemia Protein Interacts with Sp1 and Inhibits Its Transactivation of the Epidermal Growth Factor Receptor Promoter. *Mol Cell Biol* 18: 7147–7156

Varela I, Tarpey P, Raine K, Huang D, Ong CK, Stephens P, Davies H, Jones D, Lin M-L, Teague J, *et al* (2011) Exome sequencing identifies frequent mutation of the SWI/SNF complex gene PBRM1 in renal carcinoma. *Nature* 469: 539–542

Vernier M, Bourdeau V, Gaumont-Leclerc M-F, Moiseeva O, Bégin V, Saad F, Mes-Masson A-M & Ferbeyre G (2011) Regulation of E2Fs and senescence by PML nuclear bodies. *Genes Dev* 25: 41–50

Vito A, El-Sayes N & Mossman K (2020) Hypoxia-Driven Immune Escape in the Tumor Microenvironment. *Cells* 9: 992

Voisset E, Moravcsik E, Stratford EW, Jaye A, Palgrave CJ, Hills RK, Salomoni P, Kogan SC, Solomon E & Grimwade D (2018) Pml nuclear body disruption cooperates in APL pathogenesis and impairs DNA damage repair pathways in mice. *Blood* 131: 636–648

Wallace EM, Rizzi JP, Han G, Wehn PM, Cao Z, Du X, Cheng T, Czerwinski RM, Dixon

DD, Goggin BS, *et al* (2016) A small-molecule antagonist of HIF2α is efficacious in preclinical models of renal cell carcinoma. *Cancer Res* 76: 5491–5500

Wang D, Deng Z, Lu M, Deng K, Li Z & Zhou F (2023) Integrated analysis of the roles of oxidative stress related genes and prognostic value in clear cell renal cell carcinoma. *J Cancer Res Clin Oncol* 149: 11057–11071

Wang J, Shiels C, Sasieni P, Wu PJ, Islam SA, Freemont PS & Sheer D (2004) Promyelocytic leukemia nuclear bodies associate with transcriptionally active genomic regions. *J Cell Biol* 164: 515–26

Wang P, Benhenda S, Wu H, Lallemand-Breitenbach V, Zhen T, Jollivet F, Peres L, Li Y, Chen SJ, Chen Z, *et al* (2018) RING tetramerization is required for nuclear body biogenesis and PML sumoylation. *Nat Commun* 9: 1–10

Wang Z-G, Ruggero D, Ronchetti S, Zhong S, Gaboli M, Rivi R & Pandolfi PP (1998) Pml is essential for multiple apoptotic pathways. *Nat Genet* 20: 266–272

Weng W, Wang M, Xie S, Long Y, Li F, Sun F, Yu Y & Li Z (2014) YY1-C/EBPα-miR34a regulatory circuitry is involved in renal cell carcinoma progression. *Oncol Rep* 31: 1921–1927

Wingender E, Chen X, Hehl R, Karas H, Liebich I, Matys V, Meinhardt T, Prüß M, Reuter I, Schacherer F, *et al* (2000) Nucl. Acids Res.-2000-Wingender-316-9.pdf. 28: 316–319

Wolf, MM, Kimryn Rathmell, W & Beckermann, K.E (2020) Modeling clear cell renal cell carcinoma and therapeutic implications. *Oncogene* **39**, 3413–3426

Wu CH, Van Riggelen J, Yetil A, Fan AC, Bachireddy P & Felsher DW (2007) Cellular senescence is an important mechanism of tumor regression upon c-Myc inactivation. *Proc Natl Acad Sci U S A* 104: 13028–13033

Wu HC, Lin YC, Liu CH, Chung HC, Wang YT, Lin YW, Ma HI, Tu PH, Lawler SE & Chen RH (2014) USP11 regulates PML stability to control Notch-induced malignancy in brain tumours. *Nat Commun* 5: 1–15

Wu W-S, Xu Z-X, Hittelman WN, Salomoni P, Pandolfi PP & Chang K-S (2003) Promyelocytic Leukemia Protein Sensitizes Tumor Necrosis Factor α-Induced Apoptosis by Inhibiting the NF-κB Survival Pathway. *J Biol Chem* 278: 12294–12304

Wu X, Xie W, Gong B, Fu B, Chen W, Zhou L & Luo L (2023) Development of a TGF-

β signaling-related genes signature to predict clinical prognosis and immunotherapy responses in clear cell renal cell carcinoma. *Front Oncol* 13: 1–13

Xie L, Wang Q, Dang Y, Ge L, Sun X, Li N, Han Y, Yan Z, Zhang L, Li Y, *et al* (2019) OSkirc: a web tool for identifying prognostic biomarkers in kidney renal clear cell carcinoma. *Futur Oncol* 15: 3103–3110

Xue X, Taylor M, Anderson E, Hao C, Qu A, Greenson JK, Zimmermann EM, Gonzalez FJ & Shah YM (2012) Hypoxia-Inducible Factor-2α Activation Promotes Colorectal Cancer Progression by Dysregulating Iron Homeostasis. *Cancer Res* 72: 2285–2293

Yamada N, Tsujimura N, Kumazaki M, Shinohara H, Taniguchi K, Nakagawa Y, Naoe T & Akao Y (2014) Colorectal cancer cell-derived microvesicles containing microRNA-1246 promote angiogenesis by activating Smad 1/5/8 signaling elicited by PML down-regulation in endothelial cells. *Biochim Biophys Acta - Gene Regul Mech* 1839: 1256–1272

Yu Q, Katlinskaya Y V., Carbone CJ, Zhao B, Katlinski K V., Zheng H, Guha M, Li N, Chen Q, Yang T, *et al* (2015) DNA-Damage-Induced Type I Interferon Promotes Senescence and Inhibits Stem Cell Function. *Cell Rep* 11: 785–797

Yuan WC, Lee YR, Huang SF, Lin YM, Chen TY, Chung HC, Tsai CH, Chen HY, Chiang CT, Lai CK, *et al* (2011) A Cullin3-KLHL20 Ubiquitin Ligase-Dependent Pathway Targets PML to Potentiate HIF-1 Signaling and Prostate Cancer Progression. *Cancer Cell* 20: 214–228

Zhang R, Poustovoitov M V., Ye X, Santos HA, Chen W, Daganzo SM, Erzberger JP, Serebriiskii IG, Canutescu AA, Dunbrack RL, *et al* (2005) Formation of MacroH2A-Containing Senescence-Associated Heterochromatin Foci and Senescence Driven by ASF1a and HIRA. *Dev Cell* 8: 19–30

Zhang X-W, Yan X-J, Zhou Z-R, Yang F-F, Wu Z-Y, Sun H-B, Liang W-X, Song A-X, Lallemand-Breitenbach V, Jeanne M, *et al* (2010) Arsenic Trioxide Controls the Fate of the PML-RARα Oncoprotein by Directly Binding PML. *Science (80-)* 328: 240–243

Zhao J, Du F, Shen G, Zheng F & Xu B (2015) The role of hypoxia-inducible factor-2 in digestive system cancers. *Cell Death Dis* 6: e1600–e1600

Zhou W & Bao S (2014) PML-mediated signaling and its role in cancer stem cells. *Oncogene* 33: 1475–1484

Zindy F, Eischen CM, Randle DH, Kamijo T, Cleveland JL, Sherr CJ & Roussel MF (1998) Myc signaling via the ARF tumor suppressor regulates p53-dependent apoptosis and immortalization. *Genes Dev* 12: 2424–2433

Chiara Menegazzi